

AD-A068 088

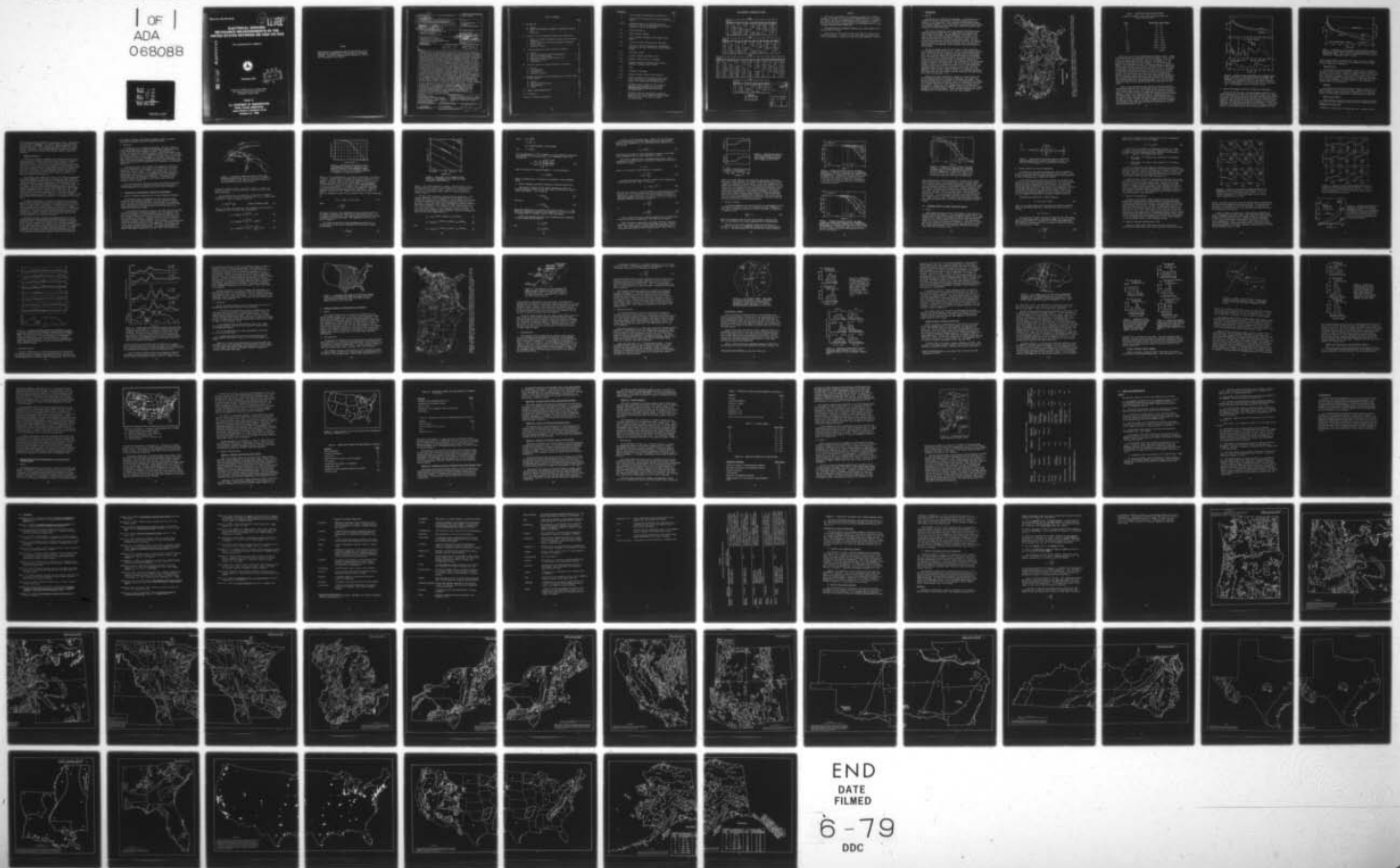
COLD REGIONS RESEARCH AND ENGINEERING LAB HANOVER NH F/G 20/14  
ELECTRICAL GROUND IMPEDANCE MEASUREMENTS IN THE UNITED STATES B--ETC(U)  
DEC 78 S A ARCONE, A J DELANEY DOT-FATQWAI-707

UNCLASSIFIED

FAA-RD-78-103

NL

OF  
ADA  
068088



END  
DATE  
FILMED  
6-79  
DDC

Report No. FAA-RD-78-103

12  
NW

LEVEL

# ELECTRICAL GROUND IMPEDANCE MEASUREMENTS IN THE UNITED STATES BETWEEN 200 AND 415 KHZ

S.A. Arcone and A.J. Delaney

AD A068088

DDC FILE COPY



December 1978

DDC  
APR 26 1979  
A

Document is available to the U.S. public through  
the National Technical Information Service,  
Springfield, Virginia 22161.

Prepared for

79 04 25 017

**U.S. DEPARTMENT OF TRANSPORTATION**  
**FEDERAL AVIATION ADMINISTRATION**  
**Systems Research & Development Service**  
**Washington, D.C. 20590**

NOTICE

This document is disseminated under the sponsorship of the Department of Transportation in the interest of information exchange. The United States Government assumes no liability for its contents or use thereof.

1. Report No. 18 FAA-RD-78-103	2. Government Accession No.	3. Recipient's Catalog No.	
4. Title and Subtitle 6 ELECTRICAL GROUND IMPEDANCE MEASUREMENTS IN THE UNITED STATES BETWEEN 200 AND 415 KHZ.		5. Report Date	6. Performing Organization Code USACRREL
7. Author(s) 10 A. Arcone and J. Delaney		8. Performing Organization Report No.	
9. Performing Organization Name and Address U.S. Army Cold Regions Research and Engineering Laboratory Hanover, New Hampshire 03755		10. Work Unit No. (TRAIS)	11. Contract or Grant No. 15 DOT-FATQWAI-707 new
12. Sponsoring Agency Name and Address FAA/Department of Transportation Systems Research and Development Service Washington, D.C. 20591 SRDS, ARD-60		13. Type of Report and Period Covered 9 Final Report. Oct 1976 - Mar 1978	
15. Supplementary Notes 11 Dec 78		14. Sponsoring Agency Code FAA/SRDS 12 92 p.	
<p>6. Abstract</p> <p>The objectives of the work described in this report were to use and evaluate new radiowave methods of measuring earth resistivity in the low-frequency (LF) (200-415 kHz) band, and to develop estimated effective ground resistivity maps in this same band for the United States including Alaska. Both airborne and ground methods were investigated by using the wavetilt and surface impedance techniques. The airborne methods discussion concentrates on the use of the wavetilt technique in the very-low-frequency (VLF) (10-30 kHz) band because LF transmitters operate at a wide range of frequencies and supply inadequate coverage. It is concluded from the VLF study that over much of the central United States VLF airborne resistivity might well approximate LF ground resistivity. The ground methods discussion concerns the surface impedance method in the LF band using a device developed by a commercial organization for the purposes of this study. Geological and physiographic effects on LF resistivity are demonstrated in several studies and the data are used later to produce an estimated effective conductivity map of the United States. It is concluded from the LF studies that the present conductivity map based on the field strength attenuation method for BCB (Broadcast Band: 550-1600 kHz) transmitters, and in current use by the FAA, is fairly accurate for BCB purposes but inapplicable to LF purposes, mainly because of the inadequate penetration of BCB radiation. The LF estimated conductivity maps for the United States, including Alaska, show patterns similar to those in previous resistivity maps but with different values. The most resistive areas are the granitic, mountainous regions. The most conductive areas are generally the coastal and loess deposits. The formerly glacially covered states of the Midwest have intermediate values and show much more variation than in previous mapping; this is because of the various types of glacially produced sediments. In addition to the resistivity mapping, a very generalized estimated LF surface impedance phase mapping is presented. Both resistivity and phase and their estimated seasonal variations are presented in one map of Alaska.</p>			
17. Key Words Conductivity mapping Electromagnetic resistivity mapping Ground resistivity Surface impedance Low frequency measurements Resistivity mapping Wavetilt		18. Distribution Statement Document is available to the U.S. public through the National Technical Information Service, Springfield, Virginia 22161	
19. Security Classif. (of this report) Unclassified	20. Security Classif. (of this page) Unclassified	21. No. of Pages 79	22. Price

039 100 mt

## TABLE OF CONTENTS

	<u>Page</u>
I. Introduction. . . . .	1
A. General. . . . .	1
B. Modern electromagnetic methods of resistivity measurement . . . . .	4
C. Objectives . . . . .	7
II. Principles of Electromagnetic Conductivity Measurements. . . . .	7
A. Theory of radiowave propagation in the earth-ionosphere waveguide. . . . .	7
B. Surface impedance and wavetilt methods of measuring conductivity . . . . .	11
C. Dielectric effects . . . . .	13
III. Airborne Approach to Ground Resistivity Mapping . . . . .	15
A. General. . . . .	15
B. Airborne quadrature wavetilt measurements. . . . .	16
C. Resolution considerations. . . . .	17
D. Range and altitude considerations at VLF . . . . .	17
E. Topographic effects. . . . .	20
F. Conclusions. . . . .	22
IV. Intensive Approach to Ground Resistivity Surveying . . . . .	23
A. General. . . . .	23
B. LF transmitters. . . . .	23
C. Instrumentation. . . . .	25
D. Comparative studies. . . . .	26
V. Estimated Resistivity and Phase Mapping of the United States Including Alaska. . . . .	34
A. General. . . . .	34
B. Regional classifications . . . . .	36
C. Phase mapping. . . . .	40
D. Alaska . . . . .	42
VI. Summary and Recommendations. . . . .	45
VII. References. . . . .	48
Glossary of Geologic Terms Used . . . . .	51

Appendixes

Page

A	Local Methods of Measuring Earth Resistivity . .	55
B	Operation of the Geonics EM-32 Surface Impedance Meter. . . . .	57
C1-C12	Estimated Ranges of Ground Conductivity as Measured by the Surface Impedance Method Between 200 and 415 kHz (in folded form)	
C-1	Oregon, Washington	
C-2	Idaho, Montana, Wyoming	
C-3	Iowa, Minnesota, Nebraska, North Dakota, South Dakota	
C-4	Illinois, Indiana, Michigan, Ohio, Wisconsin	
C-5	Connecticut, Maine, Massachusetts, New Hampshire, New Jersey, New York, Pennsylvania, Rhode Island, Vermont	
C-6	California, Nevada	
C-7	Arizona, Colorado, New Mexico, Utah	
C-8	Arkansas, Kansas, Missouri, Oklahoma	
C-9	Delaware, Kentucky, Maryland, North Carolina, Tennessee, Virginia, West Virginia	
C-10	Texas	
C-11	Louisiana, Mississippi	
C-12	Alabama, Florida, Georgia, South Carolina	
C-13	Urban and Industrial areas where ground conductivity values given in Appendixes C1-C12 are likely to be ineffective (in folded form)	
D	Estimated ranges of phase for the contiguous United States as measured by the surface impedance method between 200 and 415 kHz (in folded form)	
E	Estimated ranges of conductivity and phase as measured by the surface impedance method between 200 and 415 kHz for the state of Alaska (in folded form)	

# ENGLISH/METRIC CONVERSION FACTORS

## LENGTH

From \ To	cm	m	km	in	ft	mi	nmi
cm	1	0.01	1x10 <sup>-5</sup>	0.3937	0.0328	6.21x10 <sup>-6</sup>	5.39x10 <sup>-6</sup>
m	100	1	0.001	39.37	3.281	0.0006	0.0005
km	100,000	1000	1	39370	3281	0.6214	0.5395
in	2.540	0.0254	2.54x10 <sup>-5</sup>	1	0.0833	1.58x10 <sup>-5</sup>	1.37x10 <sup>-5</sup>
ft	30.48	0.3048	3.05x10 <sup>-4</sup>	12	1	1.89x10 <sup>-4</sup>	1.64x10 <sup>-4</sup>
mi	160,900	1609	1.609	63360	5280	1	0.8688
nmi	185,200	1852	1.852	72930	6076	1.151	1

## AREA

From \ To	cm <sup>2</sup>	m <sup>2</sup>	km <sup>2</sup>	in <sup>2</sup>	ft <sup>2</sup>	mi <sup>2</sup>	nmi <sup>2</sup>
cm <sup>2</sup>	1	0.0001	1x10 <sup>-10</sup>	0.1550	0.0011	3.86x10 <sup>-11</sup>	5.11x10 <sup>-11</sup>
m <sup>2</sup>	10,000	1	1x10 <sup>-6</sup>	1550	10.76	3.86x10 <sup>-7</sup>	5.11x10 <sup>-7</sup>
km <sup>2</sup>	1x10 <sup>10</sup>	1x10 <sup>6</sup>	1	1.55x10 <sup>9</sup>	1.08x10 <sup>7</sup>	0.3861	0.2914
in <sup>2</sup>	6.452	0.0006	6.45x10 <sup>-10</sup>	1	0.0069	2.49x10 <sup>-10</sup>	1.88x10 <sup>-10</sup>
ft <sup>2</sup>	929.0	0.0929	9.29x10 <sup>-8</sup>	144	1	3.59x10 <sup>-8</sup>	2.71x10 <sup>-8</sup>
mi <sup>2</sup>	2.59x10 <sup>10</sup>	2.59x10 <sup>6</sup>	2.590	4.01x10 <sup>9</sup>	2.79x10 <sup>7</sup>	1	0.7548
nmi <sup>2</sup>	3.43x10 <sup>10</sup>	3.43x10 <sup>6</sup>	3.432	5.31x10 <sup>9</sup>	3.70x10 <sup>7</sup>	1.325	1

## VOLUME

From \ To	cm <sup>3</sup>	liter	m <sup>3</sup>	in <sup>3</sup>	ft <sup>3</sup>	yd <sup>3</sup>	fl. oz.	fl. pt.	fl. qt.	gal.
cm <sup>3</sup>	1	0.001	1x10 <sup>-6</sup>	0.0610	3.53x10 <sup>-5</sup>	1.31x10 <sup>-6</sup>	0.0338	0.0021	0.0010	0.0002
liter	1000	1	0.001	61.02	0.0353	0.0013	33.81	2.113	1.057	0.2642
m <sup>3</sup>	1x10 <sup>6</sup>	1000	1	61,000	35.31	1.308	33,800	2113	1057	264.2
in <sup>3</sup>	16.39	0.0163	1.64x10 <sup>-5</sup>	1	0.0006	2.14x10 <sup>-5</sup>	0.5541	0.0346	2113	0.0043
ft <sup>3</sup>	28,300	28.32	0.0283	1728	1	0.0370	957.5	59.84	0.0173	7.481
yd <sup>3</sup>	765,000	764.5	0.7646	46700	27	1	25900	1616	807.9	202.0
fl. oz.	29.57	0.2957	2.96x10 <sup>-5</sup>	1.805	0.0010	3.87x10 <sup>-5</sup>	1	0.0625	0.0312	0.0078
fl. pt.	473.2	0.4732	0.0005	28.88	0.0167	0.0006	16	1	0.5000	0.1250
fl. qt.	948.4	0.9463	0.0009	57.75	0.0334	0.0012	32	2	1	0.2500
gal.	3785	3.785	0.0038	231.0	0.1337	0.0050	128	8	4	1

## MASS

From \ To	g	kg	oz	lb	ton
g	1	0.001	0.0353	0.0022	1.10x10 <sup>-6</sup>
kg	1000	1	35.27	2.205	0.0011
oz	28.35	0.0283	1	0.0625	3.12x10 <sup>-5</sup>
lb	453.6	0.4536	16	1	0.0005
ton	907,000	907.2	32,000	2000	1

## TEMPERATURE

$$^{\circ}\text{F} = \frac{5}{9} (^{\circ}\text{C} - 32)$$

$$^{\circ}\text{C} = \frac{9}{5} (^{\circ}\text{F}) + 32$$

APPROVED BY	
4TH	DATA Section <input checked="" type="checkbox"/>
5TH	DATA Section <input type="checkbox"/>
DISTRIBUTION	
DISTRIBUTION/AVAILABILITY CODES	
Part	APPROVAL OR SPECIAL
A	

PREFACE

This report was prepared by Dr. Steven A. Arcone and Mr. Allan J. Delaney, of the Physical Sciences Branch, Research Division, U.S. Army Cold Regions Research and Engineering Laboratory, Hanover, New Hampshire. The research was funded by the Department of Transportation, Federal Aviation Administration, Systems Research and Development Service, under Interagency Agreement DOD FATQWAI-707.

The manuscript was technically reviewed by Mr. Garth Kanen and Mr. Charles Cram, of the FAA.

The contents of this report are not to be used for advertising or promotional purposes. Citation of brand names does not constitute an official endorsement or approval of the use of such commercial products.

## I. INTRODUCTION

### A. General

The design, site selection and management of low-frequency (LF) transmitters require a knowledge of the earth conductivity in the vicinity of the transmitter. This is because field strength attenuation strongly depends on earth conductivity, an increase in which causes an increase in transmitter range and, hence, possibly cochannel interference with another transmitter.

This report concerns the use of new methods for obtaining ground conductivity values appropriate for engineering in the 200-415 kHz radio navigation aid band. The development of these methods in the last 20 years now enables detailed improvements to be made of the present conductivity map (see Figure 1 and Table I) used by the FAA (pub. 6050.10) both as to actual and extrapolated values. Not only do these new methods give the most appropriate values for the frequency band considered, but they also enable a survey area to be covered in regular grids, thus improving on the statistics and extrapolations of older methods.

The map in present use by the FAA is that of Fine (1954) based on an eight-year study by Kirby et al. (1954) of field strength attenuation of radiation from 621 transmitters in the 550-1660 kHz broadcast band. Ten to twelve radial sections, extending about 25 miles apiece, were taken from each transmitter, giving 7237 conductivity determinations. In Fine's map, extrapolations of conductivity values for areas not covered by BCB stations were made on the basis of correlations between conductivity and subsoil type (the term "subsoil" was not defined by Fine) existing in the known areas. This procedure was undoubtedly adopted in view of the conclusion of Kirby et al. of "some association of ground conductivity with soil type but so little that its use in predicting future values of ground conductivity for given soil type generally yields too wide a range of values to be sufficiently precise." Fine states that measured conductivities for paths over the same terrain often varied by more than 2 to 1.

Although the field strength decay method is a valid practice for determining gross measures of surface conductivity, the present FAA map is inappropriate for LF purposes for the following reasons. First, the depth through which conductivity values are integrated is much deeper at LF, being proportional to the square root of the frequency for any one material. Second, the field strength method at both BCB and LF wavelengths is topographically sensitive, thus giving question to values obtained in mountainous regions. Third, the field behavior over local inhomogeneities is understood for only very simple examples.

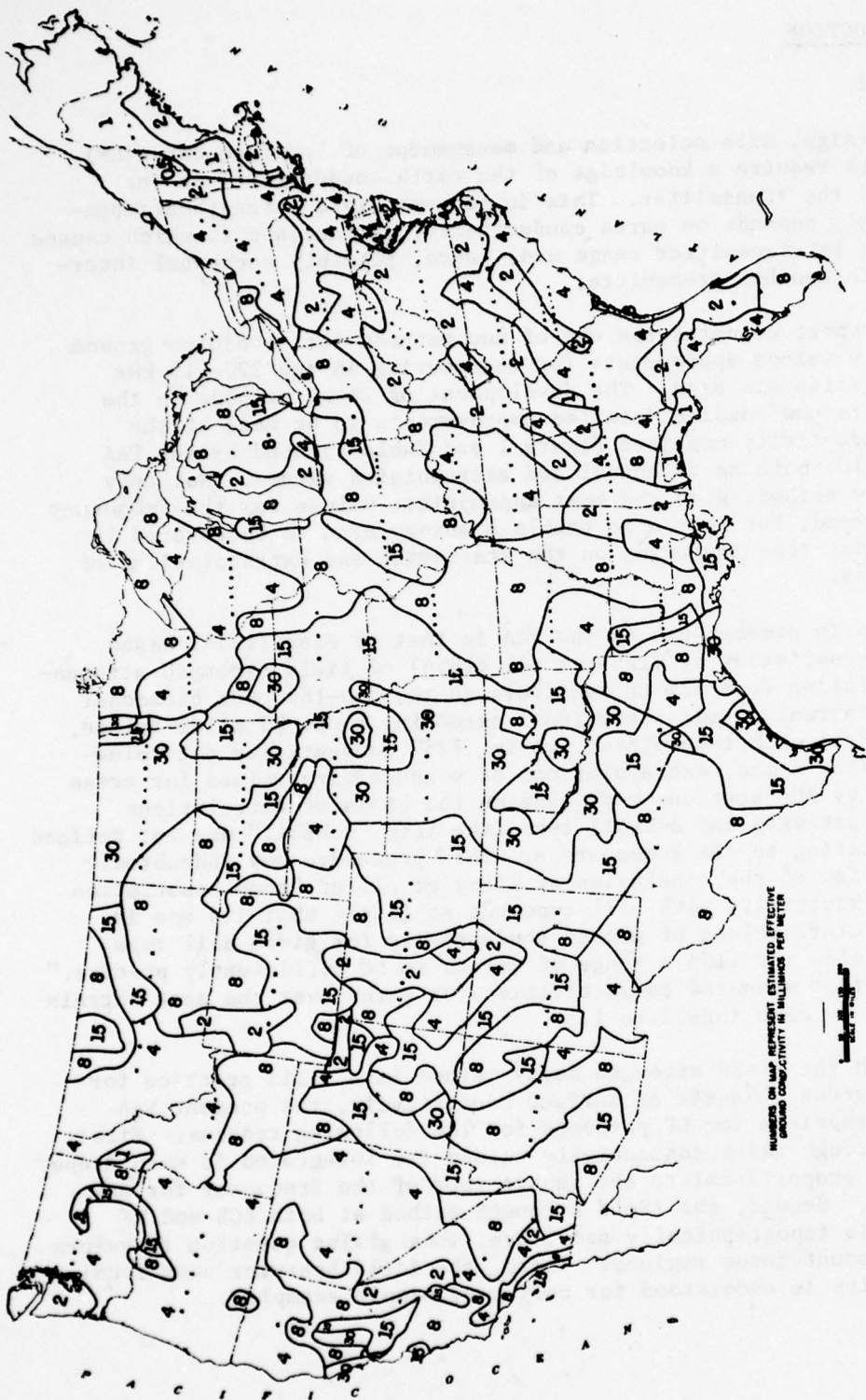


FIGURE 1. ESTIMATED EFFECTIVE GROUND CONDUCTIVITY IN THE CONTIGUOUS 48 STATES (AFTER FINE 1954). Each number refers to the approximate average conductivity in millimhos/m for the area designated. The conductivity range of each class is given in Table I.

TABLE I. RESISTIVITY CLASSIFICATION SCHEME  
 Classes 30 through 0.5 and their associated ranges are  
 taken from Fine (1954).

<u>Class</u>	<u>Resistivity range (ohm-m)</u>
30	22 - 47
15	47 - 91
8	91 - 177
4	177 - 354
2	354 - 707
1	707 - 1,414
0.5	1,414 - 2,829
0.25	2,829 - 5,000
0.14	5,000 - 10,000
0.06	10,000 - 20,000
0.03	> 20,000

These last two points are demonstrated in Figures 2 and 3. Figure 2 shows theoretical and experimental horizontal magnetic field strength ("H<sub>y</sub>" in the figures) attenuation curves for a 276-kHz, 25-Watt Non-Directional Beacon (NDB) located in Hanover, New Hampshire, a topographically and geologically complex region. At the bottom of the figure is the topographic profile. The bedrock geology is composed of various types of schist (see Glossary of Geologic Terms) metamorphosed from volcanic rocks and overlain by a marginal till cover. Also shown in this figure are galvanically (direct current method, see Appendix A) determined resistivity profiles for two effective depths of penetration. As the resistivity profiles reveal for both penetration depths resistivity varies over a very wide range (60-100,000 ohm-m). The field strength profile shows many large perturbations superimposed upon a general decay with radial distance, and some of the perturbations are associated with the rugged topography. At best, the average resistivity seen at LF is crudely estimated at between 200 and 1000 ohm-m.

Figure 3 shows experimental and theoretical horizontal magnetic field strength profiles for a 248-kHz NDB located at Glenallen, Alaska. In this case, there is very little relief and the geology to several tens of meters depth consists of unconsolidated glacial and lacustrine deposits. A best fit to the data places the average resistivity between 200 and 500 ohm-m. This agrees with the d.c. investigations over 1 to 20-m depth (vertical bars) that indicate values ranging from 20 to 600 ohm-m. However, although the field strength decay seems to follow the 500 ohm-m curve, there is at present no adequate way of estimating the resistivity along the large perturbations seen between 25 and 60 km and between 90 and 125 km.

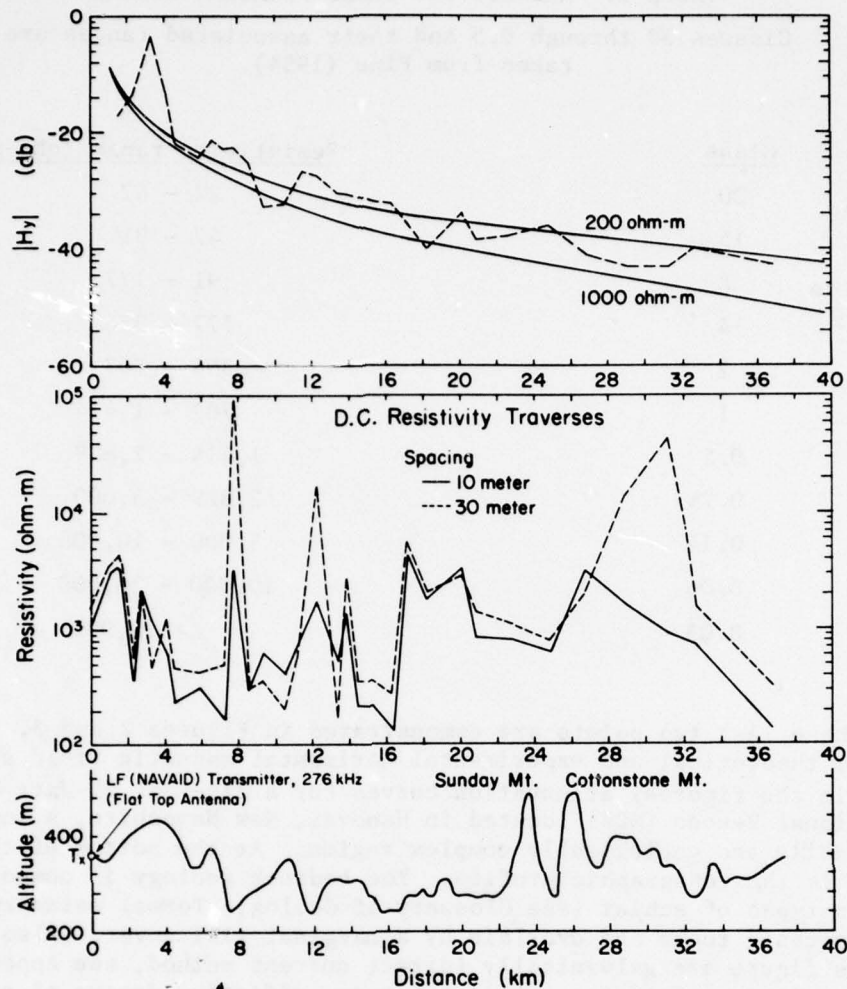


FIGURE 2. THEORETICAL AND EXPERIMENTAL FIELD STRENGTH ATTENUATION CURVES FOR A 276-KHZ BEACON LOCATED IN HANOVER, NEW HAMPSHIRE. The spacings indicated in the center plots are interelectrode separations for which the depths of penetration are approximately 7 m (10-m spacing) and 21 m (30-m spacing). The topographic profile is given at bottom.

#### B. Modern Electromagnetic Methods of Resistivity Measurement

Within the last 20 years, new electromagnetic methods of subsurface exploration have come into practice that enable local resistivity determinations not practical with field strength decay methods to be made. With the exception of subsurface radar which operates between 100 and 1000 MHz and relies on contrasts in dielectric polarizability, these methods rely primarily on contrasts in electrical conductivity to make subsurface material distinctions. In many cases therefore, electromagnetic methods are able to determine earth conductivity locally and directly, thus offering alternatives to the

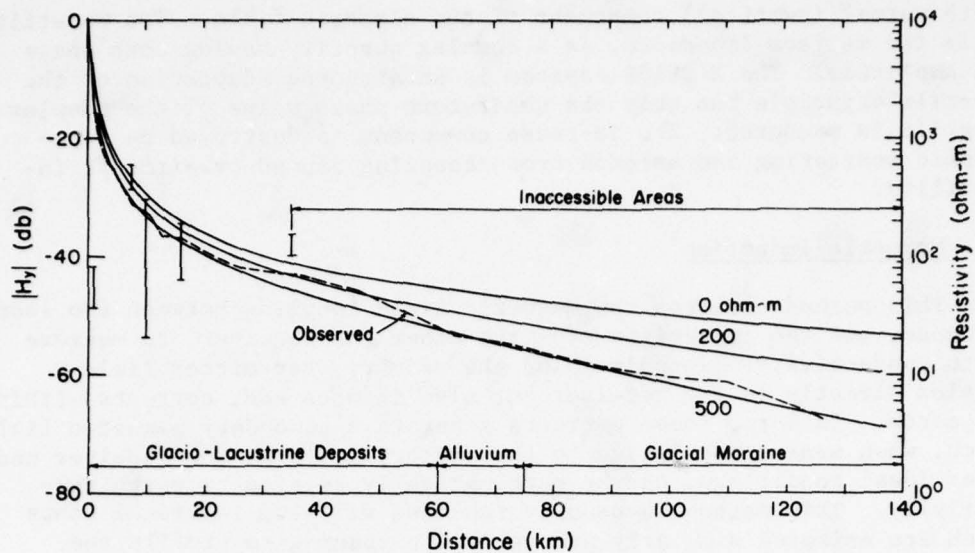


FIGURE 3. THEORETICAL AND EXPERIMENTAL FIELD STRENGTH ATTENUATION CURVES FOR A 248-KHZ BEACON LOCATED AT GLENALLEN, ALASKA, IN THE COPPER RIVER BASIN. The section runs approximately north from the transmitter. Topographic relief is minor.

field strength method of measuring earth resistivity. The methods are as follows, listed under their more common or commercial names. They are summarized in Appendix A.

#### Magnetotelluric

This method utilizes electromagnetic energy in VLF (3-30 kHz), ELF (10 Hz-30 kHz) and ULF (below 10 Hz) bands generated worldwide by atmospheric and ionospheric discharges, magnetic field micropulsations, etc. The quantity related to earth resistivity is the ratio of the earth tangential components of the electric and magnetic field known as the surface impedance. Readings covering a broad spectrum of frequencies allow interpretations to be made as to the resistivity of various layers of earth materials.

#### Radiohm\*

This method also utilizes the surface impedance principle but at higher frequencies in the VLF and LF bands. Powerful transmitters at VLF and numerous though less powerful transmitters at LF allow this method to be used almost anywhere over the North American Continent.

#### Wavetilt and E-Phase<sup>†</sup>

These methods are similar to the above surface impedance methods except that the earth tangential electric field is compared with the

\* Radiohm is a patent name.

<sup>†</sup> E-PHASE is a patent name of the Barringer Corp., Rexdale, Ontario.

earth normal (vertical) component of the electric field. The wavenumber, as is the surface impedance, is a complex quantity having both phase and amplitude. The E-PHASE system is an airborne adaptation of the wavenumber principle but only the quadrature phase value of the complex wavenumber is measured. The in-phase component is destroyed by topographic scattering and antenna cross coupling caused by aircraft instability.

#### Magnetic Induction

This method utilizes the magnetic field coupling between two loop antennas, one the transmitter and the other the receiver, to measure earth conductivity. In principle, the primary transmitter field couples directly to the receiver but also induces eddy currents within the earth. In turn, these currents generate a secondary magnetic field which, when measured relative to the primary field at the receiver and under ideal conditions, can be mathematically related to earth conductivity. This method is usually realized with two identical loops which are oriented similarly and varied in spacing to profile the earth's conductivity with depth.

Many authors, most notably Wait (1970), have shown that specifying the surface impedance of the ground will produce the same theoretical results for propagation prediction as will specifying the entire resistivity substructure. Calculations based on this procedure are now possible with the mathematical developments of Ott and Berry (1970) and Ott (1971). Thus the surface impedance approach vastly simplifies propagation studies because only one easily measurable complex number need be associated with each surface point, rather than a set of subsurface resistivity values. However, one of our purposes was to map conductivity for future LF engineering (e.g. transmitter placement and power assignment) purposes. Therefore, it may seem redundant to have used a method that requires the existence of a transmitter in the first place.

To counter this objection, it must be realized that the approximately 1500 LF transmitters in present use probably do not cover even 20% of the United States. Therefore, if a sampling procedure is to be used, as it must for so large an area, it is far easier to measure surface impedance about these existing transmitters and to extrapolate the values to other areas of similar geology rather than to use a self-contained d.c. current or magnetic induction sounding system to determine the resistivity structure, then theoretically calculate the surface impedance at LF, and then extrapolate.

The obvious choice of conductivity mapping methods is then the radiohm method with instrumentation developed originally by Collett and Becker (1967). Their instrumentation was originally developed to monitor the VLF transmitters in regular use for military communications. Recently, however, this technique has been applied to frequencies in the 200-415 kHz radio navigation aid band, primarily for purposes of geologic exploration via ground conductivity mapping. As these instruments are capable of measuring both amplitude and phase, the total complex surface impedance boundary condition may be obtained.

More commonly, however, these surface impedance values are readily converted to equivalent effective conductivity values.

### C. Objectives

The objective of this research was twofold. The first objective was to use and evaluate new means of mapping ground conductivity values in the 200-415-kHz radio navigation aid band. Two approaches are covered. For large-scale extensive mapping, airborne measurements using the E-PHASE technique at VLF are discussed in Chapter III. This technique may be possible because in some regions of the United States the VLF airborne conductivity may well approximate the LF ground conductivity. For small-scale intensive mapping, ground measurements using the Radiohm system for monitoring local LF navigational aid transmitters are discussed in Chapter IV.

The second objective was to produce an estimated LF conductivity map of the United States. The 1500 or so LF transmitters in present use provide sufficient field strength to cover only about 20% of the country with a usable signal. Of all these transmitters, only about 20 were used, but in a variety of circumstances to allow geologic and physiographic correlations to be established. Some of the specific studies undertaken are presented in Chapter IV. Estimates of both LF ground conductivity and phase for the United States including Alaska are given in Chapter V.

We first begin with a discussion of the electromagnetic principles of ground wave propagation (Chapter II) because they are essential to an understanding of the techniques used and the results presented.

## II. PRINCIPLES OF ELECTROMAGNETIC CONDUCTIVITY MEASUREMENTS

### A. Theory of Radiowave Propagation in the Earth-Ionosphere Waveguide

Two different means of propagation at radio frequencies exist within the earth-ionosphere waveguide. They are usually referred to as the sky waves and the ground wave (often referred to as a surface wave). Sky waves are actually the sum of many modes of multiple reflections formed between the ionosphere and the earth and exist at all frequencies below about 50 MHz.

At AM broadcast frequencies and below, vertically polarized antennas are used which generate transverse magnetic (i.e. the magnetic field vector is orthogonal to the direction of propagation) radiation. The field vectors of both the ground and sky waves at the earth's surface are represented in Figure 4. E denotes the electric field components, H denotes the magnetic field component, and x,y,z refer to a local right-hand Cartesian coordinate system. The coordinate z is perpendicular to the earth's surface and x and y are tangential. The symbols  $\alpha$  and  $\psi$  refer to the incidence angles of the first order sky wave mode upon the ionosphere and earth respectively. As has been experimentally shown by Hollingworth (1926) and by Al'pert (1963), both modes do not

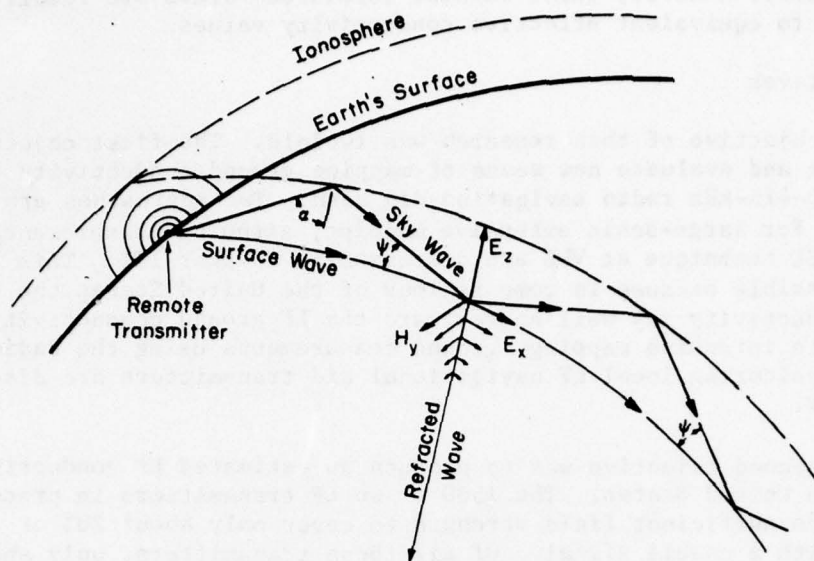


FIGURE 4. TWO RADIO WAVE PROPAGATION MODES IN THE EARTH-IONOSPHERE WAVEGUIDE (see text for explanation of symbols). The electromagnetic field components are characteristic of radiation from a vertical electric dipole.

necessarily combine in phase at the earth's surface. However, depending on distance from the transmitter, usually one or the other mode predominates.

The ground wave has less range than the sky wave but dominates in amplitude within a few tens of kilometers from, say, a 25-Watt transmitter at LF. Within a distance  $d$  such that

$$d \leq 80/f^{1/3} \text{ (km)} \quad \text{(Jordan and Balmain 1968)} \quad (1)$$

where  $f$  is in MHz, the ground wave field components at the surface of a homogeneous flat earth model may be expressed as

$$E_z = i60\beta Id\ell F \frac{e^{-i(\beta r - \omega t)}}{r} (1-u^2) \quad (2)$$

$$E_x = i60\beta Id\ell F \frac{e^{-i(\beta r - \omega t)}}{r} (u\sqrt{1-u^2}) \quad (3)$$

$$H_y = -i60\beta Id\ell F \frac{e^{-i(\beta r - \omega t)}}{r} \sqrt{\frac{\epsilon_0}{\mu_0}} (1-u^2) \quad (4)$$

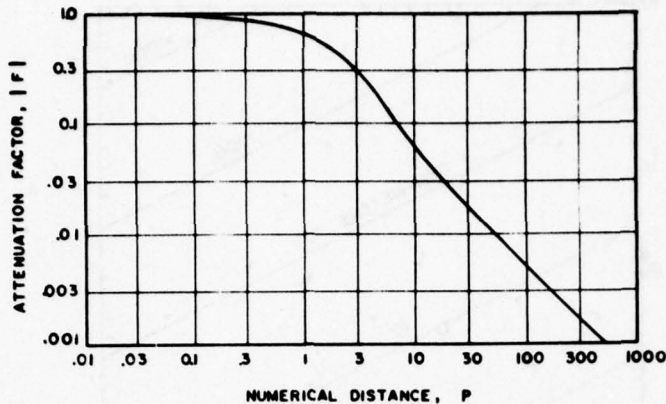


FIGURE 5. VARIATION OF THE ABSOLUTE VALUE OF THE SOMMERFELD ATTENUATION FUNCTION  $|F|$  WITH NUMERICAL INSTANCE  $P$  OVER HOMOGENEOUS GROUND. Displacement currents are considered negligible in comparison to conduction currents.

where  $\omega = 2\pi f$  in radians/second,  $t$  is time in seconds and  $r$  is distance in meters. The free space wave number is  $\beta$  and is determined by the formula  $\beta = \omega\sqrt{\mu_0\epsilon_0}$  where  $\epsilon_0 = 8.85 \times 10^{-12}$  Farad/m, and  $\mu_0 = 4\pi \times 10^{-7}$  Henry/m. The quantity  $Idl$  is the current moment of the transmitter, ( $dl$  is assumed to be much shorter than the free space wavelength),  $i$  is  $\sqrt{-1}$ ,  $\sigma$  is the conductivity in mhos/m, and  $u = \sqrt{1/(\kappa - i\sigma/\omega\epsilon_0)}$  where  $\kappa$  = relative permittivity.  $F$  is known as the Sommerfeld attenuation function which strongly depends upon earth conductivity. When displacement currents are small compared with conduction currents,  $u = \sqrt{\frac{i\omega\epsilon_0}{\sigma}}$  for homogeneous ground and the absolute value of  $F$  may be expressed as

$$|F| = 1 - i\sqrt{\pi p} e^{-P} \operatorname{erfc}(i\sqrt{p}) \quad (5)$$

where

$$p = \frac{\beta r \epsilon_0 \omega}{2\sigma}$$

The term  $\operatorname{erfc}$  refers to the complement of the error function  $\operatorname{erf}$  [see, for example, Abramowitz and Stegun (1967)] which equals  $(1 - \operatorname{erf})$ .  $F$  is usually plotted against  $p$ , the numerical distance, which is actually a normalized function of distance. The dependency of  $|F|$  on  $p$  is given in Figure 5.

The depth of penetration within homogeneous earth for the refracted ground and sky waves is measured by the skin depth  $\delta$  given by the formula

$$\delta = \sqrt{2\rho/\omega\mu_0} \quad (6)$$

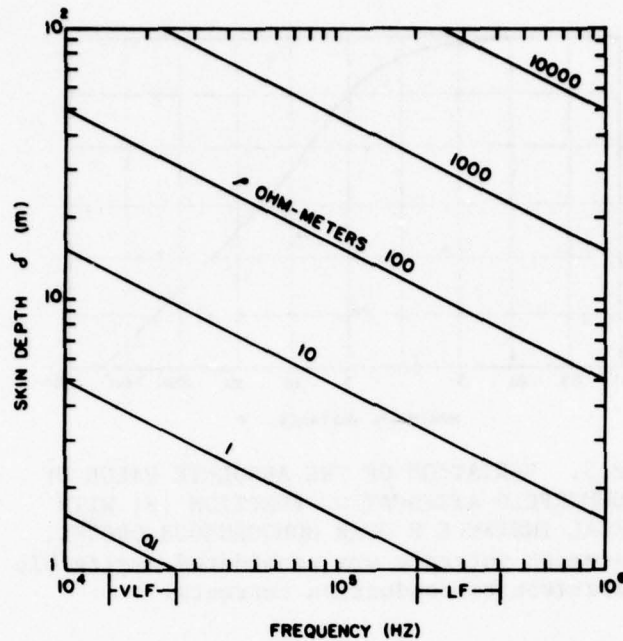


FIGURE 6. SKIN DEPTH  $\delta$  AS A FUNCTION OF FREQUENCY FOR A HOMOGENEOUS MODEL EARTH OF DIFFERENT VALUES OF RESISTIVITY  $\rho$ .

where  $\rho = 1/\sigma$  is the resistivity in ohm-m. The skin depth  $\delta$  is the depth at which the refracted field strengths will have attenuated to  $e^{-1}$  (37%) of their surface values. Values of  $\delta$  as a function of frequency for a homogeneous model earth of varying resistivity are given in Figure 6.

Sky waves have much greater coverage than the ground wave. They usually predominate in field strength beyond about 800 km for the powerful VLF transmitters in present use. At LF, however, the low power of existing transmitters rarely allows significant excitation of the sky waves. The sky wave modes may be approximated as several different plane waves undergoing various numbers of "hops" (reflections) from the earth and ionosphere. For an observer at the earth's surface, the first order mode (usually a single ionospheric skip) is dominant. For this mode the electromagnetic field components (using the coordinates of Figure 4) may be well approximated by

$$H_y = -H_0 e^{-i\beta x \sin\theta} (e^{i\beta z \cos\theta} + \text{Re } e^{-i\beta z \cos\theta}), \quad (7)$$

$$E_z = H_0 Z_0 \sin\theta e^{-i\beta x \sin\theta} (e^{i\beta z \cos\theta} + \text{Re } e^{-i\beta z \cos\theta}) \quad (8)$$

and

$$E_x = H_0 Z_0 \cos\theta e^{-i\beta x \sin\theta} (e^{i\beta z \cos\theta} - \text{Re } e^{-i\beta z \cos\theta}), \quad (9)$$

where  $Z_0 = \sqrt{\mu_0/\epsilon_0}$   
 $\theta = 90^\circ - \psi$

$H_0$  = incident magnetic field strength

and  $\beta = \omega\sqrt{\mu_0\epsilon_0}$ .

The time dependency of  $e^{i\omega t}$  is assumed. R is the reflection coefficient which depends on earth conductivity. For a homogeneous earth, R is expressed as

$$R = \frac{\cos\theta - \frac{\beta}{\beta_1} \sqrt{1 - \left(\frac{\beta}{\beta_1} \sin\theta\right)^2}}{\cos\theta + \frac{\beta}{\beta_1} \sqrt{1 - \left(\frac{\beta}{\beta_1} \sin\theta\right)^2}} \quad (10)$$

when the radiation is transverse magnetic. In this expression,

$$\beta_1 = \sqrt{-i\omega\mu_0\sigma}.$$

Again, the permittivity of the earth is considered to have negligible effect.

#### B. Surface Impedance and Wavetilt Methods of Measuring Conductivity

The wavetilt W method and the surface impedance  $Z_s$  method are actually different versions of the same thing, but each has its special area of application. W is defined as

$$W = \left. \frac{E_x}{E_z} \right|_{z=0} \quad (11)$$

and  $Z_s$  as

$$Z_s = \left. \frac{E_x}{H_y} \right|_{z=0} \quad (12)$$

where both quantities are evaluated at the earth's surface  $z = 0$ . This definition automatically applies to the ground wave, but for a sky wave the grazing angle of incidence  $\psi$  must be near zero degrees.

W and  $Z_s$  are complex quantities and, in general, may be expressed in terms of amplitude and phase as

$$W = |W|e^{i\phi_1}$$

and

$$Z_s = |Z_s|e^{i\phi_2}.$$

$\phi_1$  and  $\phi_2$  are not generally equal. However, for an earth model of vertically stratified, uniform homogeneous layers (the standard model for data comparison)  $\phi_1 = \phi_2$  and both will be referred to as  $\phi$ . In this case,

$$Z_s = \sqrt{\mu_o/\epsilon_o} W \quad (13)$$

so that  $Z_s$  and  $W$  convey the same information. Equation 13 and subsequent formulations apply to both ground and sky waves.

The surface impedance above a homogeneous model earth is well approximated for either ground or sky waves at frequencies below about 10 MHz by the formula

$$Z_s = Z_o/n \quad (14)$$

where  $n$  is the index of refraction and is expressed as

$$n = \sqrt{\kappa - \frac{i}{\omega\epsilon_o\rho}} \quad (15)$$

For most earth materials, dielectric effects can be neglected at frequencies below about 1 MHz. In this case

$$Z_s = \sqrt{\omega\mu_o\rho} e^{i45^\circ} \quad (16)$$

When the earth consists of uniform homogeneous layers, equation 13 still holds but the  $Z_s$  or  $W$  dependency upon  $\rho$  and layer depths becomes more complicated. Common practice is to define an apparent resistivity  $\rho_a$  from the homogeneous earth model and relate it to  $W$  or  $Z_s$  through the amplitude inversion of equations 13 and 16 as

$$\rho_a = \frac{|Z_s|^2}{\omega\mu_o} \quad (17)$$

or

$$\rho_a = \frac{|W|^2}{\omega\epsilon_o} \quad (18)$$

These formulas will give a good approximation to the actual resistivity if the earth is homogeneous to at least the skin depth  $\delta$ .

Where the earth's conductivity is layered, equation 17 must be modified to account for the various layer depths and layer resistivities. Wait (1970) presents a simple scheme for generating  $Z_s$  or  $W$  values above any number of plane, parallel layers. Wait (1970) and

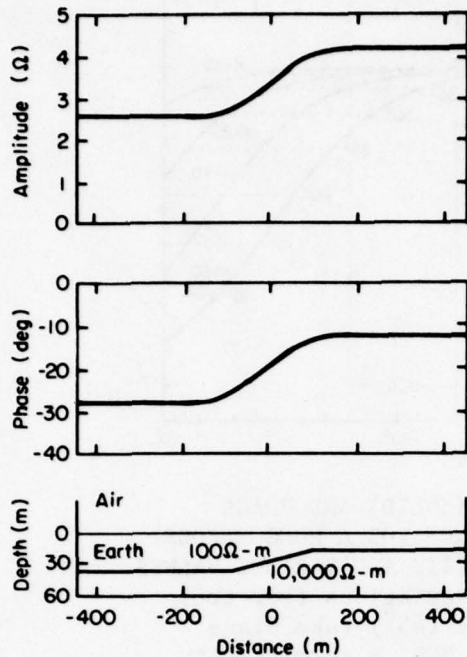


FIGURE 7. AMPLITUDE AND PHASE OF THE SURFACE IMPEDANCE AT 10 KHZ OVER A CHANGE IN STRATIFICATION (after Hughes and Wait 1975).

others (e.g. King 1968) have also shown that specifying a priori the plane wave surface impedance as a boundary condition along the air-earth boundary is equivalent to accounting for all the layer parameters for solving the propagation problem. Present theoretical practice (Ott 1971, Johler 1975) is to extend this idea by replacing all variations in earth conductivity and topography with an equivalent surface impedance when predicting the propagation of low frequency radiowaves. In support of this idea, Hughes and Wait (1975) have calculated surface impedance values above layers of varying depths (Figure 7). Their results show that the local surface impedance could correspond to the local layering very well, giving values equivalent to those for an infinite horizontal extension of the local vertical stratification.

### C. Dielectric Effects

It has been assumed so far that the effects of displacement currents are negligible compared to those of conduction currents. Mathematically, this is expressed using the two terms of the index of refraction  $n$  (equation 15) as

$$\left| \frac{i}{\omega \epsilon_0 \rho} \right| \gg \kappa . \quad (19)$$

Where this inequality does not hold, both apparent resistivity and phase as determined by the surface impedance will be misinterpreted.

Figures 8, 9 and 10 show apparent resistivity and phase as a function of frequency for a homogeneous model earth of various values of  $\rho$  and  $\kappa$ . The bands marked VLF, LF, and BCB cover those frequencies

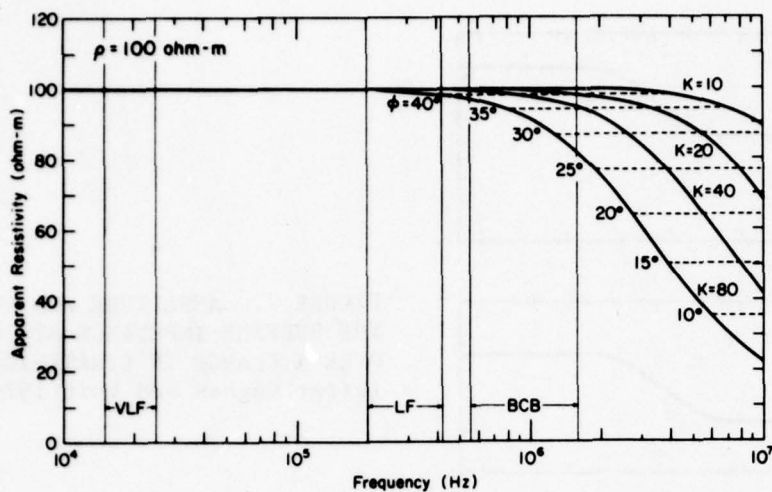


FIGURE 8. APPARENT RESISTIVITY (SOLID) AND PHASE (DASHED) AS A FUNCTION OF FREQUENCY FOR A HOMOGENEOUS MODEL EARTH OF 100 OHM-M RESISTIVITY AND VARIOUS VALUES OF PERMITTIVITY. Insignificant deviations from true resistivity (100 ohm-m) and phase ( $45^{\circ}$ ) take place in the VLF and LF bands. In the BCB, a permittivity  $\kappa = 80$  (water) will significantly lower both apparent resistivity and phase.

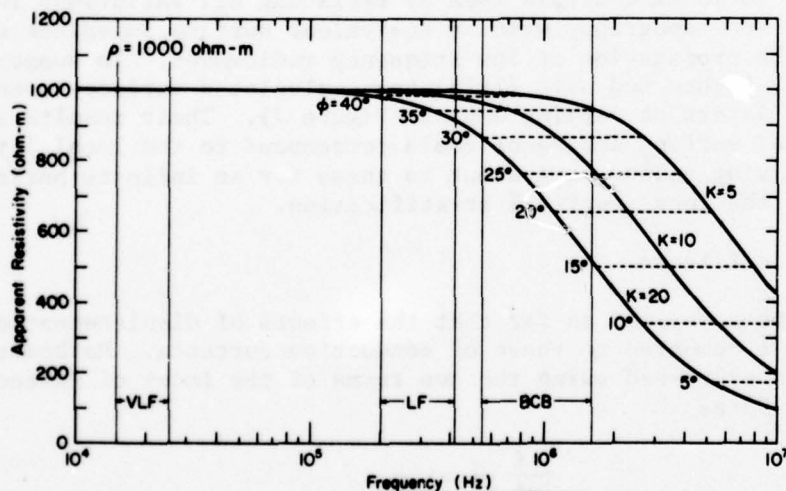


FIGURE 9. APPARENT RESISTIVITY (SOLID) AND PHASE (DASHED) AS A FUNCTION OF FREQUENCY FOR A HOMOGENEOUS MODEL EARTH OF 1000 OHM-M RESISTIVITY AND VARIOUS VALUES OF PERMITTIVITY. Significant changes occur only in the BCB for the range of permittivities expected at this value of resistivity.

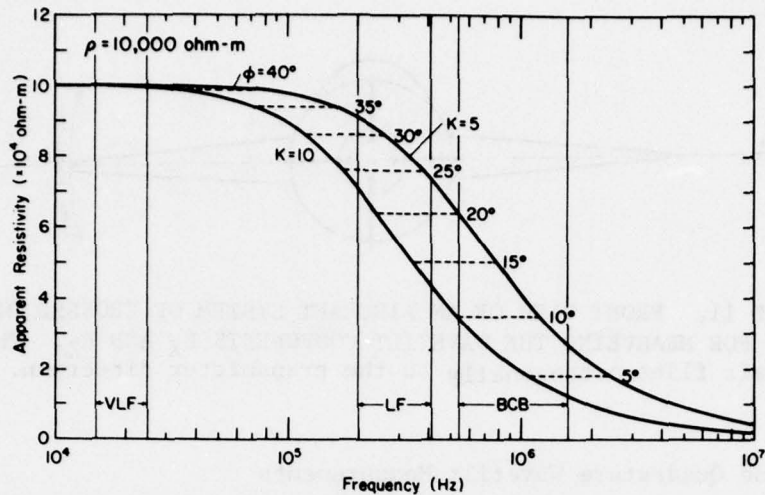


FIGURE 10. APPARENT RESISTIVITY (SOLID) AND PHASE (DASHED) AS A FUNCTION OF FREQUENCY FOR A HOMOGENEOUS MODEL EARTH OF 10,000 OHM-M RESISTIVITY AND TWO VALUES OF PERMITTIVITY. Significant changes occur in both the LF and BCB ranges for the range of permittivities expected at this value of resistivity.

where transmitters are presently operating. Figures 8 and 9 reveal that dielectric effects are insignificant in the LF and BCB ranges for the normal ranges of permittivity encountered at 1000 ohm-m or less (e.g. fresh water is usually at 100-300 ohm-m and  $\kappa=80$  while dry earth materials at about 1000 ohm-m usually have  $\kappa$  values of between 3 and 10). Figure 10 shows that, at resistivities of about 10,000 ohm-m or greater, dielectric properties significantly influence apparent resistivity and phase in the LF band and above. For example, at 300 kHz the value  $\kappa = 10$  (e.g. granite) depresses the actual resistivity to an apparent value of 5600 ohm-m and gives a phase value of about  $17^\circ$ . Values above or below  $45^\circ$  normally indicate resistivity gradients with depth (see Chapter III), but in this case the material is homogeneous.

### III. AIRBORNE APPROACH TO GROUND RESISTIVITY MAPPING

#### A. General

This chapter discusses the use of VLF signals to aid large-scale LF ground conductivity mapping of the contiguous 48 United States. The limited range of existing LF transmitters and the necessity for constant retuning to the numerous frequencies used would nullify any possible large scale use of the airborne techniques at LF. VLF transmitters, however, have ranges of thousands of kilometers. Therefore, if regions can be found where airborne measured partial apparent resistivity at VLF closely approximates the total apparent resistivity at LF, this large range may be extremely useful.

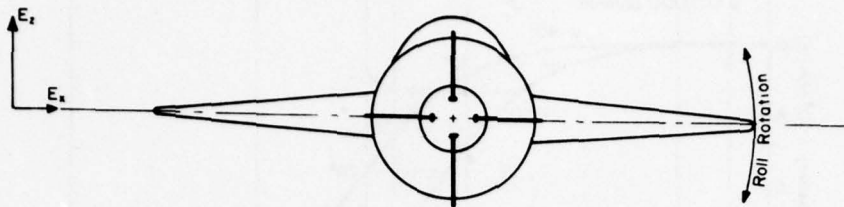


FIGURE 11. FRONT VIEW OF AN AIRCRAFT SYSTEM OF CROSSED DIPOLES FOR MEASURING THE WAVETILT COMPONENTS  $E_x$  AND  $E_z$ . The aircraft flies orthogonally to the transmitter direction.

### B. Airborne Quadrature Wavetilt Measurements

In Chapter I it was briefly mentioned that only the quadrature value of the complex wavetilt can be measured from an aircraft. Here, we will discuss this more thoroughly and show how this shortcoming may be used to advantage for LF conductivity mapping.

In the airborne system illustrated in Figure 11, horizontal and vertical electric dipole antennas are mounted on a nose cone extending from a Short Take Off and Landing (STOL) aircraft. The horizontal antenna is mounted orthogonally to the long axis of the nose cone. The aircraft must then fly perpendicularly to the transmitter direction for maximum coupling with  $E_x$ . This allows the more intense  $E_z$  to couple with the horizontal antenna when the aircraft rolls so that only the total  $E_z$  and the component of  $E_x$  in quadrature phase with  $E_z$  can be measured successfully to determine a wavetilt value  $W_q$ .

Expressing the wavetilt as a complex quantity,

$$W = |W| (\cos\phi + i\sin\phi) \quad (20)$$

where  $\phi$  is the phase angle and the parallel bars denote the absolute value of the wavetilt amplitude. The quadrature wavetilt value  $W_q$  is then

$$W_q = |W| \sin\phi. \quad (21)$$

Since  $W_q$  does not equal the actual  $W$  except when the phase angle is  $45^\circ$ , a phase angle must be arbitrarily assumed in trying to approximate the true value of  $W$ . An angle of  $45^\circ$  is the usual assumption. The formula for converting  $W_q$  at  $45^\circ$  to apparent resistivity, defined as  $\rho_q$  in this case, is then

$$\rho_q = \frac{2|W_q|^2}{\omega\epsilon_0} \quad (22)$$

which gives the correct value of resistivity only for a homogeneous earth.  $\rho_q$  is related to  $\rho_a$  by the formula

$$\rho_q = 2 \rho_a \sin^2 \phi . \quad (23)$$

When the earth is layered, the amplitude and phase of  $W$  change according to the resistivities and layer dimensions involved. For vertically stratified homogeneous layers, the phase varies between  $0^\circ$  and  $90^\circ$ . In general, the following rules apply:

- 1) Phase angles  $>45^\circ$  indicate that resistivity is decreasing with depth.
- 2) Phase angles  $<45^\circ$  indicate that resistivity is increasing with depth.

Since  $\rho_q$  biases the actual apparent resistivity  $\rho_a$  by the factor  $2\sin^2\phi$ ,  $\rho_q$  will always be more indicative of the surficial layers because, when rule 1 applies,  $2\sin^2\phi > 1$ , and when rule 2 applies,  $2\sin^2\phi < 1$ . This may then allow  $\rho_q$  at VLF to closely approximate  $\rho_a$  at LF since LF waves penetrate less deeply than VLF waves under any resistivity condition, as was shown by the skin depth formula (equation 6).

Figures 12 and 13 illustrate some specific comparisons between the variations with layer depth of  $\rho_q$  at 20 kHz (VLF) and those of  $\rho_a$  at 300 kHz (LF) for various two-layer earth models. Figure 12 is of prime importance because the models consider a less resistive second layer which is a common situation encountered in the contiguous 48 states in areas of no relief (the decrease in resistivity with depth is due to the increase of moisture content with depth). Although the values are not identical, there is a close proximity in value for many cases for first layer depths of less than 20 m.

#### C. Resolution Considerations

Presently, the airborne wavetilt method is used for small scale geophysical surveying wherein flight altitude is maintained between 75 and 150 m depending on the severity of the topography and flightline spacing between 100 and 400 m. At these altitudes, which are much less than a VLF wavelength (15 km at 20 kHz), an approximate measure of the resolution of the airborne antenna is arrived at from the directivity pattern of an electrically short dipole in the near field (quasi-static zone) which is the region within a wavelength's distance from the antenna. In this region the intercept of the -10 db field strength contour (relative to the ground point directly below the aircraft) with the ground is a circle of approximately 2 h diameter where h is the survey altitude. 2 h is then usually chosen for the flightline spacing.

#### D. Range and Altitude Considerations at VLF

Analysis in Watt (1967) shows that at VLF the total field at ground level is essentially equal to the ground wave field out to about

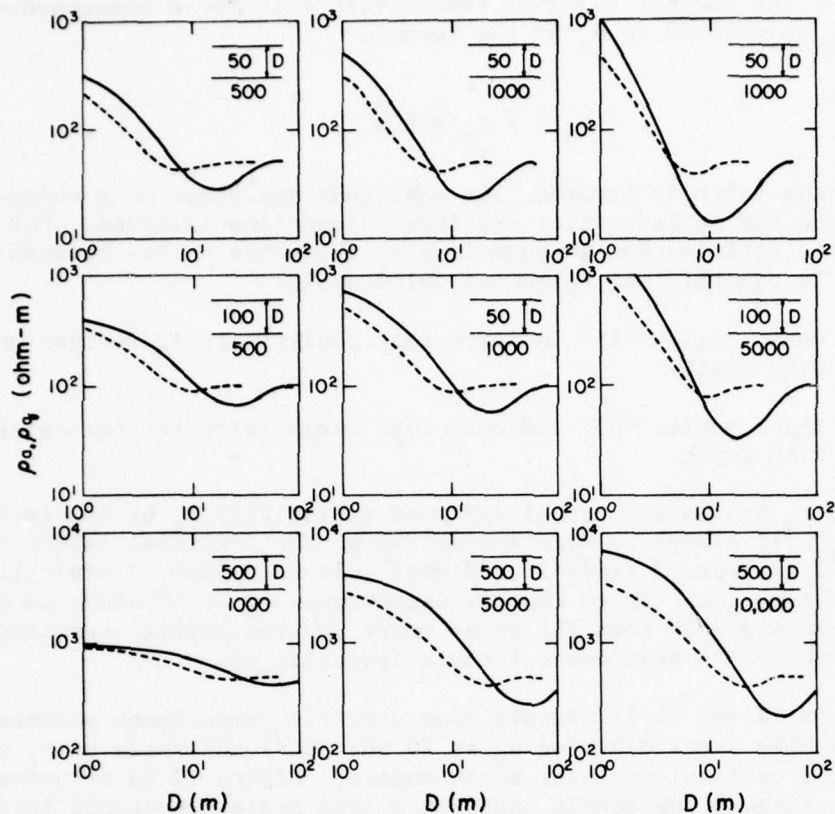


FIGURE 12. CURVES OF 2-LAYER EARTH APPARENT RESISTIVITY AS MEASURED AT 20 KHZ (SOLID) AND 300 KHZ (DASHED). The 20 kHz curves are of  $\rho_q$  and the 300 kHz curves are of  $\rho_a$ . A dielectric permittivity of 10 has been assumed for all layers. Layer resistivities are in ohm-m.

400 km. From 400 to 800 km the first hop sky wave makes an appreciable contribution and predominates beyond about 800 km. The grazing angle of incidence  $\psi$  for the first hop sky wave (see Figure 4), which must be near zero for this method to be of use, decreases with range from about  $27^\circ$  at 300 km to  $9^\circ$  at 1500 km.

Figure 14 shows the variation of  $\rho_q$  with altitude, parametric in  $\psi$ , for a homogeneous flat earth model. The curves show serious degradation of apparent resistivity at the larger values of  $\psi$  when the survey altitude is increased beyond 100 m. Beyond the 1500-km range where  $\psi < 9^\circ$ , survey altitude may be increased to as much as 1 km without serious degradation. Since 1 km is still a small fraction of a free space VLF wavelength, ground level would still be in the near field of the airborne antennas. The ground resolution at this altitude is approximately  $\pi h^2(\text{km}^2)$  or about  $3.1 \text{ km}^2$ .

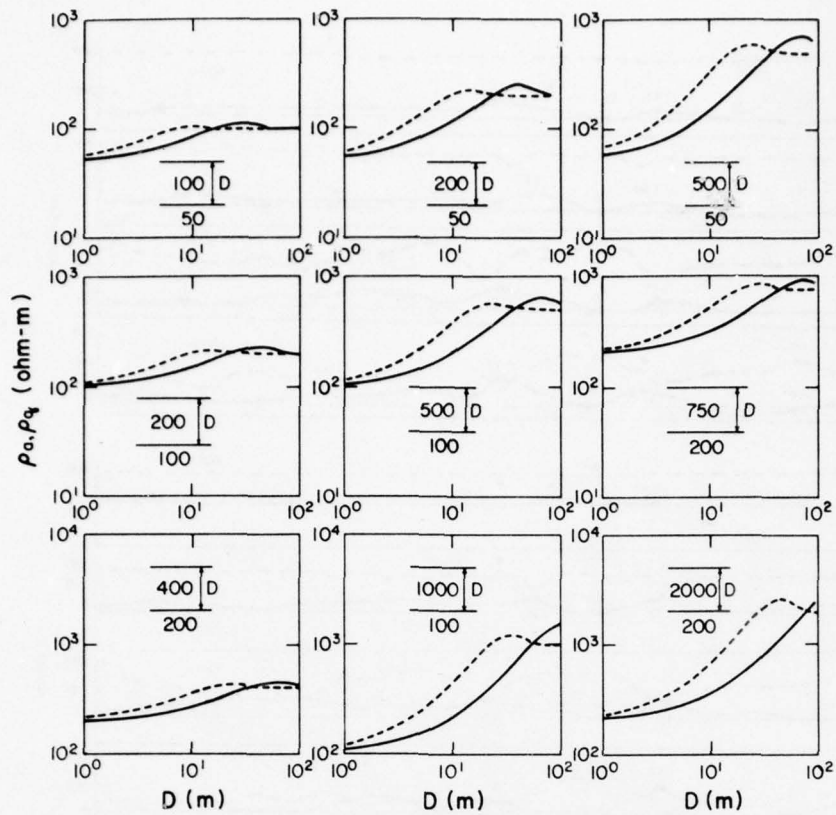


FIGURE 13. CURVES OF 2-LAYER EARTH APPARENT RESISTIVITY AS MEASURED AT 20 KHZ (SOLID) AND 300 KHZ (DASHED). The 20 kHz curves are of  $\rho_q$  and the 300 kHz curves are of  $\rho_a$ . A dielectric permittivity of 10 has been assumed for all layers. Layer resistivities are in ohm-m.

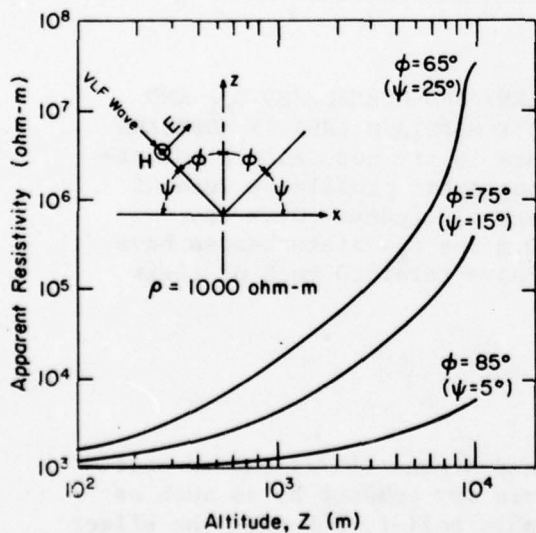


FIGURE 14. APPARENT RESISTIVITY AS A FUNCTION OF ALTITUDE ABOVE A MODEL HOMOGENEOUS EARTH OF  $\rho = 1000$  OHM-M. The apparent resistivity is determined by the airborne wavetilt method for a VLF sky wave at 20 kHz incident upon the earth at three different values of the grazing angle  $\psi$ .

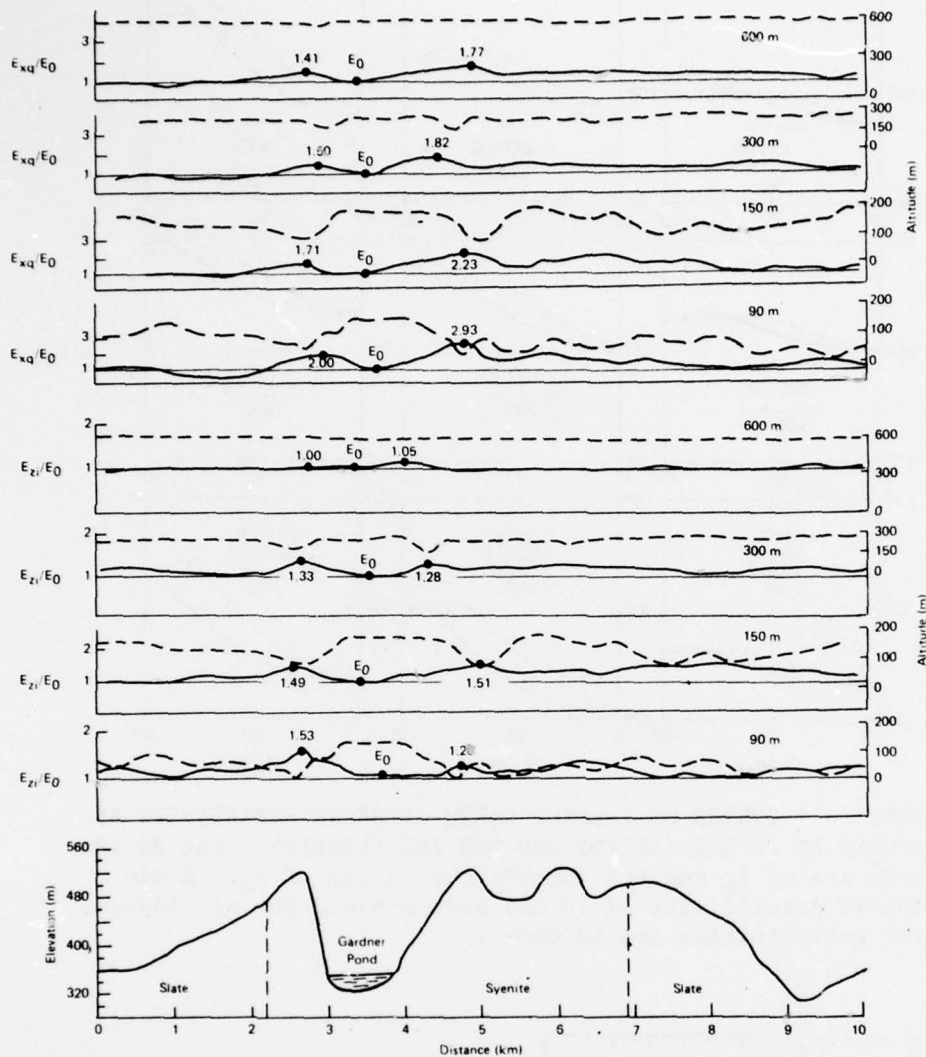


FIGURE 15. CALIBRATED ALTIMETRY (BROKEN) AND NORMALIZED  $E_{zi}$  AND  $E_{xq}$  (SOLID) PROFILES OVER THE DEBOUILLIE MOUNTAIN AREA IN NORTHERN MAINE. The profiles and those of Figure 16 are not exactly coincidental with each other or with the topographic profile because of changes in flight speed at the different altitudes. Over the ridges  $E_{zi}$  is always enhanced. At 600 m the  $E_{zi}$  disturbances have nearly disappeared while those of  $E_{xq}$  have retained much of their lower altitude strength.

#### E. Topographic Effects

The work of Harrison et al. (1971) and Arcone (1977) showed that the vertical electric field  $E_z$  of VLF waves may enhance by as much as 6 db immediately above prominent topographic relief, but that the effect becomes negligible at an altitude equal to approximately twice the height

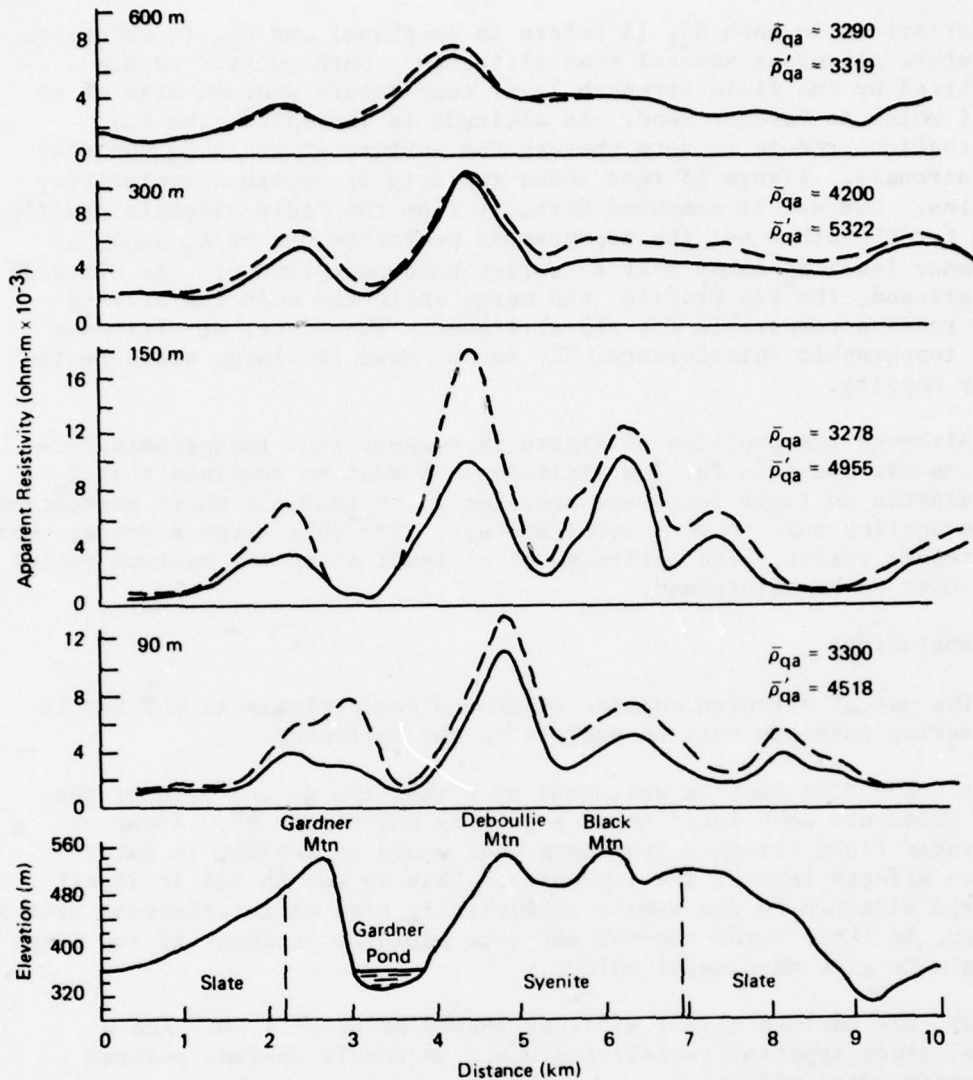


FIGURE 16. APPARENT RESISTIVITY PROFILES COMPUTED FROM THE VALUES OF  $E_{xq}$  AND  $E_{z1}$  OF FIGURE 15. At 600 m the perturbations have decreased but the mean is still comparable to those of the lower altitudes. The solid lines are computed directly from  $E_{z1}$  and  $E_{xq}$  of Figure 15 while the broken lines use the constant values of  $E_0$  for  $E_{z1}$ , thus topographically correcting the solid profiles. Mean values (the prime quantity refers to the broken curve) are given at the right of the profiles.

of the relief (all quantities measured from sea level). Arcone's work also showed that this effect does not happen to the component of  $E_x$  in quadrature phase with  $E_z$ , allowing airborne VLF resistivity values to be modified for topographic effects by modifying only  $E_z$ .

Some of Arcone's profiles of VLF field strengths and apparent resistivity at various altitudes above a small mountain range in northern Maine are presented in Figures 15 and 16. Figure 15 shows

the variations in both  $E_{zi}$  (i refers to in-phase) and  $E_{xq}$  (q refers to quadrature phase) at several mean altitudes. Both quantities are normalized by the field strength level that occurs over an area of no relief which is Gardner Pond. As altitude is increased, the  $E_{zi}$  perturbations reduce to zero whereas the perturbations in  $E_{xq}$  persist more strongly. Figure 16 then shows two sets of apparent resistivity profiles. One set is computed directly from the field strength profiles, while for the other set the topographic perturbations of  $E_z$  about a reference level  $E_0$  taken over no relief have been removed. As altitude is increased, the two profile sets merge while the mean resistivity level remains comparable for all altitudes. Therefore, at altitudes above topographic interference, VLF can be used for large scale resistivity mapping.

Although the profiles of Figure 16 suggest that topographic corrections are possible for low altitudes, it must be realized that  $E_z$  also depends on range (e.g. see equation 2) so that the above correction scheme applies only to very local surveys. For very large surveys, over topographic relief, high altitudes of at least twice the maximum relief would have to be maintained.

#### F. Conclusions

The use of airborne mapping of ground conductivity at VLF for LF engineering purposes must be subject to the following:

- 1) The area must be dominated by either the ground wave or the first order sky wave incident at a grazing angle near  $0^\circ$ . Areas of comparable field strength from each mode would be subject to interference effects between the two modes. This is not so bad in itself if field strength levels remain sufficiently high at interference minima. However, in these areas the VLF sky mode would be incident at too large an angle to give meaningful values.

- 2) The maximum flight altitude should be about 1 km. Above this altitude apparent resistivity would seriously degrade because of standing wave effects.

- 3) At 1 km flight altitude, severe physiographic relief must be no more than about 500 m.

- 4) Survey areas should be those where conductivity does not change radically with depth so that  $\rho_q$  at VLF will approximate  $\rho_a$  at LF.

Figure 17 is a map of the United States in which the shaded area reasonably meets these requirements using station NAA in Cutler, Maine. At 1 km altitude the optimum flight line spacing would then be about 2 km and flight lines would be oriented in parallel, concentric, circular arcs around station NAA.

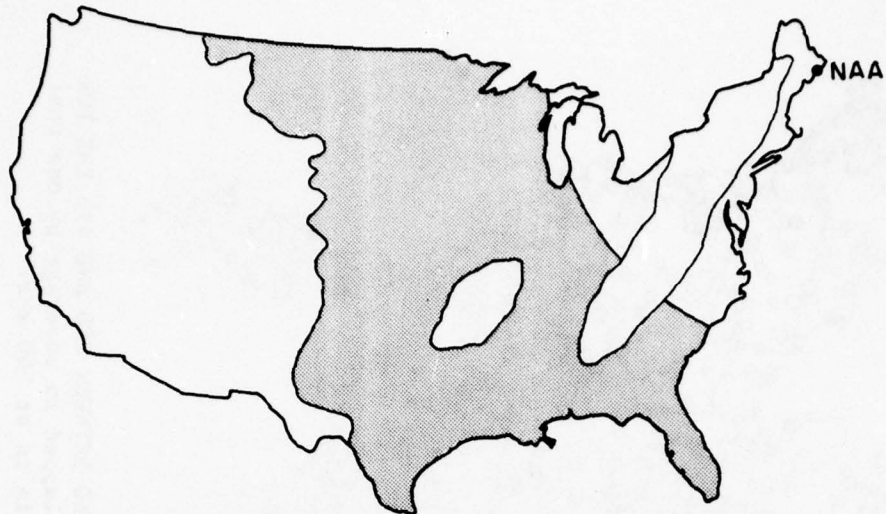


FIGURE 17. APPROXIMATE AREA WHERE VLF STATION NAA (CUTLER, MAINE) CAN BE MONITORED FOR MEASURING APPARENT RESISTIVITY THAT WOULD WELL APPROXIMATE VALUES THAT WOULD BE DETERMINED IN THE 200 TO 415 KHZ BAND.

#### IV. INTENSIVE APPROACH TO GROUND RESISTIVITY SURVEYING

##### A. General

This chapter discusses local resistivity surveying using the surface impedance method at LF. The first two sections discuss transmitters and the equipment used for measuring surface impedance. The third section discusses three studies of ground resistivity surveying, each performed in a different geologic and physiographic setting. The data compilations in these studies are the same as those of about 20 other studies undertaken for this and other investigations over the past few years and used in Chapter V. The three studies of this chapter, however, are presented because each study contains two or more areas mapped by Fine (1954) as different in conductivity, thus giving a few examples where multiple comparisons can be made between BCB and LF measurements.

##### B. LF Transmitters

The typical LF transmitter in the United States is a Non-Directional Beacon (NDB) that is a vertically polarized monopole radiating from 25 to 50 Watts at a frequency between 200 and 415 kHz. There are about 1500 transmitters operating in the 50 states. A small percentage of these operate at greater power levels, typically 100, 200 or 400 Watts.

The coverage for most of these beacons in the contiguous 48 states is shown in Figure 18 where the circles represent the approximate limits to the use of our instrumentation. Within these ranges ground level

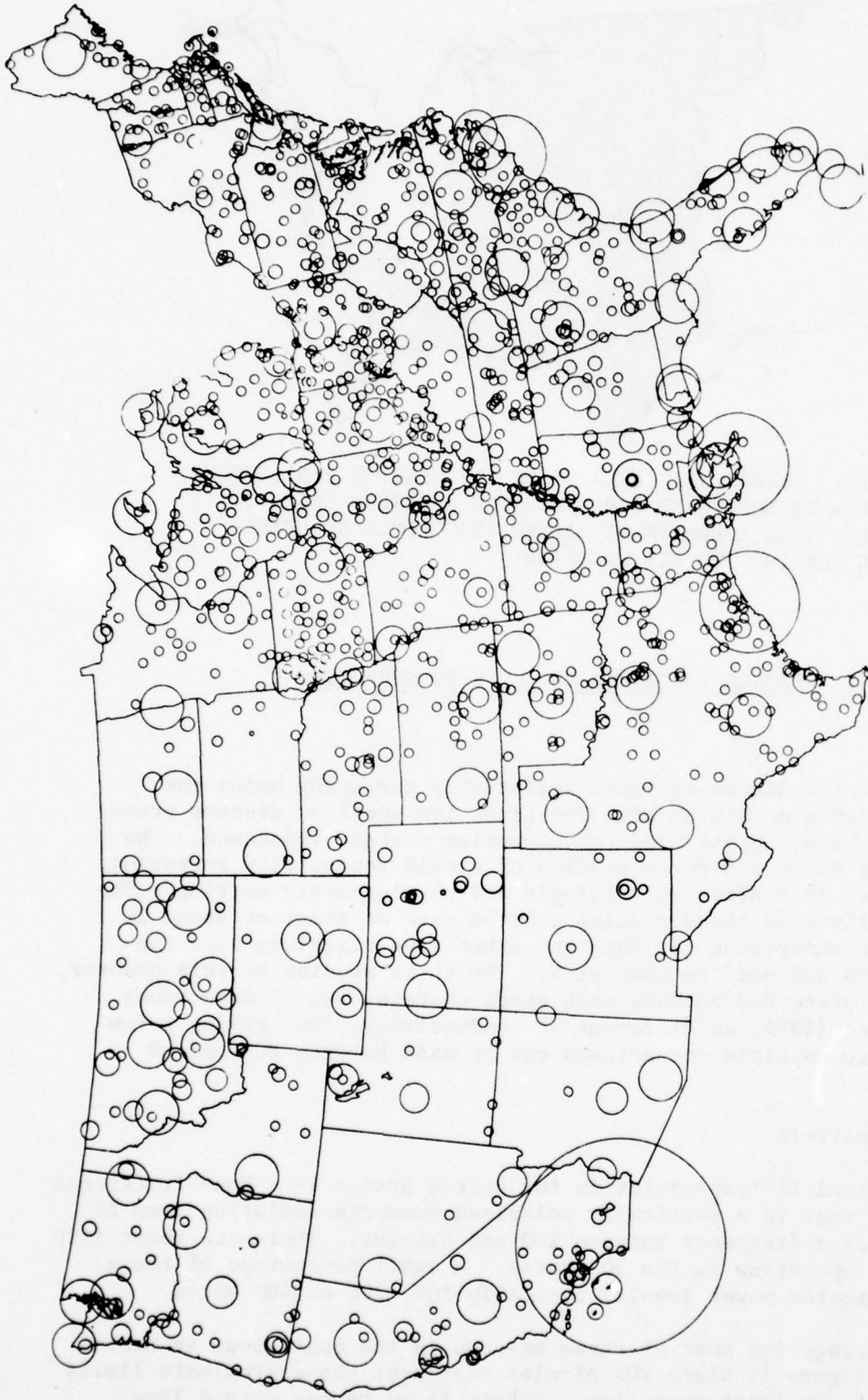


FIGURE 18. ESTIMATED USEFUL RANGE OF MOST OF THE TRANSMITTERS OPERATING BETWEEN 200 AND 415 KHZ FOR LF CONDUCTIVITY MAPPING. Many transmitters are not shown but are overlapped in coverage by one that is shown. The large coverage of one beacon shown in southern California is at 500 khz.

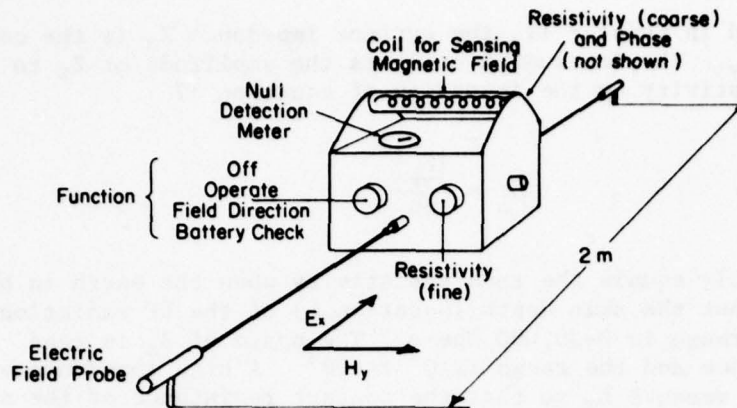


FIGURE 19. THE GEONICS EM-32, WHICH MEASURES THE COMPLEX SURFACE IMPEDANCE OF RADIO GROUNDWAVES BETWEEN 200 AND 415 KHZ. The instrument is shown in its proper measurement orientation with respect to the field vectors  $E_x$  and  $H_y$ .

field strength is determined by the ground wave. The ranges were determined by the accuracy of resistivity observations using 25-, 50- and 200-Watt beacons situated in areas where ground resistivity was typically 100 ohm-m or less. However, these ranges are approximately true for ground of higher resistivity also, because the increase in strength of  $E_x$  (compare equations 2 and 3) with resistivity can compensate for the greater attenuation experienced during propagation.

The map of Figure 18 shows that the range of many 25-Watt beacons is also covered by beacons mostly between the 200 and 400-Watt level, with two as high as 2 kW in Galveston, Texas and Grand Isle, Louisiana. The overlapping coverages are usually of different frequencies. Alaska (not shown) has the greatest number of transmitters with 125. Montana, Iowa, North and South Carolina, Indiana, Ohio and Massachusetts are the only states with as much as 40-50 percent of their areas covered by usable signal strength.

### C. Instrumentation

The instrument used for measuring the complex surface impedance at LF was designed and manufactured by Geonics Ltd. of Mississauga, Ontario, and is known as the EM-32. The operation of the EM-32 instrument is described in Appendix B. The instrument is represented in Figure 19, where it is shown in its proper measurement orientation with respect to the field vectors  $E_x$  and  $H_y$ . The earth tangential  $E_x$  is determined between the two earth probes which are spaced 2 m apart. The earth tangential  $H_y$  is measured with a ferrite-loaded coil located in the instrument handle. The device must be pretuned to any frequency between 200 and 415 kHz.

As discussed in Chapter II, the surface impedance  $Z_s$  is the complex ratio of  $E_x$  to  $H_y$ . The instrument converts the amplitude of  $Z_s$  to ohm-m of apparent resistivity by the inversion of equation 17

$$\rho_a = \frac{|Z_s|^2}{\omega\mu_0} \quad (17)$$

which approximately equals the true resistivity when the earth is homogeneous to at least the skin depth (equation 6) of the LF radiation. The calibration range is 0-30,000 ohm-m. The phase of  $Z_s$  is read directly in degrees and the range is  $0^\circ$  to  $90^\circ$ . A high impedance voltmeter is used to measure  $E_x$  so that the contact resistance of the probes poses no problem.

Both apparent resistivity and phase are obtained by tuning for a single, inaudible null. Therefore, the accuracy of the readings depends on the signal to noise ratio which is mainly determined by transmitter range and power for the ground wave, and by the value of ground resistivity itself because as resistivity decreases so does the amplitude of  $E_x$ . Reading accuracy has been estimated at about  $\pm 5\%$  for apparent resistivity and  $\pm 1\%$  for phase within two or three miles from a 25-Watt beacon. By about 11-16 km phase and amplitude accuracy falls to about  $\pm 10\%$ . These figures are estimates of the width of the inaudible null.

#### D. Comparative Studies

The following studies are three of several that were made at selected areas in the United States for the purpose of compiling a map of United States ground conductivity between 200 and 415 kHz (Chapter V). These studies in particular, however, were made in specific areas where the previous conductivity mapping at BCB (Figure 1) had indicated transitions between two or three different conductivity classes. The studies thus allowed many comparisons to be made between the old and the new mapping.

The areas discussed cover a broad range of geologic and physiographic conditions. We attempted to cover all physiographic situations present within a particular study, such as open fields, mountainsides and ridges. The first study, in the Williamstown, Vermont area, is a mountainous region of thin soil over metamorphic and granitic bedrock. The second study, in the Lake Champlain area, is primarily sedimentary bedrock, both folded and non-folded. The third study, along the Michigan-Indiana border, is a region of deep glacial deposits.

Each study consisted of 55 to 70 measurement stations. At each measurement station, five to eight readings of resistivity and phase were made and then averaged to give a reading for that particular station. The resistivity data are presented in terms of averages and statistical distributions because of the large variation in the readings. The phase data were much less variable and so averages and standard deviations are mainly presented.

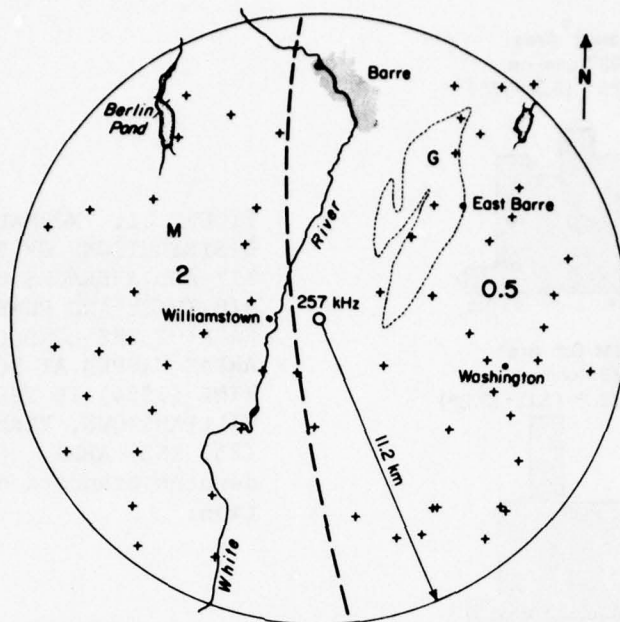


FIGURE 20. WILLIAMSTOWN, VERMONT, STUDY SHOWING TRANSMITTER LOCATION (CIRCLE), MEASUREMENT STATIONS (+), MAJOR GEOLOGIC BOUNDARIES (M - METAMORPHIC SCHISTS AND SLATES, G - GRANITE) AND BCB RESISTIVITY BOUNDARIES OF FINE (1954).

#### Williamstown, Vermont

Figure 20 presents a simplified map of the Williamstown area located in central Vermont. The entire area is mountainous with elevations ranging between about 270 and 730 m. The bedrock geology is mainly metamorphic\* grades of slate and schist (Doll 1961), but also includes the granite stock where the Barre quarries are located. The surficial geology (Flint et al. 1959) is a glacial till of probably no more than 1 to 2-m depth on hillsides but probably more than 10 m deep in level pastures.

Figure 20 also shows the location of the transmitter which is a 25-Watt NDB operating at 257 kHz. The crosses indicate where measurement stations were located. The heavy dotted line divides the area into two BCB conductivity sections mapped by Fine (1954). The BCB Class 2 area represents resistivity values from 354 to 707 ohm-m and the BCB Class 0.5 area represents values from 1414 to 2829 ohm-m. Sixty-seven stations were established.

Figure 21 gives statistical comparisons between the BCB Class 2 and BCB Class 0.5 areas for the resistivity and phase readings. The

\*See glossary for definitions of geologic terms used.

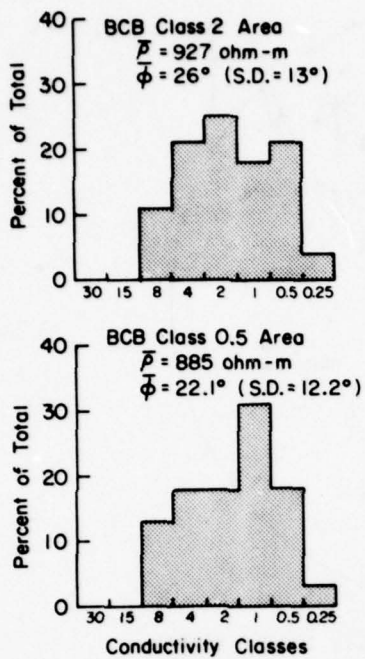


FIGURE 21. NORMALIZED DISTRIBUTIONS OF RESISTIVITY AND AVERAGES OF RESISTIVITY AND PHASE FOR EACH OF THE CONDUCTIVITY AREAS MAPPED AT BCB BY FINE (1954) IN THE WILLIAMSTOWN, VERMONT (257 KHZ) AREA. S.D. denotes standard deviation.

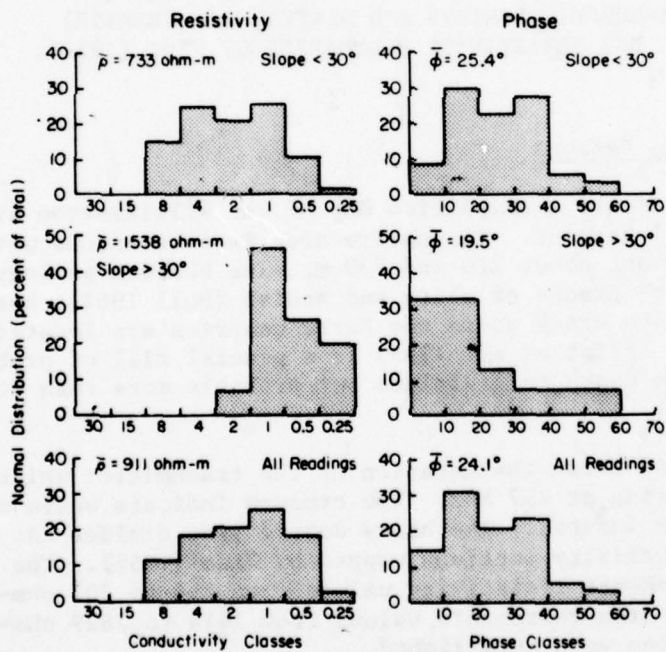


FIGURE 22. NORMALIZED DISTRIBUTIONS OF RESISTIVITY AND PHASE ACCORDING TO SLOPE OF THE TOPOGRAPHIC RELIEF IN THE WILLIAMSTOWN, VERMONT, AREA.

statistics show that at LF both are nearly identical. They both have similar means in the Class 1 range for resistivity, the mean phase and standard deviation for phase are similar, and there is a similar spread of resistivity values from Class 8 to Class 0.25. The average phase readings of  $22.1^\circ$  and  $26^\circ$  indicate that resistivity is increasing with depth from the surface so that, at BCB, the entire area is most probably a resistivity Class 2 with no transition. For example, a two-layer model of 125 ohm-m material of 1.4-m thickness above 2500 ohm-m material will give Class 2 readings between 550 and 1200 kHz, while at 257 kHz the model will give 922 ohm-m at  $24.6^\circ$ , which is similar to the data\*. The study of Kirby et al. (1954), upon which the map of Fine (1954) was based, shows that the nearest BCB transmitter used is located 56 km northeast of Williamstown and that the nearest BCB measurement was made 16 km from Williamstown. Therefore, Fine's mapping for this area is an extrapolation.

A topographic analysis of these readings is given in Figure 22. The top set of graphs is for areas where the slope of the relief was less than  $30^\circ$ , while the middle set is for areas where the slope of the relief was greater than  $30^\circ$ . For slopes greater than  $30^\circ$ , the till cover was always marginal and the average of the resistivity readings falls within Class 0.5. For slopes less than  $30^\circ$ , the average resistivity is barely within Class 1. The phases are still comparable for both cases. This analysis demonstrates that relief widens the dispersion of resistivity values through its effect on sediment cover and drainage. For this area, it causes the LF average resistivity to fall within the Class 1 designation.

The readings taken over the granite section where bedrock was exposed were not exceptionally high, ranging individually (within each station) from 400 to 2700 ohm-m. However, other studies over more extensive granite areas near Hanover, New Hampshire, revealed much higher values in the 0.5 range.

#### Champlain Valley of Vermont and New York

Figure 23 presents a simplified map of the survey area situated in the Lake Champlain Valley of western Vermont and upper New York State. The New York shores and the islands of Lake Champlain are fairly flat. The western end of the survey area becomes hilly while the eastern end is the rugged terrain of the Vermont Green Mountains. The flat areas have only a marginal marine or lacustrine sediment overlying limestone, dolostone, shale, argillite, and sandstone bedrock (Denny 1967, 1970). The New York uplands are of similar bedrock geology only with a heavy cover of coarse glacial till. The mountainous area of Vermont is primarily metamorphic schists and quartzites.

A 200-Watt NDB in Burlington, Vermont, radiates at 323 kHz. The strength of this signal allowed a sector of 56 km radius to be covered. This sector presently contains a dividing line between a BCB Class 4

---

\*These and subsequent models are probably some of several that may approximate the data.

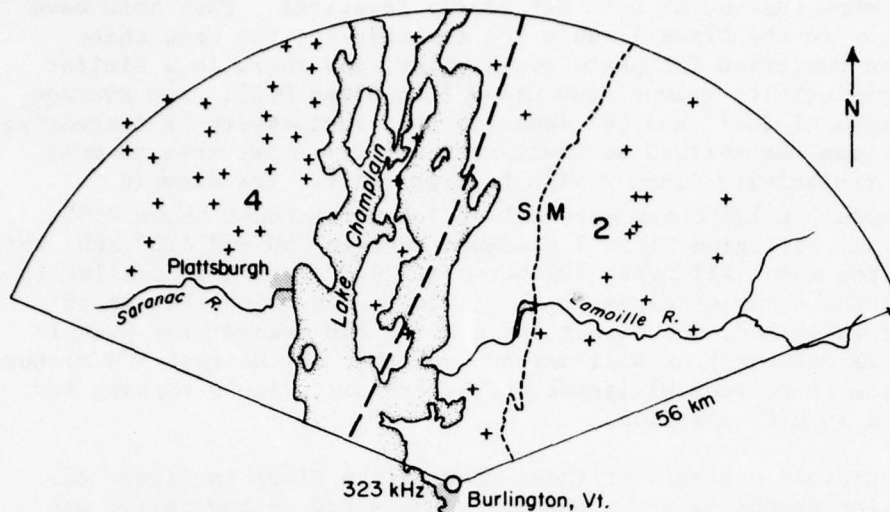


FIGURE 23. LAKE CHAMPLAIN VALLEY STUDY SHOWING TRANSMITTER LOCATION (CIRCLE), MEASUREMENT STATIONS (+), MAJOR GEOLOGIC BOUNDARIES (M - METAMORPHIC SCHISTS AND QUARTZITES, S - SEDIMENTARY ROCKS) AND BCB RESISTIVITY BOUNDARIES OF FINE (1954).

and a BCB Class 2 area. Lake Champlain is a BCB and LF Class 8 area but is not of concern as the other areas continue extensively into New York and Vermont. Fifty-five stations were established.

Figure 24 gives statistical comparisons between the BCB Class 4 and 2 areas for the resistivity and phase readings. The mean resistivity of the BCB Class 4 area falls slightly above the Class 4 range (177-354 ohm-m) at 398 ohm-m. The average phase is just slightly above  $45^\circ$ , so that, on the average, earth resistivity is probably fairly uniform over the depth of LF radiowave penetration. For the BCB Class 2 (354-707 ohm-m) area which is a different part of the BCB Class 2 area of the Williamstown study, the mean resistivity is 944 ohm-m and the LF resistivity values are in the Class 1 range just as they were in Williamstown. The marginal till cover in the mountainous regions and the metamorphic rocks again combine to produce these higher resistivities. The average phase of  $36.3^\circ$  indicates that the BCB mapping at Class 2 is probably correct, just as it did for the Williamstown study. The study of Kirby et al. (1954) used one transmitter in Burlington, Vermont, and one in Plattsburgh, New York. The BCB transition from Class 4 to Class 2 in Fine's mapping compares well with our transition from 2 to 1. The actual difference between BCB and LF resistivity may be only marginal considering the range of each resistivity class.

A geologic analysis of the resistivity and phase readings is shown in Figure 25. The most resistive category is the two-layer structure of till of usually less than 1 m thickness, over the metamorphic schists and quartzites. The least resistive category is the two-layer structure of marine and lacustrine sediments of usually less than 1-m thickness over the sedimentary bedrock types referred to above. On the New York shores of Lake Champlain, the fine-grained sediment is only of marginal

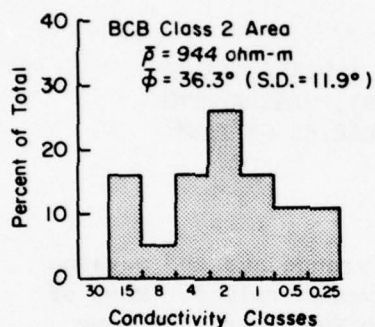
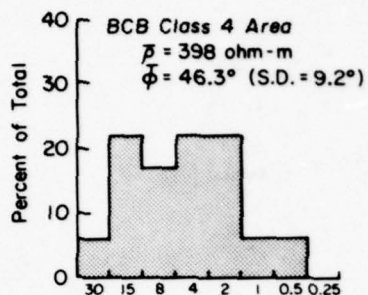


FIGURE 24. NORMALIZED DISTRIBUTIONS OF RESISTIVITY AND AVERAGES OF RESISTIVITY AND PHASE FOR EACH OF THE CONDUCTIVITY AREAS MAPPED AT BCB BY FINE (1954) IN THE BURLINGTON, VERMONT (323 KHZ), AREA.

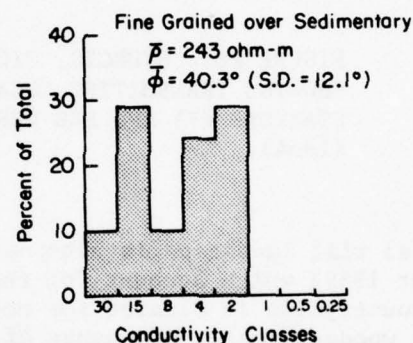
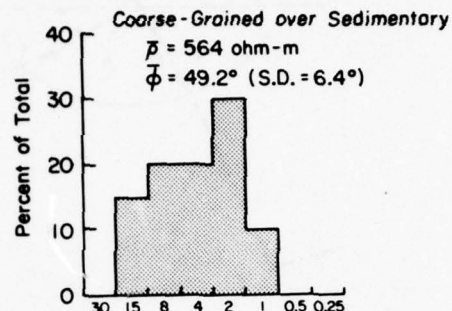
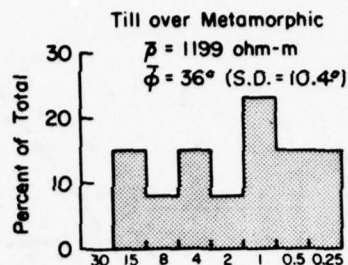


FIGURE 25. NORMALIZED DISTRIBUTIONS OF RESISTIVITY AND AVERAGES OF RESISTIVITY AND PHASE FOR DIFFERENT GEOLOGICAL SITUATIONS OCCURRING IN THE CHAMPLAIN VALLEY AREA.

thickness due to prehistoric wave action. The coarse-grained ground moraines, alluvium, sands and gravels which overlie sedimentary bedrock and have thicknesses of several meters or more have intermediate values. In the New York uplands section, the depth of the coarse-grained glacial deposits is extensive and great enough to obscure the nature of the bedrock (Denny 1967).

Sturgis, Michigan- Angola, Indiana

Figure 26 presents a simplified map of this study area which is located about the Michigan-Indiana border. The area consists of a deep

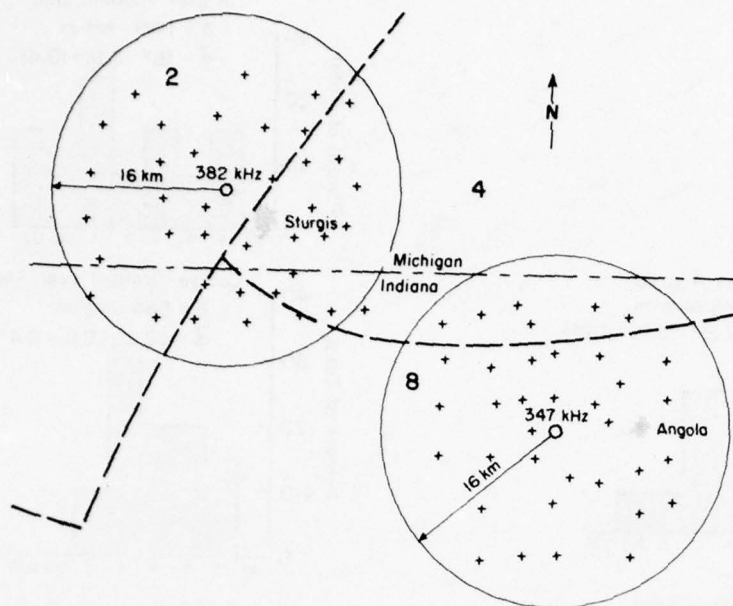


FIGURE 26. STURGIS, MICHIGAN-ANGOLA, INDIANA, STUDY SHOWING TRANSMITTER LOCATIONS (CIRCLES), MEASUREMENT STATIONS (+) AND BCB RESISTIVITY BOUNDARIES OF FINE (1954).

glacial till landscape in alternating bands of ground and end moraine (Flint 1959) which account for the minor topographic relief. Most of the countryside is cleared for corn or soy beans but there are some small wooded areas. Outwashes of sand and gravel are also present.

The signal strengths from two 25-Watt NDB's situated near Sturgis, Michigan (382 kHz), and Angola, Indiana (347 kHz), were sufficient to allow areas of approximately 16-km radius to be surveyed as shown in Figure 26. The total area surveyed contains an intersection of three different BCB conductivity classes as mapped by Fine et al. (1954). A total of 74 stations were established with 19 in the BCB Class 4 area, 34 in the BCB Class 8 area and 21 in the BCB Class 2 area.

Figure 27 shows a statistical summary of the LF results from all three BCB areas. The mean apparent resistivity of each area falls within the Class 4 range, but with a wide dispersion of values, probably due to the large dispersion in sediment grain size associated with glacial till. In the BCB Class 4 area, the LF averages of 224 ohm-m and  $56.5^\circ$  imply that, at BCB, Class 4 is probably correct. For example, a two-layer model of 500 ohm-m material of 4-m thickness above 125 ohm-m material will give Class 4 readings up to 1500 kHz, while at 365 kHz (midway between 347 and 382 kHz) the model will give 227 ohm-m at  $55.3^\circ$ , which is similar to the data. In the BCB Class 2 area, the LF averages of 288 ohm-m and  $64.3^\circ$  imply that, at BCB, Class 2 is probably correct. For example, a two-layer model of 2000-ohm-m material of 5.5-m thickness

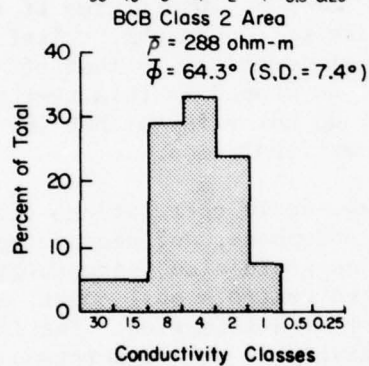
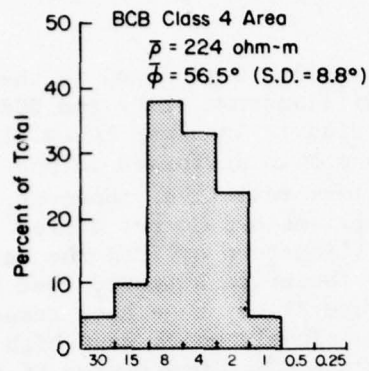
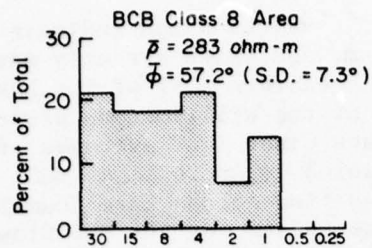


FIGURE 27. NORMALIZED DISTRIBUTIONS OF RESISTIVITY AND AVERAGES OF RESISTIVITY AND PHASE FOR EACH OF THE CONDUCTIVITY AREAS MAPPED AT BCB BY FINE (1954) IN THE STURGIS, MICHIGAN (382 KHZ)-ANGOLA, INDIANA (347 KHZ), AREA.

above 90-ohm-m material will give Class 2 readings between 600 and 1450 kHz, while at 365 kHz the model will give 289 ohm-m at 64.7°, which is similar to the data. The only LF results that differ significantly from the BCB mapping are those for the BCB Class 8 area. Here the LF apparent resistivity and phase imply that, at BCB, apparent resistivity should be near the upper resistivity limit of Class 4 or within Class 2. The study of Kirby et al. (1954) shows that the nearest BCB transmitters monitored were located more than 48 km north of Sturgis and that the nearest field strength measurements were made just at the northern perimeter of the study area. Therefore, for this area, Fine's mapping is an extrapolation.

#### Summary and Conclusions for the Comparative Studies

There were several areas surveyed where the BCB mapping of Fine et al. (1954) agreed with the implications of the LF data but not with the data themselves. The western half of the Lake Champlain study

area gave LF averages of 398 ohm-m at  $46.3^\circ$ , values which indicate average homogeneity of about the upper 18 m, and which are only marginally above the BCB Class 4 mapping. The eastern half of the Lake Champlain study area and the western half of the Williamstown study area, both mapped as BCB Class 2 areas, gave Class 1 LF averages of 944 ohm-m at  $36.3^\circ$  and 927 ohm-m at  $26^\circ$ , which imply that, at BCB, Class 2 is probably correct as is the transition across Lake Champlain. In the Sturgis-Angola study, the LF average phases for the BCB Class 4 and Class 2 areas also indicated that the BCB mapping is correct for BCB propagation.

Disagreements between the BCB and LF results were found in the BCB mapped Class 0.5 eastern area of the Williamstown study and BCB mapped Class 8 area of the Sturgis-Angola study. In these cases, it is recognized that the LF measurements may have been performed in one particular area that was slightly more or less resistive. However, the geology and physiography to the east of Williamstown do not differ significantly from those to the west of Williamstown or from the eastern part of the Lake Champlain studies. It is therefore believed that topographic influences (as demonstrated in Figure 2) may have been responsible for the severe attenuation of the BCB signals which gave high BCB resistivities in northeastern Vermont. In the BCB Class 8 area of the Sturgis-Angola study, there is no possibility of topographic relief affecting any results. The geology is almost identical to that of the neighboring areas. Therefore, the transitions mapped in this region due to the existence of the Class 8 area either do not exist at BCB (or LF) or have been misplaced due to an incorrect extrapolation.

In general, it has been shown that large-scale correlations exist between ranges and averages of resistivity and phase, and geology and physiography at LF. Material texture such as grain size, permeability, and porosity, and terrain relief, which often controls soil cover, both strongly control resistivity and resistivity stratification. The influence of material texture on earth resistivity is well understood (e.g. Keller and Frischknecht 1966) and the influence of topographic relief is fairly obvious. However, the results as presented in Figures 22 and 25 provide good examples of the resistivity and phase values to be found at LF. In the next chapter, these correlations are used as guidelines for mapping LF resistivity values in unmeasured areas.

## V. ESTIMATED RESISTIVITY AND PHASE MAPPING OF THE UNITED STATES INCLUDING ALASKA

### A. General

The mapping presented in this chapter is based on the studies that we have performed near LF transmitters and on previous VLF and galvanic studies. Our own LF studies were concentrated in three main areas: New England, the formerly glaciated states of the Midwest, and Alaska; these are the areas where we believe the mapping to have the greatest validity. Of course, it is impossible to survey the entire United States at LF, even if the time were available, because of the limited coverage

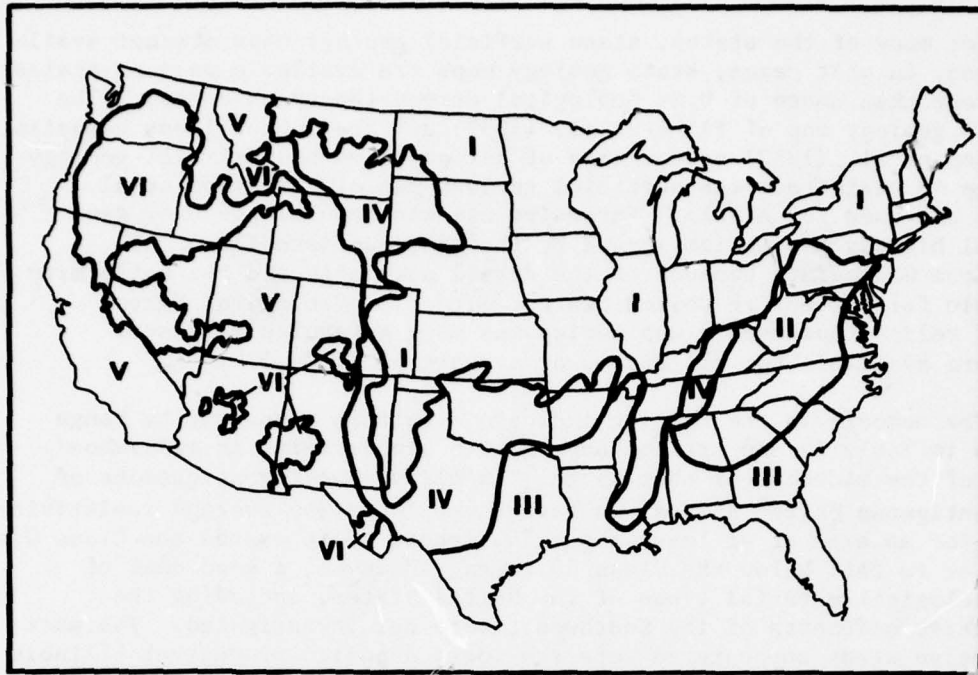


FIGURE 28. ESTIMATED U.S. REGIONS OF SIMILAR RESISTIVITY PATTERNS.

- I: Formerly glaciated and loess-covered.
- II: Moderate relief and residual soils.
- III: Deep, unconsolidated, coastal deposits.
- IV: No relief and residual soils.
- V: Severe relief with little volcanic rock.
- VI: Volcanic areas.

of existing LF transmitters (see Figure 18). Therefore, the mapping is mainly an estimation based on known geologic correlations and topographic effects. The mapping uses the same resistivity classification scheme of Table I that was used by Fine (1954) and is currently used by the FAA (publication 6050.10).

The general scheme used to develop the maps is as follows. First, the United States was divided into various regions (Figure 28) within which most of the materials that would affect an LF surface impedance measurement are of similar origin and type. Within these regions, the most prevalent materials were then assigned conductivity ranges based on our and other investigations. These ranges are given in table form later in this chapter. We then considered the effect of geological stratification. This was simplified by assuming that over the depth of LF (300 kHz was assumed for all cases) penetration, a two-layer model of sediment over bedrock, or a dryer soil over a more moist soil (within the water table), was sufficient. We then used state surficial geology maps and topographic maps to estimate upper layer thicknesses and computed apparent resistivity and phase at 300 kHz.

For many of the states, state surficial geology maps are not available and, in most cases, state geology maps are available only at scales different than those of U.S. Geological Survey topographic maps. The glacial geology map of Flint et al. (1959) and the map of loess deposits by Thorp et al. (1952) solved many of our problems of surficial geology for the 48 states and the surficial geology map of Karlstrom et al. (1964) was used for Alaska. Extensive use was made of the U.S. geological highway map series issued by the American Association of Petroleum Geologists because of the detail available and the uniformity of scale for the entire United States. The U.S. Geological Survey shaded relief topographic map series was used extensively because maps are available for all states at a scale of 1:500,000.

The numbers in the mapping indicate a certain conductivity range (given in Table I) and are the approximate conductivity in millimhos/meter of the midvalue of that range. In all of our investigations of the contiguous United States, we have never found the average resistivity value for an area of at least about 350 square km to exceed the Class 0.5 range or to fall below the Class 30 range. However, a good deal of the geological material types of the United States, including the conductive sediments of the Southwest, were not investigated. The most conductive areas encountered were the loess deposits of central Illinois and the most resistive were the granites of New Hampshire. In the latter case, some measurements at LF have been as high as 20,000 ohm-m, but these were isolated cases. It is most likely that such isolated cases would be found in the granitic outcroppings of the large mountain ranges where sediment cover is marginal.

The mapping appears in Appendixes C, D and E in folded form, and is grouped by adjacent states in Appendixes C1-C12. Figure 29 shows these groupings. Appendix C13 shows urban and industrial areas where the estimates are probably meaningless because scattering and diffraction may be more important processes affecting propagation.

## B. Regional Classifications

### Region I: Formerly glaciated and loess covered.

This is the largest region and includes the New England states, New York, northern Pennsylvania and New Jersey, Ohio, Indiana, Illinois, Michigan, northern Missouri, Iowa, Wisconsin, Minnesota, and parts of North and South Dakota, Kansas, Nebraska, Oklahoma, Texas, Mississippi, Kentucky and Tennessee. The northern states are areas covered by glacial deposits of ground and end moraine or by lacustrine and alluvial deposits. The till is coarse in some areas as in parts of Wisconsin, northern New York and northern New England, where it may also be no more than 1 or 2 m thick in the mountainous areas. In other areas, the till is quite fine and similar in resistivity to the loess deposits, as in Illinois. The areas of Mississippi, western Kentucky and western Tennessee are covered by loess originating in the Mississippi Valley.

Generally, the resistivity classes assigned in Table II were used for this region. There are many exceptions to this scheme but, in general, we believe that these are the most probable ranges for the

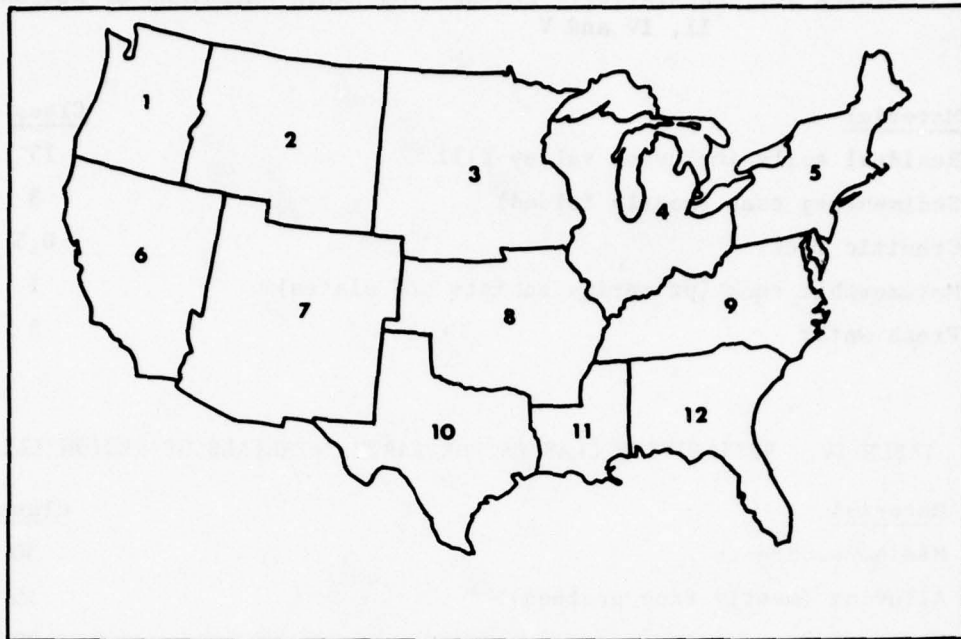


FIGURE 29. AREA DIVISIONS OF THE UNITED STATES FOR THE CONDUCTIVITY MAPPINGS OF APPENDIXES C1-C12.

TABLE II. RESISTIVITY CLASSES FOR EARTH MATERIALS OF REGION I

<u>Material</u>	<u>Class</u>
Marine sediments	30
Lacustrine sediments	30
Fresh water	8
Sands and gravels (mostly alluvial outwash)	4
End moraine	4
Ground moraine (depends on coarseness)	8, 15
Sedimentary rocks	8
Metamorphic rocks (primarily schists and slates)	1
Granitic rocks	0.5

TABLE III. RESISTIVITY CLASSES FOR EARTH MATERIALS OF REGIONS II, IV and V

<u>Material</u>	<u>Class</u>
Residual soils including valley fill	15
Sedimentary rock (mostly folded)	8
Granitic rock	0.5
Metamorphic rock (primarily schists and slates)	1
Fresh water	8

TABLE IV. RESISTIVITY CLASSES FOR EARTH MATERIALS OF REGION III

<u>Material</u>	<u>Class</u>
Marine sediments	30
Alluvium (mostly fine grained)	15
Marl	30
Sedimentary rock	8

materials in this region. In some areas such as Michigan and Iowa, the surficial geology is so complicated (Flint et al. 1959) that averages had to be made for groups of materials. The two values given for ground moraine correspond to coarse-grained moraine (Class 8) as occurs in Iowa or Wisconsin, and to fine-grained moraine (Class 15) such as occurs in central Illinois.

In the Midwest, bedrock resistivity values were of little concern as the depth of the soils usually far exceeds the LF skin depth. Some bedrock exceptions are the near surface limestones in southern Indiana, northeastern Iowa and southwestern Wisconsin. In New England and the Adirondacks, the metamorphic or granitic bedrock is often of primary importance. In most of New York, the glacial till is not considered to be of significantly different resistivity than the underlying sedimentary bedrock.

Region II: Mountains and Hills of Moderate Relief with Residual Soils.

This region covers the Appalachian region of central Pennsylvania, western Maryland and Virginia, eastern West Virginia, western North and South Carolina, northern Georgia, eastern Tennessee and Kentucky and northeastern Alabama. It includes the piedmont areas of the Atlantic coast states. In these areas we used the resistivity classifications of Table III.

The greatest margin for error probably lies in the value assigned for sedimentary rock (Class 8). The actual values encountered may be as low as 20 ohm-m for shale or even lower for coal, and as high as or higher than 5000 ohm-m for an extremely dense or dry limestone. However, in most of this region the depth of weathering or depth of soil is sufficient to bring most resistivities of soils over sedimentary formations down to Class 8 or lower.

Region III: Coastal Areas of Deep, Unconsolidated Sediment.

This region comprises the eastern and southern portions of states that border the Atlantic Ocean and the Gulf of Mexico. It includes all of Florida. In this region, the depth of conductive and unconsolidated sediments generally exceeds the LF skin depth in the same materials so that the underlying bedrock types were of little concern. The settlement and industrialization along the New Jersey, Delaware and Maryland coasts (shown in Appendix C13) make any ground conductivity estimate meaningless as propagation is probably more affected by scattering and diffraction. The resistivity classifications for this region are given in Table IV.

Region IV: Little or No Relief with Residual Soils.

This region covers a large portion of the Great Plains area of Montana, North and South Dakota and Wyoming. In the Southwest it includes portions of Colorado, Texas, Oklahoma and Kansas and Arkansas. In the East it is only a small portion of Kentucky and Tennessee. Most of these areas consist of fine soils and/or continental deposits overlying conductive sedimentary rock. The resistivity classifications of Table III were used for this area.

Region V: Primarily non-volcanic areas of severe relief.

This region begins with the eastern boundary of the Rocky Mountains and extends to the Pacific Coast. It includes the granitic batholiths of Idaho and California, the coastal mountain ranges and the Colorado plateau. It also includes the valleys and basins within and about the separate ranges. It does not include the volcanic plateaus and mountains and their associated valleys and basins; these are included in Region VI.

In the mountainous areas we have used our own results of LF values for sedimentary, granitic and metamorphic rocks. The validity of this for one small area in Colorado is verified in Keller et al. (1970). Although many areas of the Rockies were glaciated, there was no attempt to differentiate the moraine or coarse-grain alluvium filled valleys, as the scale involved would be too small for the purposes of this report.

The flatter, more populated valleys and basins are deeply filled with fine-grained, low resistivity alluvial and lacustrine sediments and this is where the BCB transmitters that were used by Kirby et al. (1954) are located. Therefore, because we expect that LF and BCB values are in the same resistivity class, we have used the BCB values for these areas. Generally, we have used the resistivity classifications of Table III.

One material type encountered in Region V that is not found in Regions I-IV (except for some metamorphic varieties) is volcanic rock, which occurs in all states of this region. It is discussed separately below since it occurs most extensively in Region VI, especially in the Pacific Northwest.

#### Region VI: Volcanic Regions.

This area is composed of the large volcanic areas of Idaho, Washington, Oregon, Nevada and California, and the smaller areas of Wyoming, Colorado, New Mexico, Texas and Arizona. The volcanic areas of the Northwest are both mountainous and flat (i.e. the "flood basalts" or plateau basalts), while in much of Nevada and the Southwest the volcanic rocks are found in individual mountain ranges. Generally, basalt is the volcanic rock type, which, although igneous, in these areas is much less resistive than granite because of its greater porosity and permeability.

Field measurements of resistivity at radiowave frequencies are generally nonexistent for the mountainous areas. Culley et al. (1975) list the range of values for basalt to be about 200-1000 ohm-m. Kirby et al. (1954) generally assign these areas to Class 4. We have made no measurements over volcanic flows and so have adopted the Class 4 range for volcanic rocks. This is used for both flat and mountainous areas because the detritus in the mountainous volcanic areas of the west is expected to be predominantly coarse-grained and probably within Class 4 also. In the plateau areas the soil cover is usually thin (Fenneman 1938b) and is not electrically significant. The resistivity classes assigned to the different materials in this region are given in Table V.

#### C. Phase Mapping

As was discussed in Chapter II, the actual quantity of interest for propagation studies is the surface impedance which is complex. The mapped resistivity is actually an apparent resistivity which is derived from the surface impedance amplitude. The surface impedance phase is also important for radiowave propagation studies and a very general estimate of its variation throughout the 48 contiguous states is given in Appendix D. The phase classification scheme used is given in Table VI.

The general geological scheme used for assigning LF phase classes is given in Table VII. Class VI areas are the most extensive and are mainly where surficial, unconsolidated sediment such as loess, fine-grained till, alluvium and lacustrine deposits are of thicknesses greater than their respective LF skin depths (e.g. 9 m for 100 ohm-m material at 300 kHz). Resistivity generally decreases with depth in these areas because materials below the water table are more conductive than those above it. Our measurements in the Midwest at fine-grained soil sites were within Class VI phase limits at 5 out of 8 stations. The remaining three stations had average phases of 48, 48.7 and 61.9 degrees.

Class III areas are mainly the igneous and metamorphic bedrock areas of the Appalachians, Rockies and Sierra Nevadas, where resistivity

TABLE V. RESISTIVITY CLASSES FOR EARTH MATERIALS OF REGION VI.

<u>Material</u>	<u>Class</u>
Alluvium	15
Lacustrine sediments	15
Lake water (fresh)	8
Granitic rock	0.5
Volcanic rock	4
Metamorphic rock	1
Sedimentary rock	8
*Great Salt Lake and associated salt beds	<30

TABLE VI. LF PHASE CLASSES.

<u>Class</u>	<u>Phase Range</u>
I	0° - 10°
II	11° - 20°
III	21° - 30°
IV	31° - 40°
V	41° - 50°
VI	51° - 60°
VII	61° - 70°
VIII	71° - 80°
IX	81° - 90°

TABLE VII. GEOLOGICAL SCHEME FOR LF PHASE CLASSES

<u>Geological Condition</u>	<u>Phase Class</u>
Basins and plains of unconsolidated sediments	VI
Mountains of granitic and metamorphic bedrock	III
Volcanic mountains	IV
Flood basalts	IV
Mountains of sedimentary bedrock	V
Coarse glacial till over granitic and metamorphic rocks	V

increases with depth because of such factors as weathering and the decrease with depth of permeability and porosity of the rock types. Our measurements in Vermont, New Hampshire and Massachusetts have verified this. Dielectric properties are important for the highly resistive regions and their effect may be to lower the phase also for resistively homogeneous areas (see Figures 8-10). In the Superior Uplands of Minnesota and Wisconsin, the rock type is also granitic and metamorphic, but the till is usually of sufficient depth to assign this area to Class V, as was measured at Antigo, Wisconsin ( $\phi = 47.7^\circ$ ).

The volcanic areas have been assigned to Class IV although we have no measurements on which to base this. It is, therefore, an area of great uncertainty. Our reasoning for this classification of the mountainous, volcanic areas is that solid volcanic rock may be only slightly more resistive than the overlying erosional debris, and that the resistivity of the area, in general, is low enough to avoid dielectric effects. Therefore, the Class IV range would reflect this moderate increase of resistivity with depth. To the flatter volcanic areas, we have also assigned the Class IV phase range because there is usually only a thin residual soil and rubbly, more porous lava over the thicker lava beds at depth so that here, too, we expect only moderate resistivity increases with depth.

In the mountainous areas of sedimentary rock such as much of the Appalachians, Rockies and the Pacific coastal mountains, the rock resistivity is generally within Class 8 or the upper half of Class 15. Overlying soils are not expected to be of much different resistivity and so we have assigned these areas to Class V. This would then be the class containing the best examples of resistive homogeneity within the depth of LF penetration.

#### D. Alaska

The LF resistivity and phase mapping of Alaska requires a more extensive treatment than the contiguous 48 states because of the effect of seasonal temperature variations. Most of Alaska is underlain by permafrost, the resistivity of which strongly depends on temperature. By definition, permafrost only refers to ground which has remained below  $0^\circ\text{C}$  for at least two consecutive years. Therefore, a "warm" permafrost (i.e. within a few degrees of  $0^\circ\text{C}$ ) consisting of a fine-grained silt in which most of the water is not frozen because it is adsorbed on the particle surfaces, may only be 200-400 ohm-m, whereas at  $-10$  to  $-15^\circ\text{C}$  it may be 10,000 ohm-m or higher (Hoekstra et al. 1975). Clays and saline sediments can exhibit resistivities less than 50 ohm-m but still be permafrost.

The first attempt at mapping Alaskan ground resistivity at LF and BCB was done by Stanley (1955-1958) who used airborne measurements of field strength attenuation from 31 LF and BCB transmitters located at 25 different cities or villages. According to Stanley, "Turbulent air, poor check points or proximity to hills caused the record to indicate considerable spread," so that most radials from the transmitters were flown 3 or 4 times to find an average value or values. No attempt was made to geologically correlate the readings so that

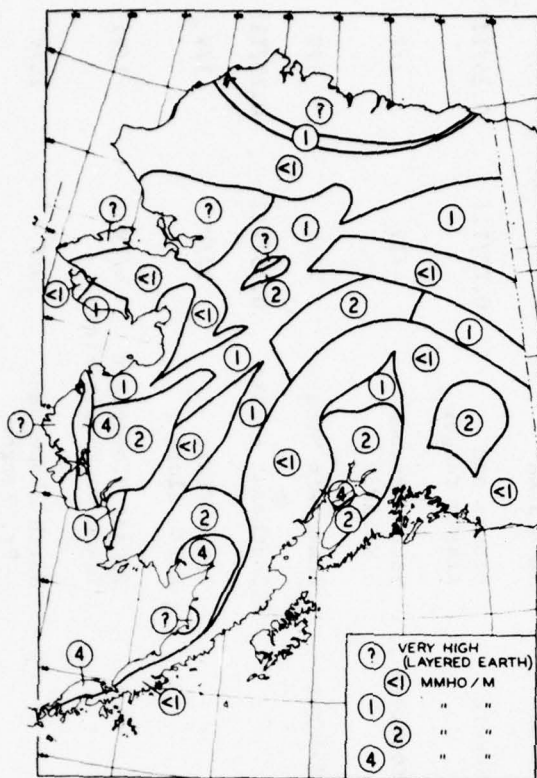


FIGURE 30. LF CONDUCTIVITY MAP OF ALASKA PRODUCED BY STANLEY (1958).

Stanley's map (Figure 30) consists of a number of arcuate sections that reflect the placement of the transmitters (in the arcuate valleys) and the flight paths. Stanley's conductivity divisions are only slightly different from those of Fine (1954). Very little attempt was made to seasonally differentiate the readings.

Resistivity measurements using galvanic, surface impedance, airborne wavetilt and magnetic induction methods have been made over the last several years (Sellmann et al. 1974; Hoekstra et al. 1975; Delaney et al. 1974; Arcone et al. 1978) in Alaska. These measurements have been in the vicinities of Fairbanks, the Copper River Basin, the North Slope and all 12 of the Alyeska pipeline pump stations. These data have been combined with Stanley's data, along with the use of geologic maps (Karlstrom et al. 1964, Ferrians 1965) to produce an estimated LF ground conductivity and phase map of Alaska (Appendix E). Within each section two sets of numbers are indicated, one set for seasonal resistivities and one for seasonal phases. The resistivity and phase schemes used for the various geologic materials and some of their locations are given in Table VIII. In this table the term fine-grain refers to silts and clays and coarse-grain refers to sands and gravels. Deep permafrost means greater than about 50 ft. The term "discontinuous" is in reference to horizontal distribution.

TABLE VIII. ALASKA RESISTIVITY CLASSES

<u>Material</u>	<u>Soil Cover or Type</u>	<u>Permafrost</u>	<u>Topography</u>	<u>Representative Locations</u>	<u>Resistivity Class/Phase Class</u>	
					<u>Late Summer</u>	<u>Late Winter</u>
Volcanic rock	Marginal	-	Moderate to severe	Aleutians, SE Alaska	4/V	4/V
SMG* rock	Marginal	Moderate to deep	Severe	Brooks and Alaska ranges	0.25/III	0.25/III
SMG rock	Fine-grain	Deep	Moderate	Yukon-Tanana Uplands	4/IV	1/V
SMG rock	Coarse-grain	Deep	Moderate	Kuskokwim Mtns	2/IV	1/V
Glaciers	-	-	-	Southeast Alaska	0.25/III	0.25/III
Alluvium	Fine-and coarse-grain	Deep	-	Yukon Flats North Slope	2/IV	1/V
Alluvium	Fine-grain	Deep	-	Tanana Floodplain Yukon-Kuskokwim Flats	4/IV	1/VI
Marine sediments	Fine-grain	Deep	-	North Slope near Pt. Barrow	30/V	15/V
Lacustrine sediments	Fine-grain	Discontinuous	-	Copper River Basin	15/V	8/VI

\*SMG-Sedimentary, Metamorphic, Granitic

## VI. SUMMARY AND RECOMMENDATIONS

### Summary

The important points of the first four chapters are as follows:

- 1) BCB mapping is inadequate for LF engineering purposes because of BCB radiowave sensitivity to normal dielectric effects at resistivities greater than 1000 ohm-m, inadequate earth penetration, and topographic effects.
- 2) Airborne VLF may possibly be used for large-scale LF mapping, mainly in flatter areas of the country such as the Midwest.
- 3) LF transmitters, though numerous, cover only about 50% of 9 particular states, and probably not more than 20% of the land area of the 48 contiguous states, with adequate field strength for resistivity mapping using the surface impedance method.
- 4) There is a great deal of dispersion in apparent resistivity values for many areas both in the BCB results as displayed by Kirby et al. (1954) and in the LF results presented in this report.
- 5) Correlations between apparent resistivity and geology and physiography exist. For example:
  - a) Fine-grain silts that cover much of the central U.S. are invariably Class 30 or Class 15. Even when extremely dry conditions prevail, these low figures may hold because of the amount of adsorbed water that may remain.
  - b) Crystalline rocks such as schists and granites are in the Class 1 - Class 0.5 range. The actual resistivity of the unweathered rocks may be much higher, but dielectric properties, weathering and the thin sediment cover usually associated with them in mountainous settings lower their surface apparent resistivity at LF.
  - c) Sedimentary rocks are generally in the Class 8-Class 4 range.
  - d) Unsorted sediments such as glacial till, which covers so much of the Northeast, Midwest and upper Midwest, show the greatest variability, but generally the values are centered around Class 15-Class 8.

e) Topography affects resistivity values through its effect on soil cover. Steep slopes are generally more resistive than gentle slopes for a given bedrock type.

6) Phase ranges for the 48 States also correlate with geology and physiography. The more important correlations are:

a) In areas of deep sedimentary cover, phases are generally greater than  $45^{\circ}$ . This means that resistivity decreases with depth as would be expected from increases of moisture with depth.

b) In mountainous areas of crystalline bedrock, phases are generally less than  $45^{\circ}$ . This means that resistivity is increasing with depth as evidenced by the less resistive till cover, a decrease of weathering with depth, and a lessening of permeability and porosity with depth.

In general, phases less than  $20^{\circ}$  and greater than  $70^{\circ}$  rarely are found.

With respect to the mapping of Chapter V, the following should be noted:

1) Large areas of the country obviously were not sampled and alternative sources of information had to be used. For example, the BCB values of Kirby et al. (1954) are used at LF for the flat areas of the West where sedimentation is deep. This is because the BCB values show little variation and are not subject to topographic influence, the sediments are sufficiently conductive so as not to be influenced by dielectric effects, and the sediments are homogeneous to sufficient depth.

2) Many areas of the mountainous regions are extremely complex geologically and the conductivity classes assigned are only estimates. Generally, the greater the relief, the more weight given to the bedrock type.

3) Of all the bedrock types, volcanic (mostly basalt) rocks were those for which the least information was available. Generally, these were assigned to Class 4.

4) The seasonal mapping of Alaska is based on our measurements along the Copper River Basin - Fairbanks - Prudhoe Bay axis and those of Stanley (1958). We disagree with Stanley's conclusion of little seasonal change in resistivity values. Even over thick permafrost where the seasonally active surface layer has thawed to depths of only 40-60 cm we have observed resistivity changes by a factor of 2.5 to 3 between late summer and late winter. Generally, some of Alaska has some of the most resistive ground of all, such as in the mountain ranges where resistivities are probably well over 10,000 ohm-m.

### Recommendations

The most important recommendation is that the LF conductivity map presented here be improved based on actual field measurements. This could be done most economically by investigating the largest areas of similar geology and physiography. Our investigations were mainly concentrated in the formerly glaciated states of the Midwest and New England. Other large areas of similar geology and physiography might be the flood basalts of the Pacific Northwest and the vast sedimentary areas of the South and the Southwest.

It is recognized that over much of the United States LF signal strength is not of sufficient amplitude to map surface impedance. It is therefore recommended that the use of commercially available instruments that measure resistivity using magnetic induction and VLF surface impedance be investigated in these areas. In the former case, easily portable instruments give less penetration than LF and require no remote transmitter. In the latter case, there is greater penetration than at LF, instrumentation is also portable and sufficient signal strength is available over the entire contiguous 48 states. The data supplied by these methods would then allow estimates of LF apparent resistivity to be made.

## VII. REFERENCES

- Abramowitz, M. and I. Stegun, eds. (1967), Handbook of mathematical functions, National Bureau of Standards, Applied Mathematics Series No. 55.
- Al'pert, Y.A. (1963), Radiowave propagation and the ionosphere, New York: Consultants Bureau, Translated from Russian.
- American Association of Petroleum Geologists (1966), United States geological highway map series (Maps 1-11). Available from AAPG, P.O. Box 979, Tulsa, Oklahoma, 74101.
- Arcone, S.A. (1977), Investigation of an airborne resistivity survey conducted at very low frequency, USACRREL Report 77-20, AD-AD44684.
- Arcone, S.A., P.V. Sellmann and A.J. Delaney (1979), Detection of arctic water supplies with geophysical techniques, USACRREL Report to be published.
- Collett, L.S. and A. Becker (1967), Radiohm method for earth resistivity surveying, Canadian Patent No. 795919.
- Culley, R.W., F.L. Jagodits, and R.E. Middleton (1975), E-phase system for detection of buried granular deposits. Paper presented at the Symposium on Modern Innovations in Subsurface Exploration, University of Toronto, Toronto, Canada.
- Delaney, A.J., P.V. Sellmann and P. Hoekstra (1974), Estimated ground resistivity for the Trans-Alaska Pipeline Route, USACRREL Internal Report 409 (unpublished).
- Denny, C.S. (1967), Surficial geologic map of the Dannemora quadrangle and part of the Plattsburgh quadrangle New York, Map GQ-635, U.S. Geological Survey.
- Denny, C.S. (1970), Surficial geologic map of the Mooers quadrangle and part of the Rouses Point quadrangle, Clinton County, New York, Map I-630, U.S. Geological Survey.
- Doll, C.G., ed. (1961), Centennial geologic map of Vermont, State of Vermont publication.
- Federal Aviation Administration (1965), An FAA handbook, Frequency management engineering principles; L/MF frequency assignment criteria. Publication 6050.10, Washington, D.C.
- Fenneman, N.M. (1938a), Physiography of eastern United States, New York: McGraw-Hill.

- Fenneman, N.M. (1938b), Physiography of western United States, New York: McGraw-Hill.
- Ferrians, O.J. (1965), Permafrost map of Alaska, Map I-445, U.S. Geological Survey.
- Fine, H. (1954), An effective ground conductivity map for continental United States, Proceedings of the IRE, September, vol. 42, p. 1405-1408.
- Flint, R.F. (1971), Glacial and Quaternary Geology, New York: John Wiley & Sons.
- Flint, R.F., R.B. Colton, R.P. Goldthwait and H.B. Willman (1959), Glacial map of the United States east of the Rocky Mountains, Geological Society of America.
- Harrison, R.P., J.L. Hecksher, and E.A. Lewis (1971), Helicopter observations of very low frequency waves over certain mountains and shorelines. Journal of Atmospheric and Terrestrial Physics, vol. 33, p. 101-110.
- Hoekstra, P., P.V. Sellmann, and A.J. Delaney (1975), Ground and airborne resistivity surveys of permafrost near Fairbanks, Alaska. Geophysics, vol. 40, no. 4, p. 641-656.
- Hollingworth, J. (1926), The propagation of radio waves, Journal of the Institute of Electrical Engineers, vol. 46, p. 579-595.
- Hughes, W.J. and J.R. Wait (1975), Effective wavetilt and surface impedance over a laterally inhomogeneous two-layer earth, Radio Science, vol. 10, no. 11, p. 1001-1008.
- Johler, J.R. (1971), Loran radio navigation over irregular inhomogeneous ground with effective ground impedance maps, Telecommunications Research and Engineering Report 22, U.S. Dept. of Commerce (Supt. of Documents, U.S. Govt. Printing Office, Washington, D.C. 20402.
- Jordan, E.C. and K.G. Balmain (1968), Electromagnetic waves and radiating systems, 2nd edition, Englewood Cliffs, New Jersey: Prentice-Hall, Inc.
- Karlstrom, T.N.V. and others (1964), Surficial Geology of Alaska, Map I-357, U.S. Geological Survey.
- Keller, G.V., and F.C. Frischknecht (1966), Electrical methods in geophysical prospecting, New York: Pergamon Press.

- Keller, G.V., A.B. Level, and F.L. Avsman (1970), Evaluation of airborne electromagnetic surveying for mapping variations in rock strength, Colorado School of Mines, Air Force Cambridge Research Laboratories, Contract Report no. F19628-69-C-0281.
- King, R.J. (1968), Crossed dipole method of measuring wavetilt, Radio Science, vol. 3, no. 4, p. 345.
- Kirby, R.S., J.C. Harman, F.M. Capps, and R.N. Jones (1954), Effective radio ground-conductivity measurements in the United States, NBS Circular 546 (supt. of Documents, U.S. Govt. Printing Office, Washington, D.C. 20402).
- Ott, R.H. and L.A. Berry (1970), An alternative integral equation for propagation over irregular terrain, Radio Science, vol. 5, no. 5, p. 767-771.
- Ott, R.H. (1971), An alternative integral equation for propagation over irregular terrain, 2, Radio Science, vol. 6, p. 429-435.
- Sellmann, P.V., P. Hoekstra, and A.J. Delaney (1974), Airborne resistivity survey: An aid in bedrock geology reconnaissance, USACRREL Special Report 202, AD 777792.
- Stanley, G.M. (1958), Studies of ground conductivity in Territory of Alaska. Geophysical Institute of Alaska, University of Alaska, Interim Scientific Report No. 1, Navy Dept. Bureau of Ships, Contract No.: NE 120308.
- Thorp, James, et al. (1952), [Map of] Pleistocene eolian deposits of the United States, Alaska, and parts of Canada. Scale 1:2,500,000 [in colors]: New York, Geological Society of America.
- United States Geological Survey shaded topographic relief map series. Scales commonly at 1:500,000 (Available from the USGS, Reston, VA., 22092).
- Wait, J.R. (1970), Electromagnetic waves in stratified media, New York: Pergamon Press. 2nd Edition.
- Watt, A.D. (1967), VLF radio engineering, New York: Pergamon Press.

GLOSSARY OF GEOLOGIC TERMS USED\*

Adsorption	Adherence of molecules to the surfaces of solids with which they are in contact. Adsorbed water in soil is resistant to the pull of gravity and capillary action.
Alluvium	A general term for sorted or unsorted clay, silt, sand or gravel or mixtures thereof deposited by running water in a stream bed, floodplain, delta, etc.
Argillite	A rock derived from clays or silts but less laminated than shale and lacking the fissility of shale.
Basalt	A dark to medium-dark, commonly volcanic, igneous rock.
Clay	(Mechanical) A particle of any composition (often a crystalline fragment of a clay mineral) that has a diameter less than 1/256 mm. (Mineralogical) Anhydrous aluminum silicate derived from feldspathic rock by weathering or by precipitation.
Cleavage	The property or tendency of a rock to split along secondary, aligned fractures or other closely spaced, planar structures or textures, produced by deformation or metamorphism.
Coarse-grain	Term referring to sand or gravel sized sediment.
Detritus	Loose rock and mineral debris mechanically eroded and removed from its place of origin.
Dolomite	A carbonate mineral including equal amounts of calcium and magnesium.
Dolostone	Sedimentary rock composed of more than 50% dolomite.
End moraine	A moraine that has been deposited at the lower or outer end of a glacier. Also called a terminal moraine.

\*Adapted from the Glossary of Geology, copyright 1972, American Geological Institute, Washington, D.C.

Feldspathic	Term used for a mineral aggregate containing feldspar.
Feldspar	A group of abundant rock forming minerals consisting of aluminum silicates most commonly in combination with potassium, calcium or sodium. Feldspars constitute approximately 60% of the earth's crust.
Ferromagnesian	Term referring to the inclusion of iron and magnesium.
Fine-grain	Term referring to silt or clay size sediment.
Flood basalt	An extensive, thick and smooth basaltic lava flow or successive flows accumulating to form a plateau. Also called plateau basalt.
Foliation	A general term used for a planar arrangement of textural or structural features in any type of rock, e.g. cleavage in slate or schistosity in schist.
Glacial till	Unsorted, unstratified and unconsolidated mixture generally of clay, sand and gravel.
Granite	A term loosely applied to any light-colored, coarse-grained igneous rock. Specifically, it refers to a definite composition of quartz, feldspar and ferromagnesian minerals.
Gravel	An unconsolidated, natural accumulation of rounded rock fragments with diameters greater than 2 mm.
Ground moraine	Rock debris dragged along in and beneath a glacier or ice sheet. After the ice has left, it refers to the smooth, gently rolling surface of till that remains.
Igneous	Term referring to a rock or mineral that solidified from a molten (magmatic) or partly molten material.
Lacustrine sediment	Fine-grained sediment deposited at the bottom of a lake. The lake may have long since disappeared or altered its shape.
Limestone	A sedimentary rock consisting chiefly of calcium carbonate.
Loess	Windblown, sedimentary deposits primarily consisting of silt.

Marine sediment	Fine-grained sediment deposited beneath a sea. The sea may have long since receded or disappeared.
Marl	A term loosely applied to unconsolidated materials consisting chiefly of clay and calcium carbonate.
Metamorphic	Term applied to a rock derived from pre-existing rock by mineralogical, chemical and structural changes in response primarily to changes in temperature and pressure.
Moraine	Any accumulation of unsorted debris deposited by a glacier in a number of topographic landforms.
Permafrost	Ground that has remained below 0°C for at least two consecutive years. The definition is based solely on temperature and does not refer to water content or material type.
Permeability	The capacity of a porous material for transmitting a fluid without impairment of the material structure.
Piedmont	An area, plain, slope, glacier, or other feature at the base of a mountain.
Plateau basalt	See "flood basalt."
Porosity	The property of a material containing interstices or voids which are not necessarily connected.
Quartzite	A metamorphic rock consisting mainly of quartz and formed by recrystallization of sandstone or other silica rich rock.
Saline	Pertaining to or consisting of salt, whether whole or dissolved.
Sand	A particle of any composition (often a rock fragment) having a diameter in the range 1/16-2 mm.
Sandstone	A sedimentary rock of sand size particles set in a silty or clayey matrix and cemented usually by silica, iron oxide or calcium carbonate.
Schist	A strongly foliated metamorphic rock which can be readily split into thin flakes or slabs; i.e. it demonstrates the property of schistosity which is a type of cleavage.

Sedimentary rock	A rock resulting from the consolidation of loose sediment that has accumulated in layers.
Shale	A fine-grained sedimentary rock formed by the consolidation of clay or silt and characterized by finely stratified laminae.
Silt	A particle of any composition (often a rock fragment) having a diameter in the range 1/256-1/16 mm.
Slate	A fine-grained metamorphic rock that cleaves along planes independent of the original bedding.
Surficial geology	The geology of surficial deposits, including rocks.

APPENDIX A

LOCAL METHODS OF MEASURING EARTH RESISTIVITY

Methods	Frequencies commonly used	Quantities measured	Comparisons made to determine resistivity	Comments
Galvanic	0-12 Hz	Injected current I Induced potential V	V/I	Also referred to as d.c. sounding method. I is introduced into 2 outer electrodes and V is measured between 2 inner electrodes. Common electrode configurations are known as Wenner, Schlumberger and Eltran arrays. Depth penetration achieved by extending the array.
Magnetic induction	1-10 kHz	Primary induction B Secondary induction B'	B'/B	B' depends on earth conductivity. Loop antennas used for transmitting and receiving. Depth penetration achieved by separating the antennas. May be adapted for airborne use.
Surface Impedance Magneto-telluric	0-10 kHz	Earth tangential components of the electric E and magnetic H fields of the propagating radiowave.	E/H	E and H are orthogonal. Signals are generated by lightning, ionospheric discharges, etc. Depth penetration increases with decreasing frequency.
Surface impedance Radiohm	10-1600 kHz	"	"	E and H are orthogonal. Signals are generated by vertically polarized transmitters in military and civilian use. Depth penetration increases with decreasing frequency.
Wavetilt	10 kHz - 40 MHz	Earth tangential and normal components of the electric field (E <sub>t</sub> and E <sub>n</sub> ) of the propagating radiowave.	E <sub>t</sub> /E <sub>n</sub>	Signals are generated by vertically polarized transmitters in military and civilian use. Depth penetration increases with decreasing frequency. Ground measurements are usually affected by vegetation. Best suited for airborne use. Usually linearly related to the surface impedance.

## APPENDIX B. OPERATION OF THE GEONICS EM-32 SURFACE IMPEDANCE METER

The ensuing discussion pertains to the more practical aspects of the operation of this instrument which was briefly outlined in Chapter IV. The theoretical basis of the data interpretation was given in Chapter II.

### Assumptions for data interpretation

The Geonics EM-32 is an instrument designed to measure the ratio of the earth tangential components of the electric and magnetic fields of a radiowave propagating over the surface of the earth. As this ratio is a complex quantity, the instrument reads both an amplitude and a phase. The calibration of this amplitude and phase, however, is based strictly on the model of a plane surface wave interacting with an earth in which variations of electrical properties may take place only in the vertical direction. In detail, the important assumptions are as follows:

#### 1) Nature of the atmospheric radiowave

The radiowave is either a classical Sommerfeld-type groundwave (see Chapter II) or a skywave that has just reflected off the ionosphere and is then incident upon the earth at a grazing angle  $\psi$  of  $0^\circ$  (this is the angle between the wave propagation vector  $\vec{\beta}$  and an earth tangent directed toward the transmitter). Such a wave is assumed to be "plane" so that the amplitude and phase of its electromagnetic field components are uniform along infinite planes that are perpendicular to the direction of propagation. If  $\psi$  is greater than  $0^\circ$ , the instrument will still perform but there is no way to tell what  $\psi$  is so as to make any corrections. Readings are reasonably accurate if  $\psi < 10^\circ$ .

Commonly, LF transmitters are of such low power that only the groundwave is important. For the few transmitters that radiate 1000 Watts or more (usually located in coastal areas), skywaves may be usable at extended ranges. However,  $\psi$  will probably be so great as to render the data meaningless. Generally, for a 25-Watt transmitter measurements are confined to within about a 16-km radius, and for a 200-Watt transmitter, to within about a 57-km radius.

#### 2) Nature of the ground structure

The fields measured at the surface of the earth are actually a combination of the incident radiation and the radiation reflected from the surface and the subsurface. It is assumed that the subsurface radiation is also plane, although it attenuates exponentially along the

direction of propagation. In order to fulfill this condition, the variations in earth electrical resistivity must take place only in the vertical direction. It is also assumed that the earth's surface is flat. This is extremely reasonable considering that the radiowave wavelength at an LF band frequency (e.g. 1 km at 300 kHz) is extremely short compared with the earth's radius.

The assumption of only vertical stratification is reasonable for most physiographic settings. Earth temperature (most importantly in permafrost areas) and ground water are significant influences upon earth resistivity and vary mainly with depth. When layering of different materials occurs such as with sedimentary rock strata or with stratified glacial deposits, the layer interfaces are usually inclined no more than a few degrees from horizontal. Only in mountainous settings will this assumption be grossly violated on a consistent basis. In these cases, experience has shown that the method gives results that are significant of a reasonable integration of subsurface conditions, but that when severely resistive inhomogeneities are encountered, earth induced currents may overly concentrate along more conductive adjacent zones, thereby giving false readings.

### 3) Nature of the ground electrical properties

This was discussed in Chapter II in detail but will be reviewed here. The most important assumption is that electrical resistivity is the only property that influences radiowave propagation. This is an excellent assumption for the LF band so long as electrical resistivity is below about 10,000 ohm-m. Above this value, dielectric permittivity may influence the readings, as was demonstrated in Figures 8, 9, and 10. Magnetic permeability is another basic earth electrical property but it is fairly constant throughout nature except for some iron bearing magnetic minerals.

When dielectric permittivity is important, the EM-32 will still function but data modeling must account for dielectric properties. The most usual high resistivity materials encountered are granites, metamorphic rocks such as quartzites and schists, ice, and extremely dry sands and gravels. For the rocks, dielectric permittivities of between 5 and 10 are reasonable values. For ice containing small amounts of impurities, values between 3 and 4 are acceptable. For dry sand or gravel, values between 3 and 5 can be used.

### Operation

The EM-32 is illustrated in Figure 19, Chapter IV, and reference should be made to that illustration. The operational procedure for

making a measurement takes less than one minute and is given as follows, along with the reasons for following it.

- 1) Turn the FUNCTION knob to the FIELD position. In this position, only the antenna coil in the instrument handle is activated and this coil senses the radiowave magnetic field "H<sub>y</sub>." The operator will now see a deflection on the NULL METER beneath the handle.
- 2) Rotate the handle clockwise or counterclockwise until a minimum is read on the NULL METER. In this position the antenna coil is decoupled to "H<sub>y</sub>."
- 3) Rotate the instrument 90° in either direction in the horizontal plane and set it down upon the ground. Extend the GROUND PROBES out orthogonally to the handle and insert them in the ground. The ground probes and antenna coil are now properly aligned with respect to the field components "E<sub>x</sub>" and "H<sub>y</sub>" of the propagating ground wave.
- 4) Turn the FUNCTION knob to the OPERATE position.
- 5) Adjust the RESISTIVITY (COARSE and FINE) and PHASE knobs until a null is achieved on the NULL METER.

The resistivity thus read is the "apparent resistivity" and is actually a calibration of the surface impedance amplitude  $|Z_s|$ . The apparent resistivity  $\rho_a$  is related to  $Z_s$  by the formula

$$\rho_a = \frac{|Z_s|^2}{\omega\mu_0}$$

as was given in equation 17 of Chapter II. Therefore  $|Z_s|$  can always be obtained regardless of any of the above assumptions. The instrument is calibrated for readings between 0 and 30,000 ohm-m. Above this range, readings will either be affected by contact resistance between the ground and the probes or by ground dielectric properties.

Phase is calibrated between 0° and 90°. This calibration is based explicitly on the above assumptions of plane wave interaction with a vertical stratification because in this model phase must lie between 0° and 90° with "E<sub>x</sub>" leading "H<sub>y</sub>." If the phase lies outside of this range, no null can be obtained but may be approached.

It is best to take several readings over a circular area when determining the LF apparent resistivity of a particular spot. The radius of this area should equal at least the skin depth  $\delta$  defined as

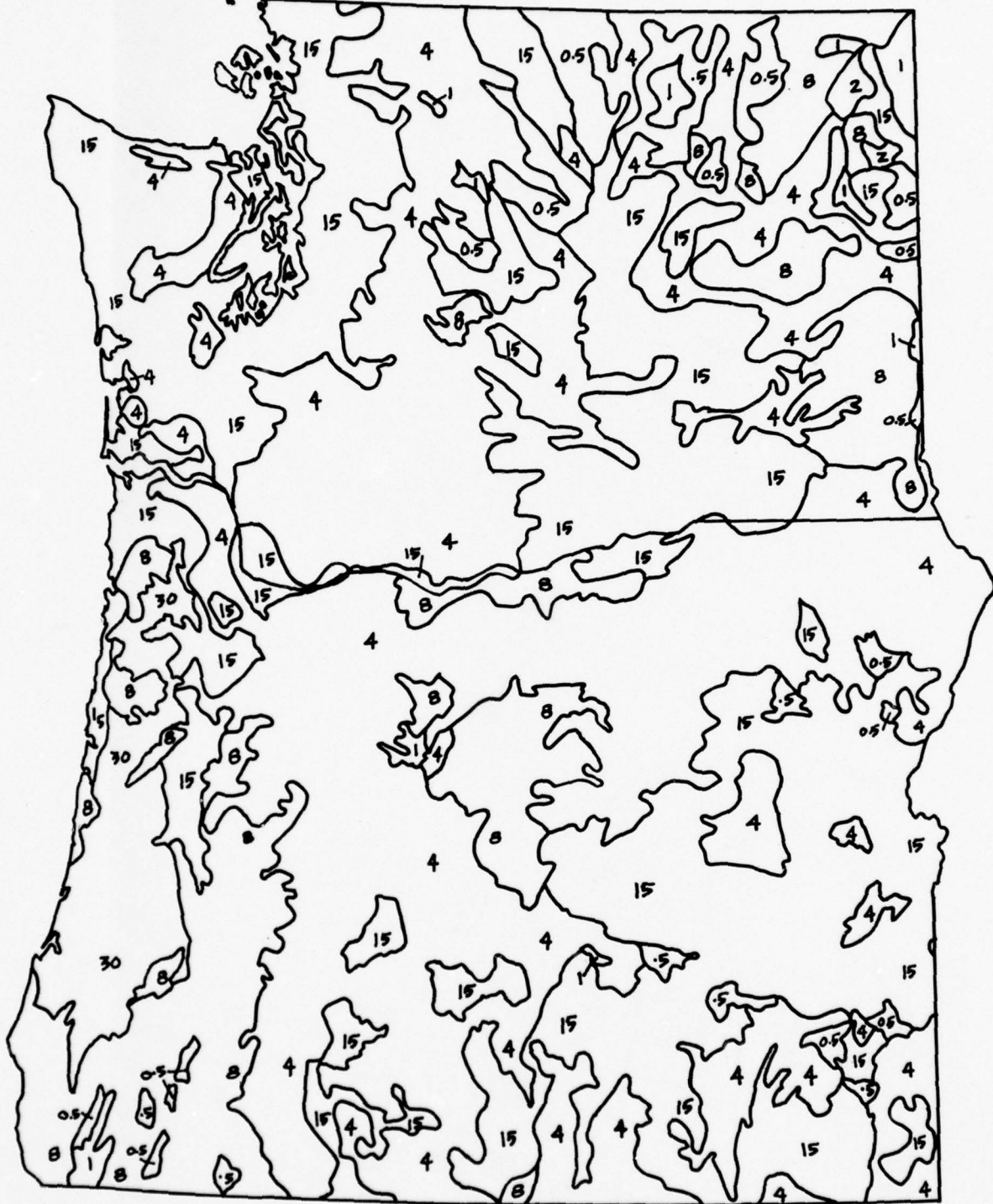
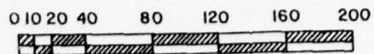
$$\delta = \sqrt{\frac{2\rho}{\omega\mu_0}}$$

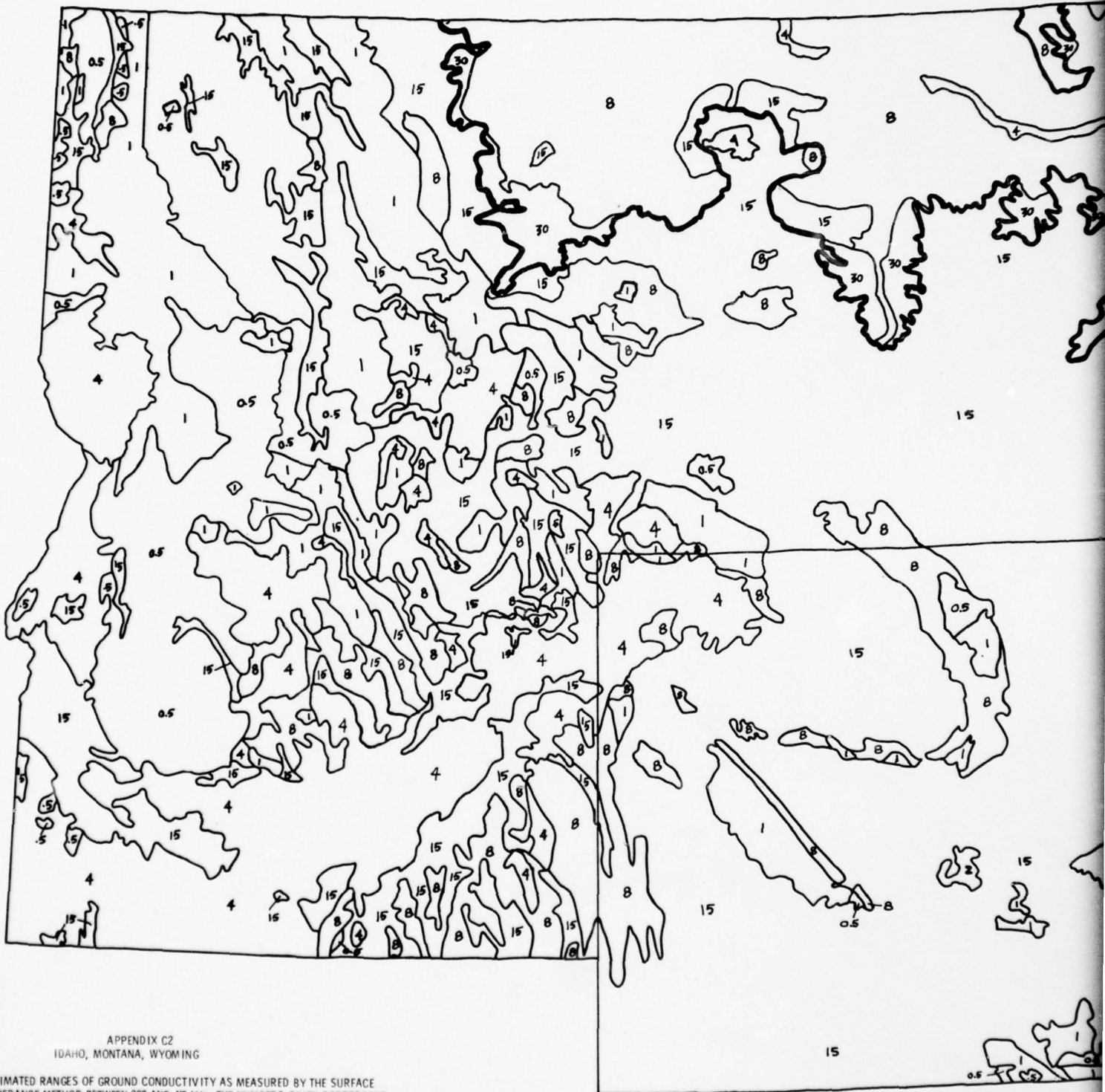
by equation 6 of Chapter II where  $\rho_a$  is the average apparent resistivity being measured. The reasoning for this is that waves that are scattered from subsurface inhomogeneities will be limited in range by the skin depth of the medium in which they occur. Therefore, such inhomogeneities may be better averaged out if several readings are taken over such an area.

APPENDIX C1

OREGON, WASHINGTON

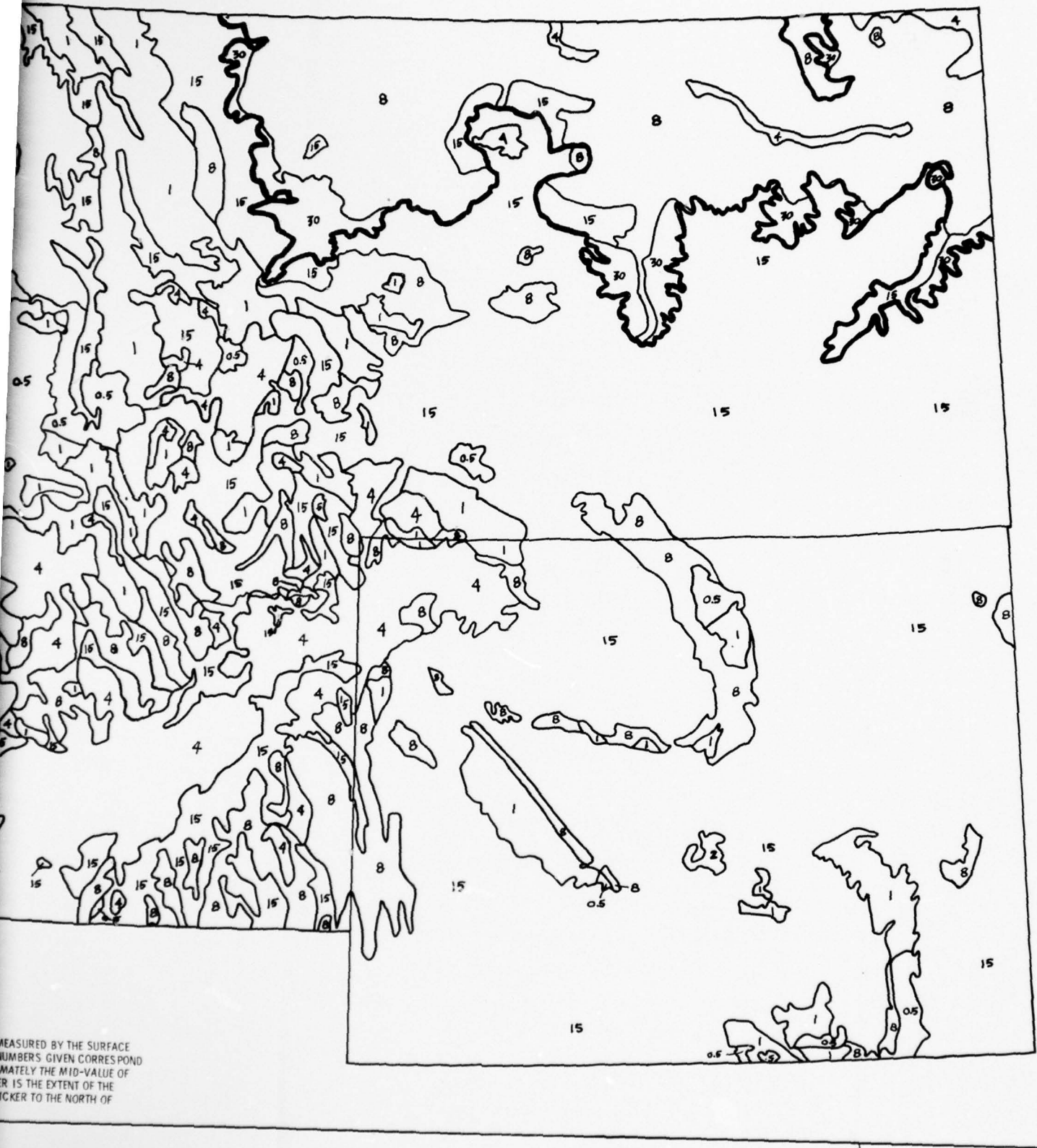
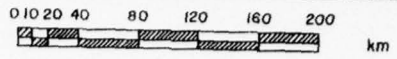
Estimated Ranges of Ground Conductivity as Measured by the Surface Impedance Method between 200 and 415 kHz. The numbers given correspond to the Ranges given in table 1 and are approximately the Mid-Value of those Ranges in Millimhos/M.

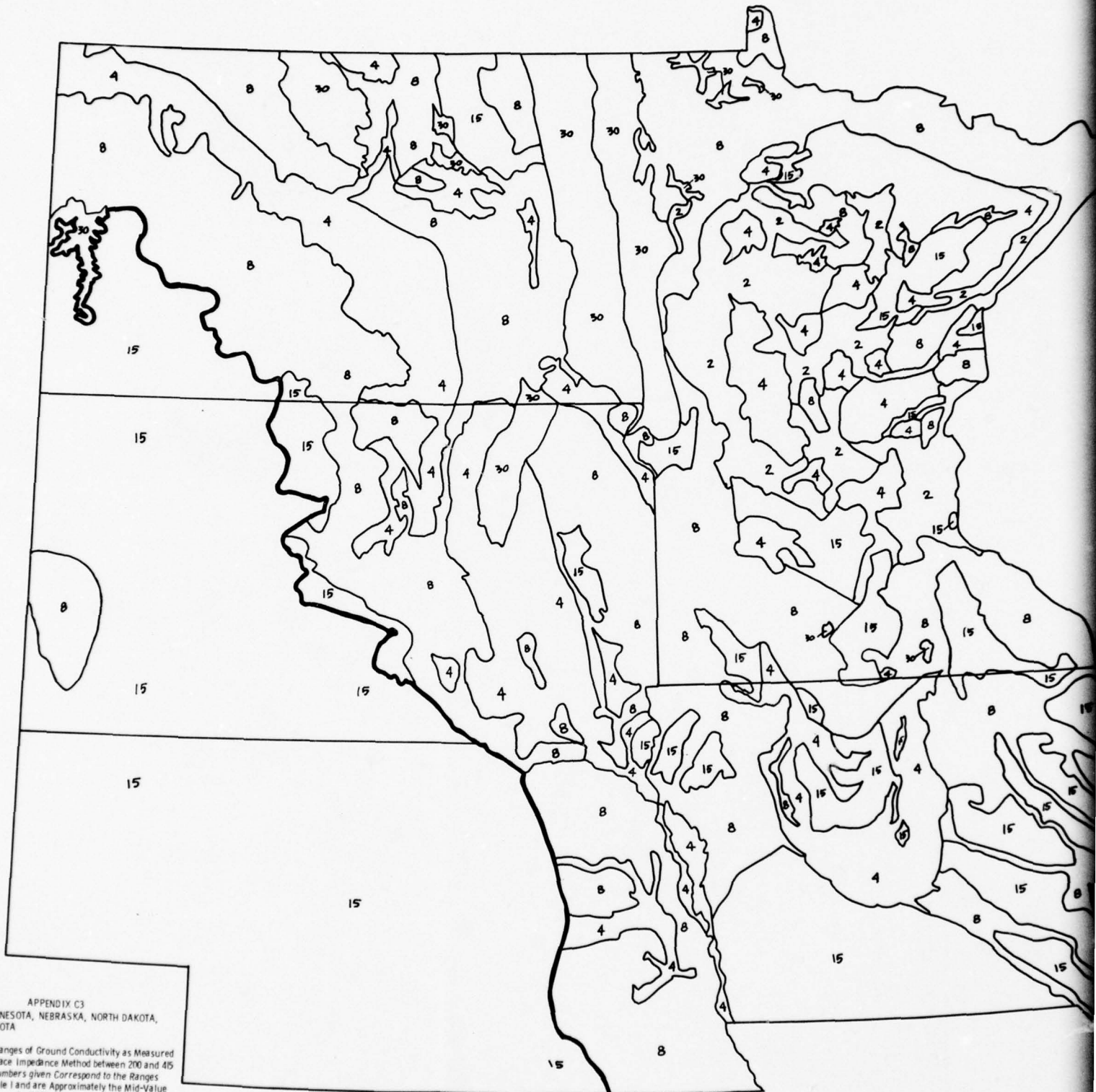




APPENDIX C2  
IDAHO, MONTANA, WYOMING

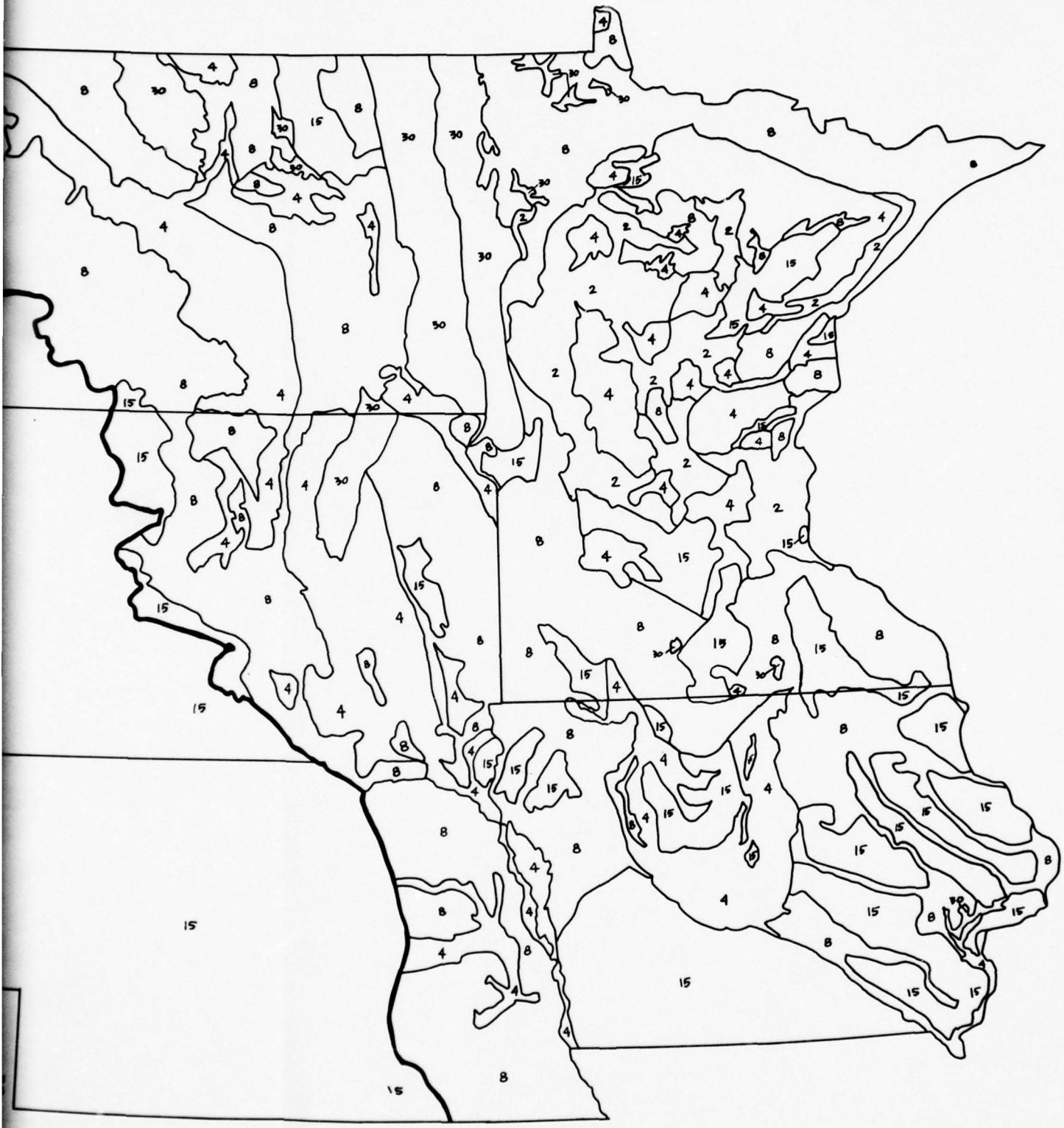
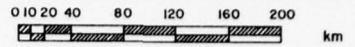
ESTIMATED RANGES OF GROUND CONDUCTIVITY AS MEASURED BY THE SURFACE IMPEDANCE METHOD BETWEEN 200 AND 415 KHZ. THE NUMBERS GIVEN CORRESPOND TO THE RANGES GIVEN IN TABLE 1 AND ARE APPROXIMATELY THE MID-VALUE OF THOSE RANGES IN MILLIMHOS/m. THE HEAVY BORDER IS THE EXTENT OF THE GLACIAL ADVANCES. SOIL COVER IS GENERALLY THICKER TO THE NORTH OF THIS BORDER THAN TO THE SOUTH.





APPENDIX C3  
IOWA, MINNESOTA, NEBRASKA, NORTH DAKOTA,  
SOUTH DAKOTA

Estimated Ranges of Ground Conductivity as Measured by the Surface Impedance Method between 200 and 415 kHz. The numbers given correspond to the Ranges given in Table I and are approximately the Mid-Value of those Ranges in Millimhos/M. The Heavy Border is the extent of the Glacial Advances. Soil Cover is Generally Thicker to the North of this Border than to the South.

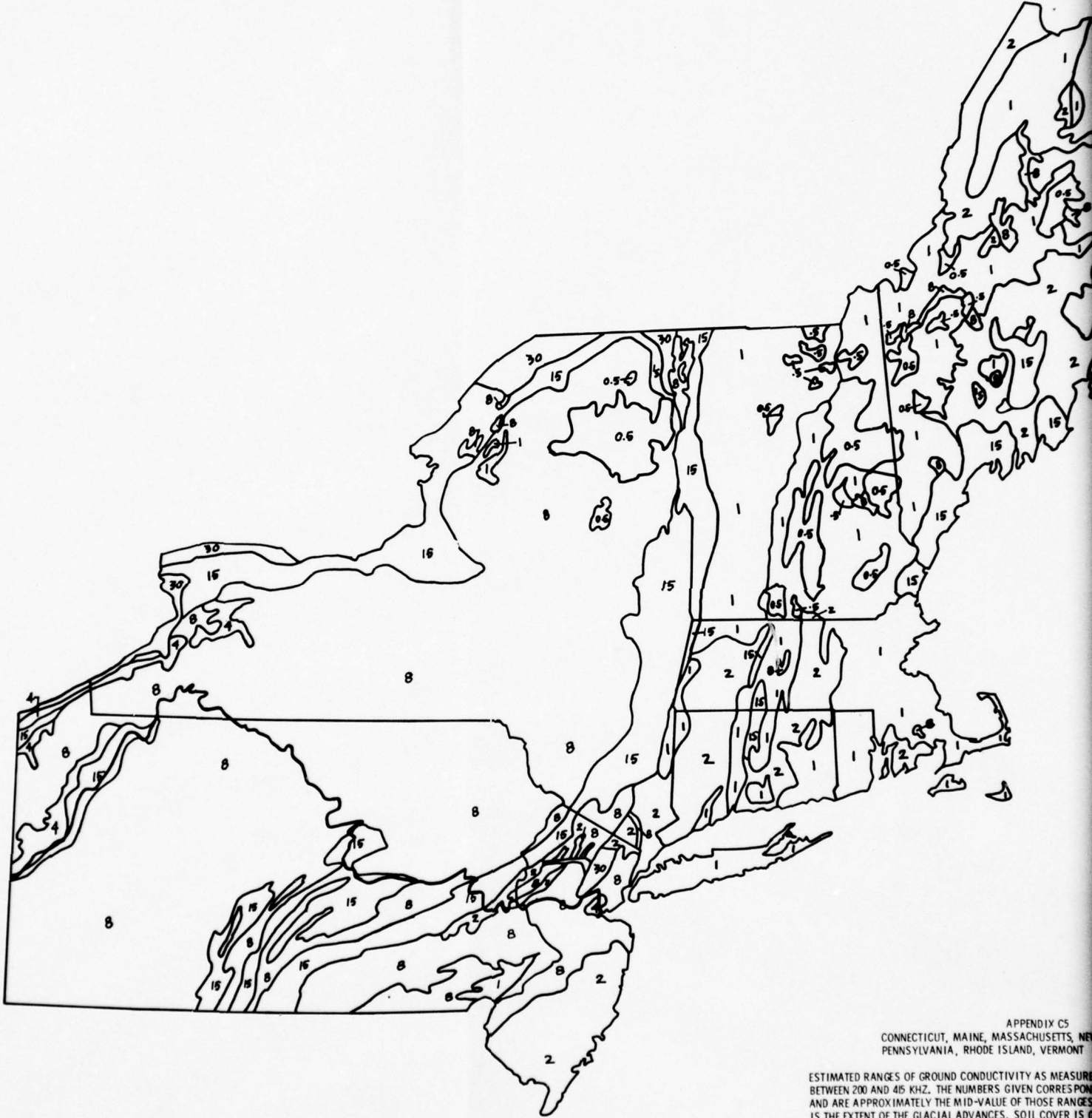


0 10 20 40 80 120 160 200  
km



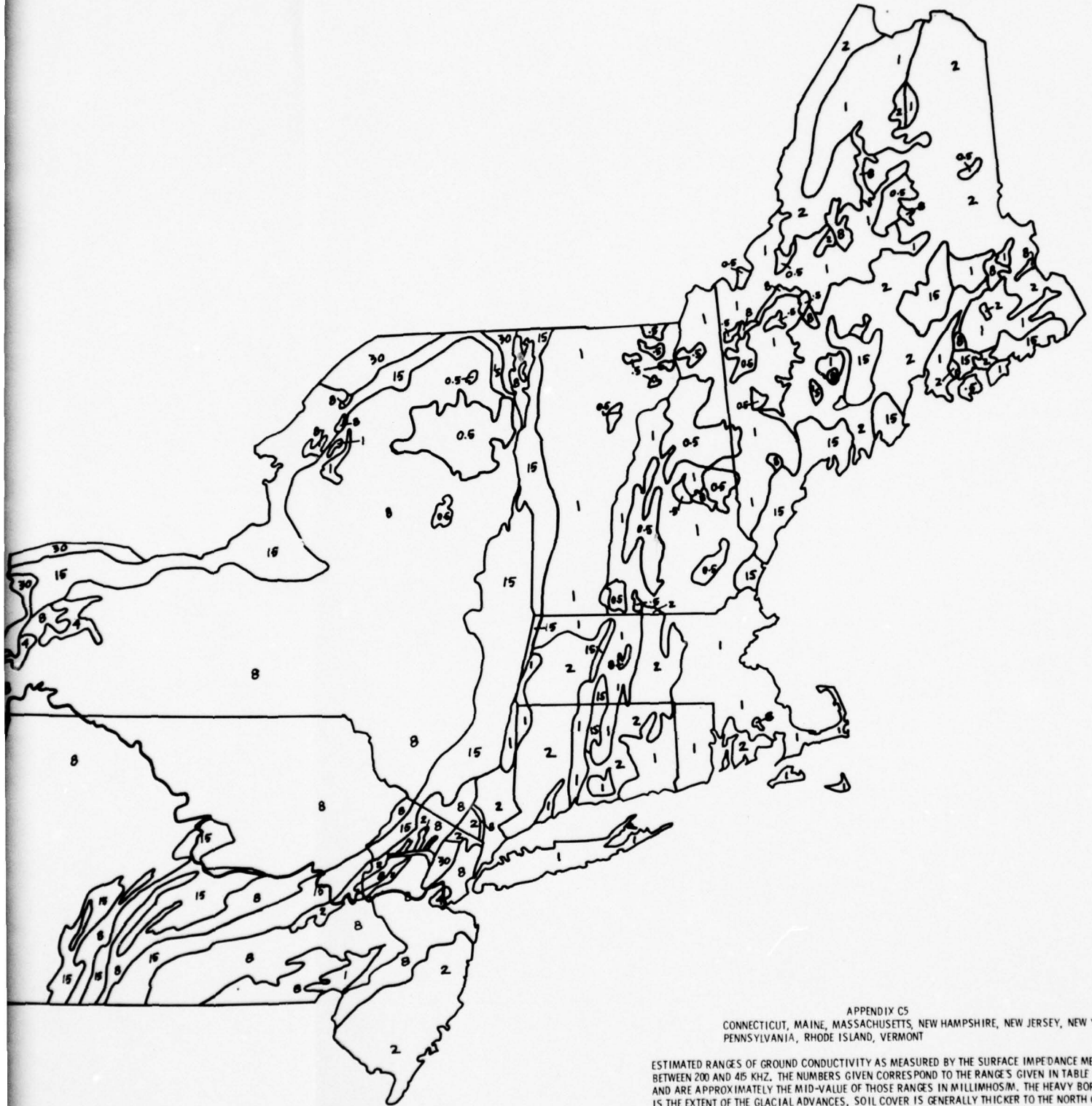
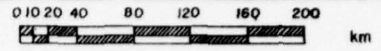
APPENDIX C4  
ILLINOIS, INDIANA, MICHIGAN, OHIO, WISCONSIN

ESTIMATED RANGES OF GROUND CONDUCTIVITY AS MEASURED BY THE SURFACE IMPEDANCE METHOD BETWEEN 200 AND 415 KHz. THE NUMBERS GIVEN CORRESPOND TO THE RANGES GIVEN IN TABLE I AND ARE APPROXIMATELY THE MID-VALUE OF THOSE RANGES IN MILLIMHOS/M. THE HEAVY BORDER IS THE EXTENT OF THE GLACIAL ADVANCES. SOIL COVER IS GENERALLY THICKER TO THE NORTH OF THIS BORDER THAN THE SOUTH.



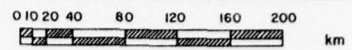
APPENDIX C5  
CONNECTICUT, MAINE, MASSACHUSETTS, NEW HAMPSHIRE,  
PENNSYLVANIA, RHODE ISLAND, VERMONT

ESTIMATED RANGES OF GROUND CONDUCTIVITY AS MEASURED BETWEEN 200 AND 415 KHZ. THE NUMBERS GIVEN CORRESPOND TO THE MID-VALUE OF THOSE RANGES. THE EXTENT OF THE GLACIAL ADVANCES. SOIL COVER IS GREATER TO THE NORTH THAN TO THE SOUTH.



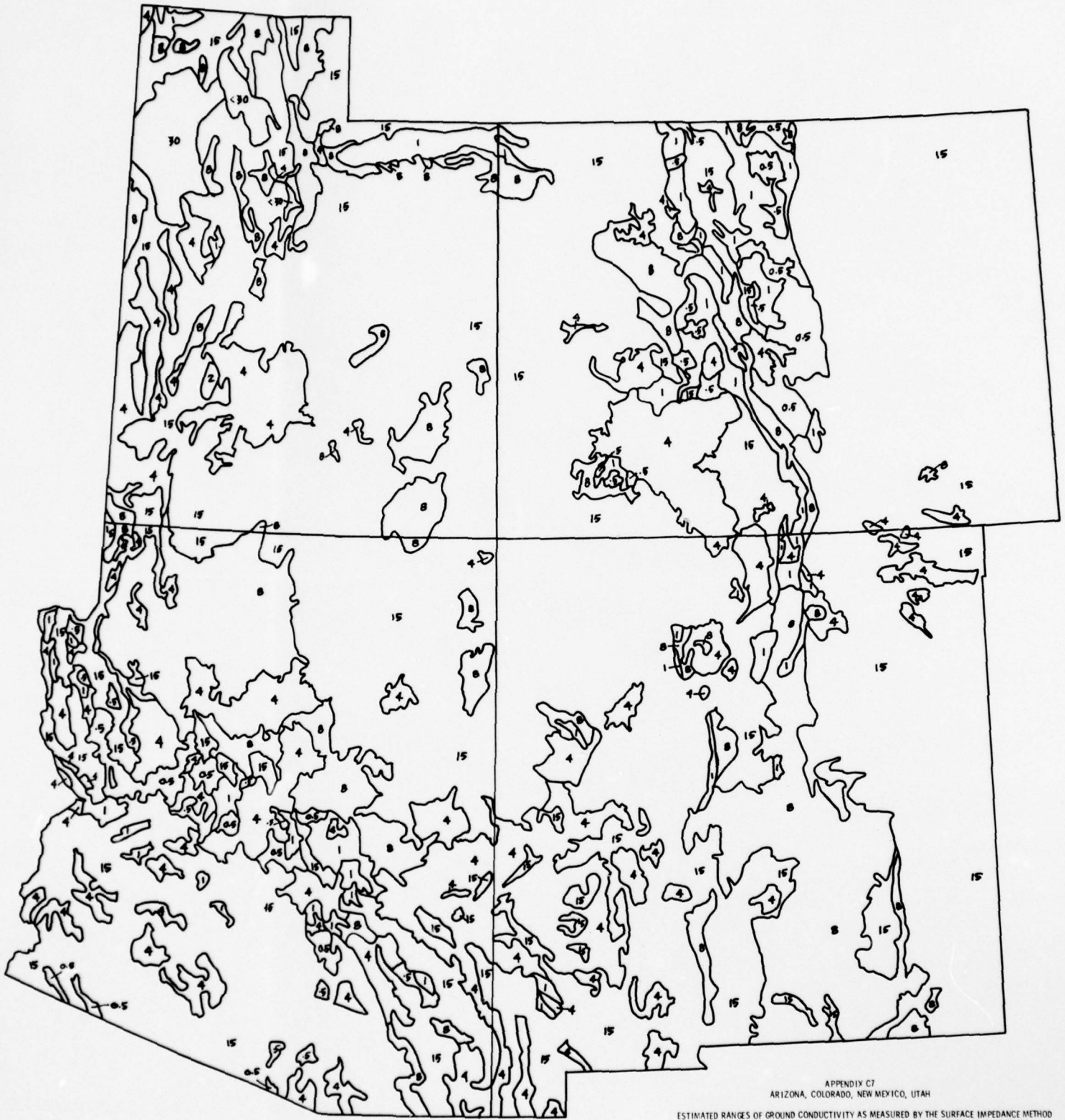
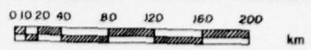
APPENDIX C5  
 CONNECTICUT, MAINE, MASSACHUSETTS, NEW HAMPSHIRE, NEW JERSEY, NEW YORK  
 PENNSYLVANIA, RHODE ISLAND, VERMONT

ESTIMATED RANGES OF GROUND CONDUCTIVITY AS MEASURED BY THE SURFACE IMPEDANCE METHOD BETWEEN 200 AND 415 KHZ. THE NUMBERS GIVEN CORRESPOND TO THE RANGES GIVEN IN TABLE 1 AND ARE APPROXIMATELY THE MID-VALUE OF THOSE RANGES IN MILLIMHOS/M. THE HEAVY BORDER IS THE EXTENT OF THE GLACIAL ADVANCES. SOIL COVER IS GENERALLY THICKER TO THE NORTH OF THIS BORDER THAN TO THE SOUTH.



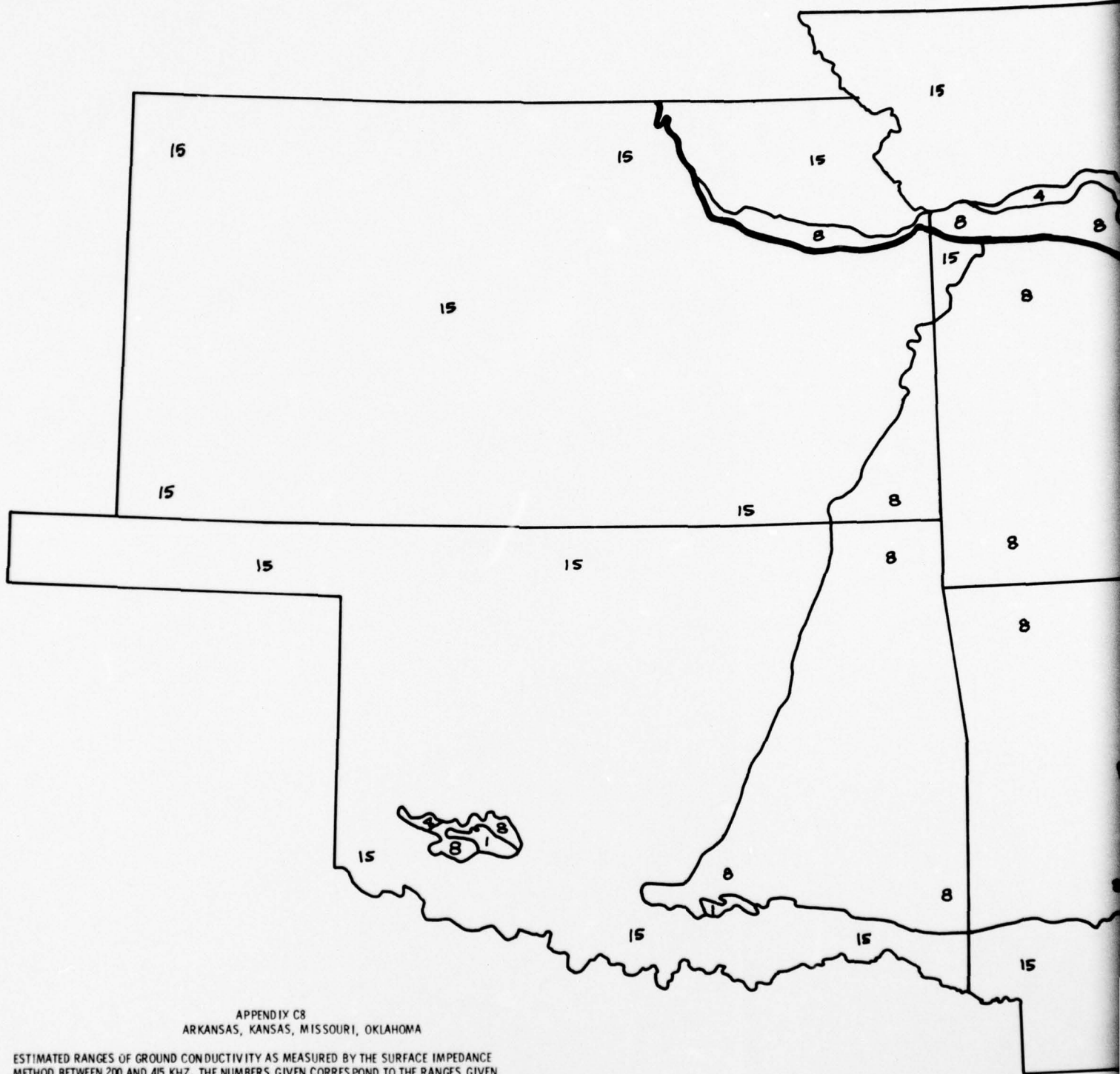
APPENDIX C6  
CALIFORNIA, NEVADA

ESTIMATED RANGES OF GROUND CONDUCTIVITY AS MEASURED BY THE SURFACE IMPEDANCE METHOD BETWEEN 200 AND 400 KHZ. THE NUMBERS GIVEN CORRESPOND TO THE RANGES GIVEN IN TABLE I AND ARE APPROXIMATELY THE MID-VALUE OF THOSE RANGES IN MILLIMHOS/M.



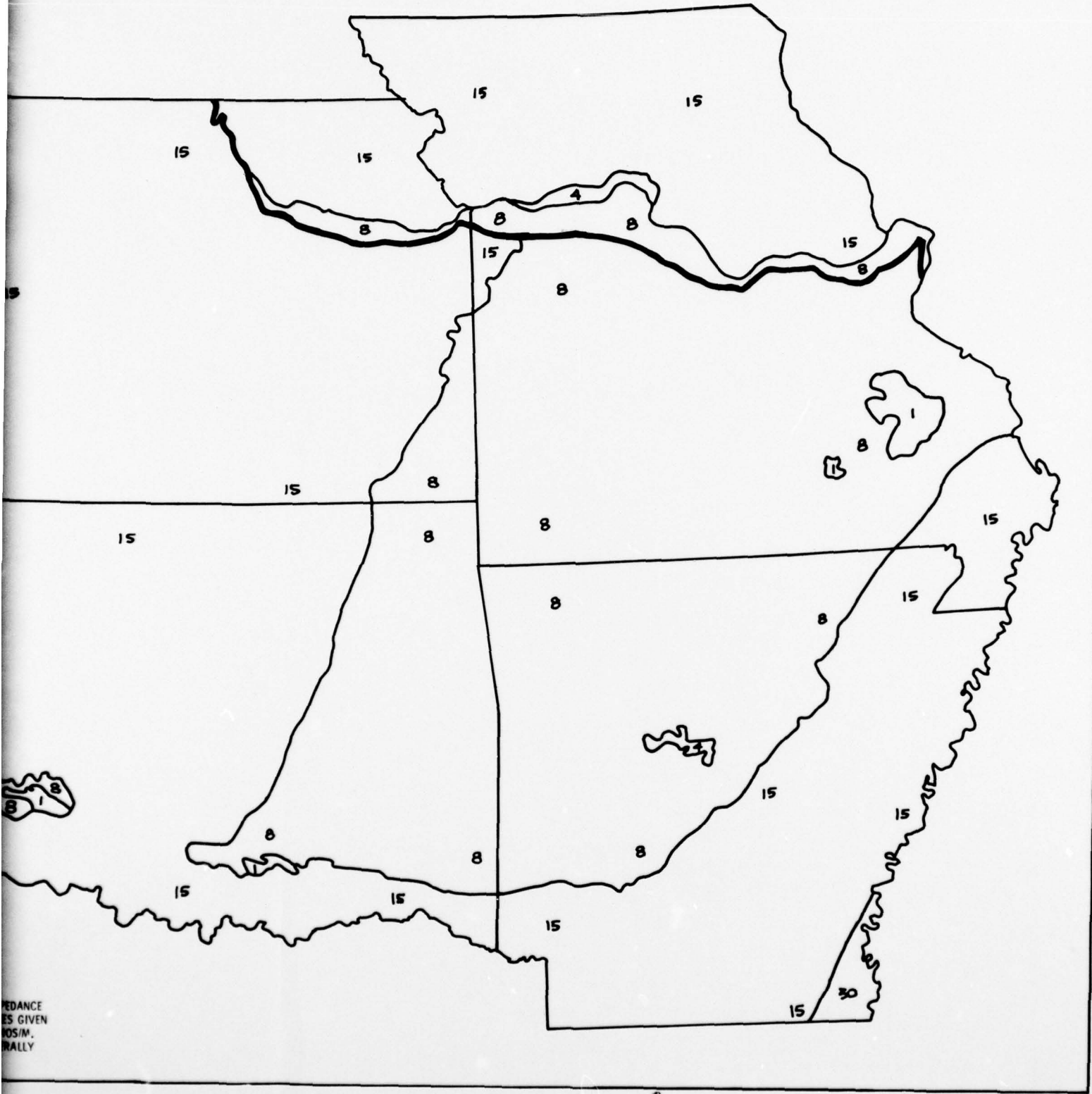
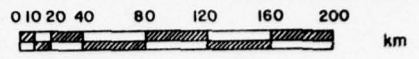
APPENDIX C7  
ARIZONA, COLORADO, NEW MEXICO, UTAH

ESTIMATED RANGES OF GROUND CONDUCTIVITY AS MEASURED BY THE SURFACE IMPEDANCE METHOD BETWEEN 200 AND 400 KHZ, THE NUMBERS GIVEN CORRESPOND TO THE RANGES GIVEN IN TABLE 1 AND ARE APPROXIMATELY THE MID-VALUE OF THOSE RANGES IN MILLIMHOS/M.

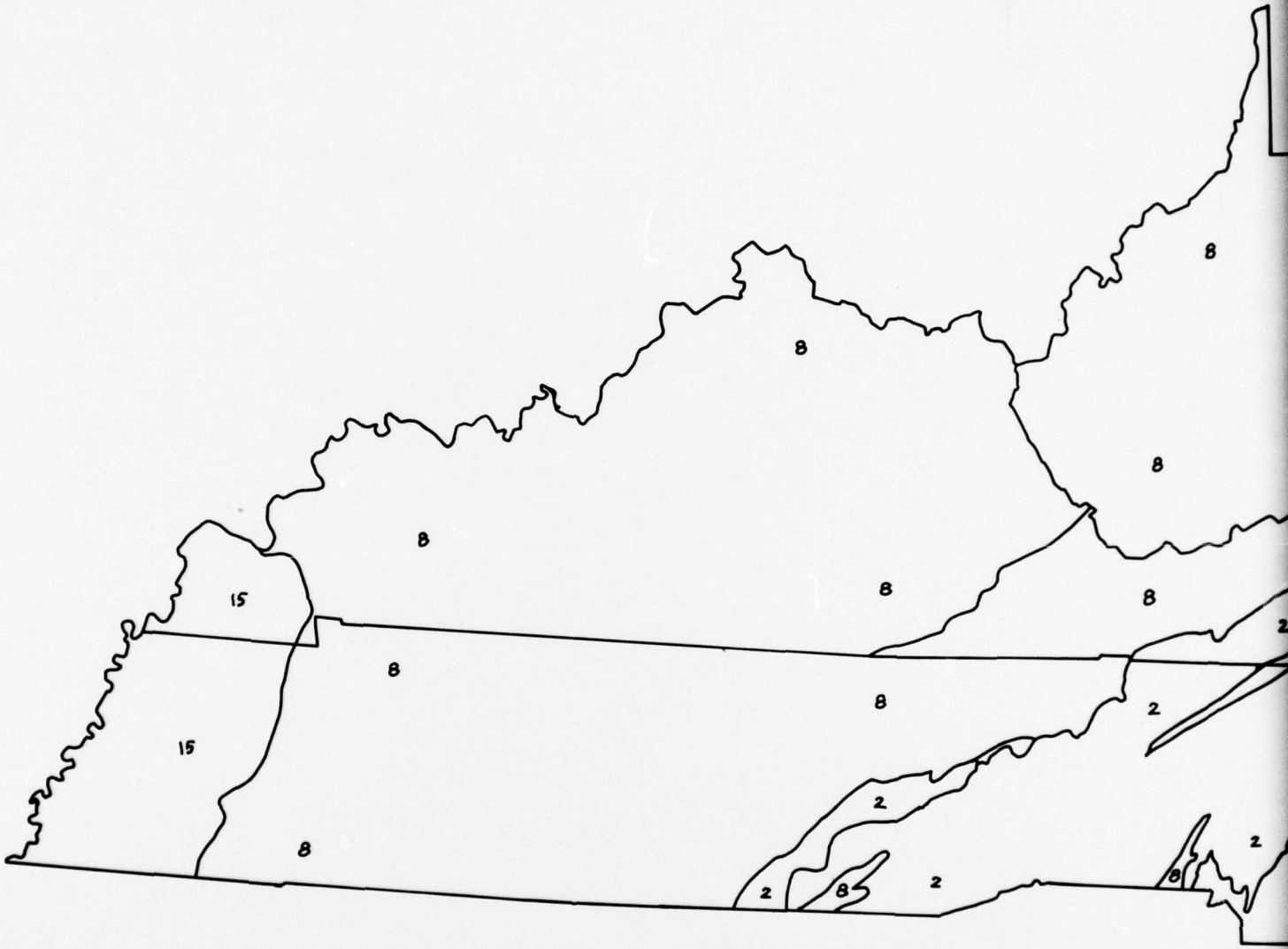


APPENDIX C8  
 ARKANSAS, KANSAS, MISSOURI, OKLAHOMA

ESTIMATED RANGES OF GROUND CONDUCTIVITY AS MEASURED BY THE SURFACE IMPEDANCE METHOD BETWEEN 200 AND 415 KHZ. THE NUMBERS GIVEN CORRESPOND TO THE RANGES GIVEN IN TABLE I AND ARE APPROXIMATELY THE MID-VALUE OF THOSE RANGES IN MILLIMHOS/M. THE HEAVY BORDER IS THE EXTENT OF THE GLACIAL ADVANCES. SOIL COVER IS GENERALLY THICKER TO THE NORTH OF THIS BORDER THAN TO THE SOUTH.

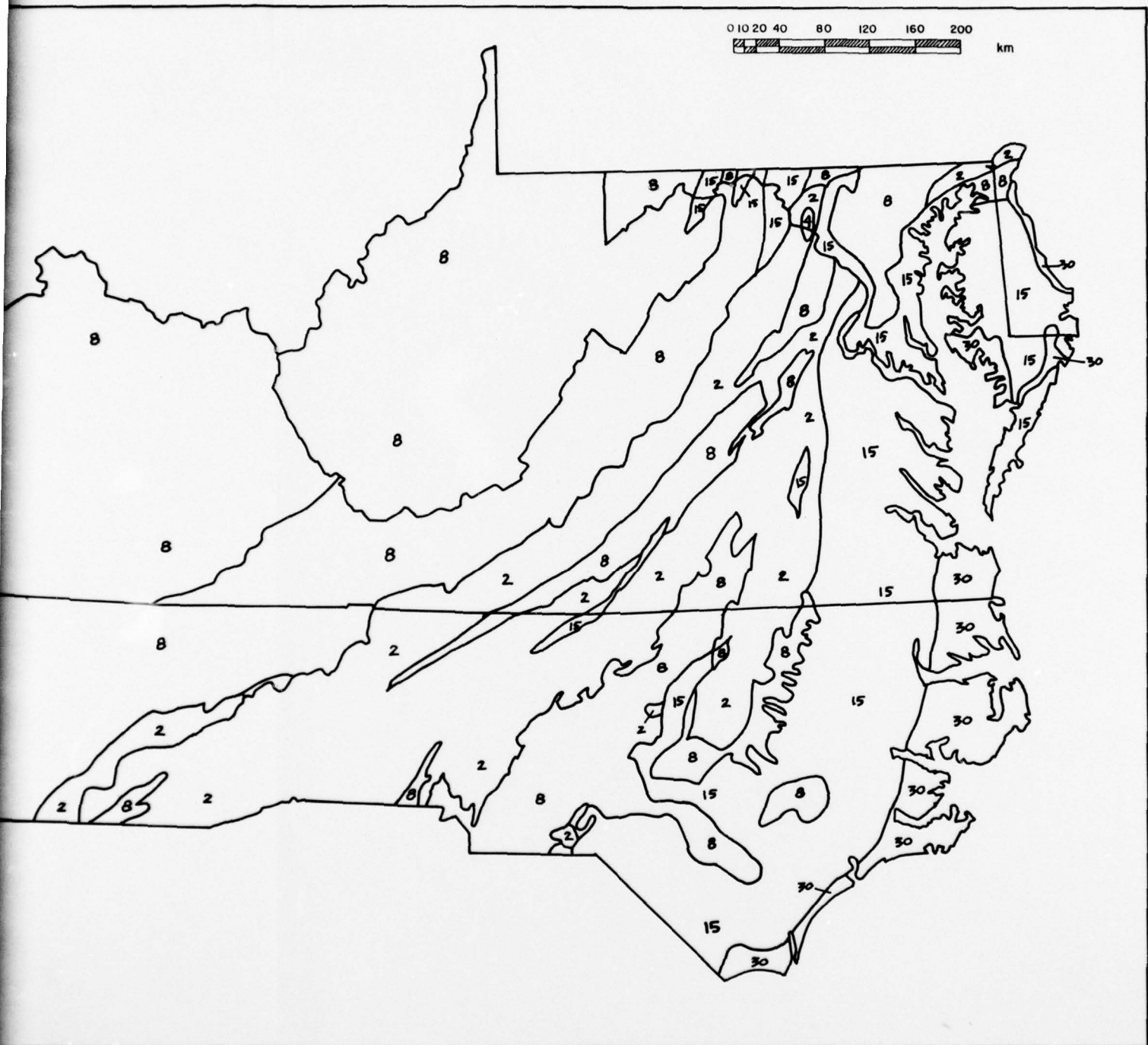
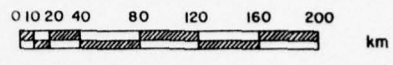


REDANCE  
ES GIVEN  
OS/M.  
RALLY

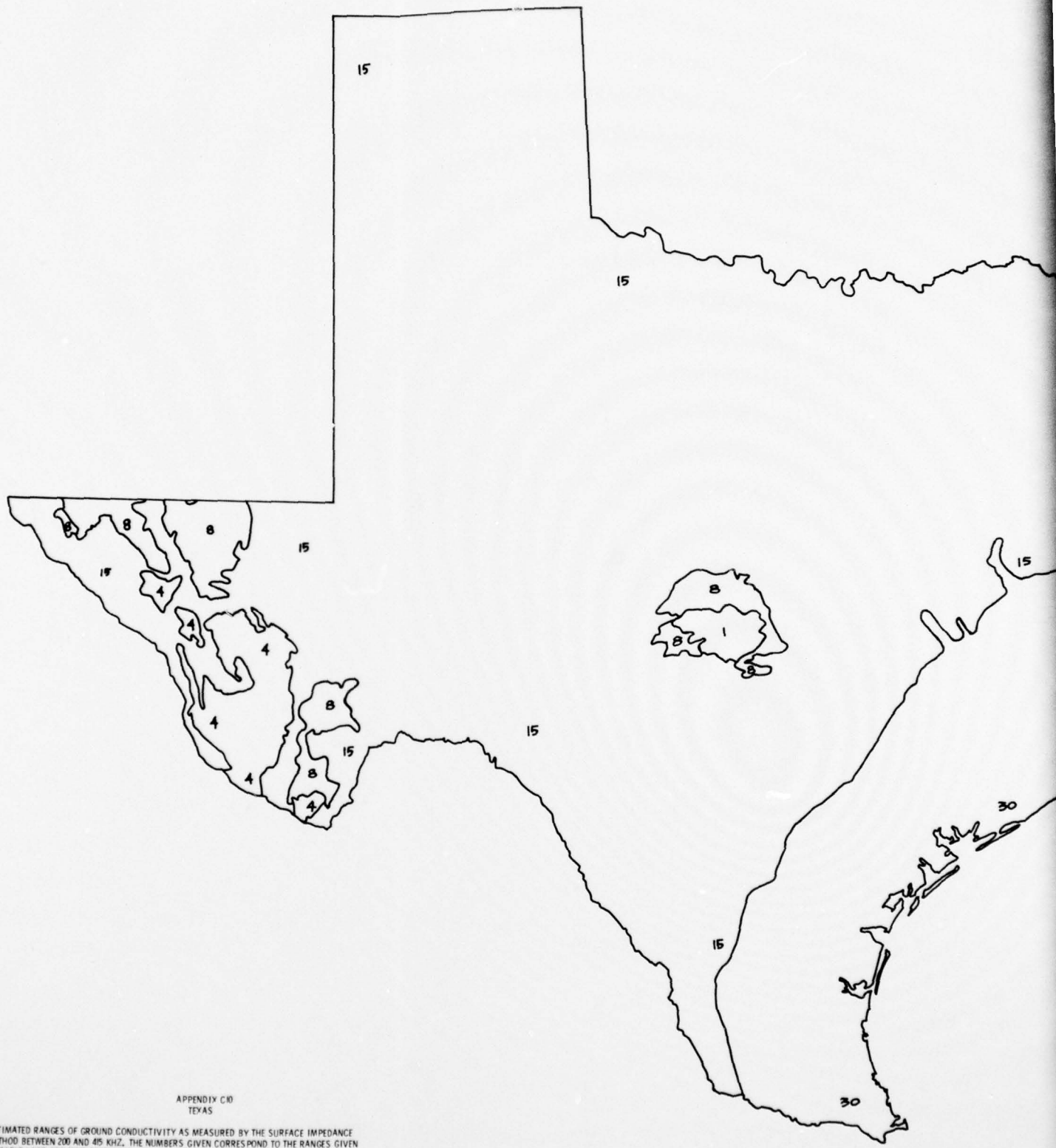


APPENDIX C9  
 DELAWARE, KENTUCKY, MARYLAND, NORTH CAROLINA, TENNESSEE, VIRGINIA  
 WEST VIRGINIA

ESTIMATED RANGES OF GROUND CONDUCTIVITY AS MEASURED BY THE SURFACE IMPEDANCE METHOD BETWEEN 200 AND 415 KHZ. THE NUMBERS GIVEN CORRESPOND TO THE RANGES GIVEN IN TABLE I AND ARE APPROXIMATELY THE MID-VALUE OF THOSE RANGES IN MILLIMHOS/CM.



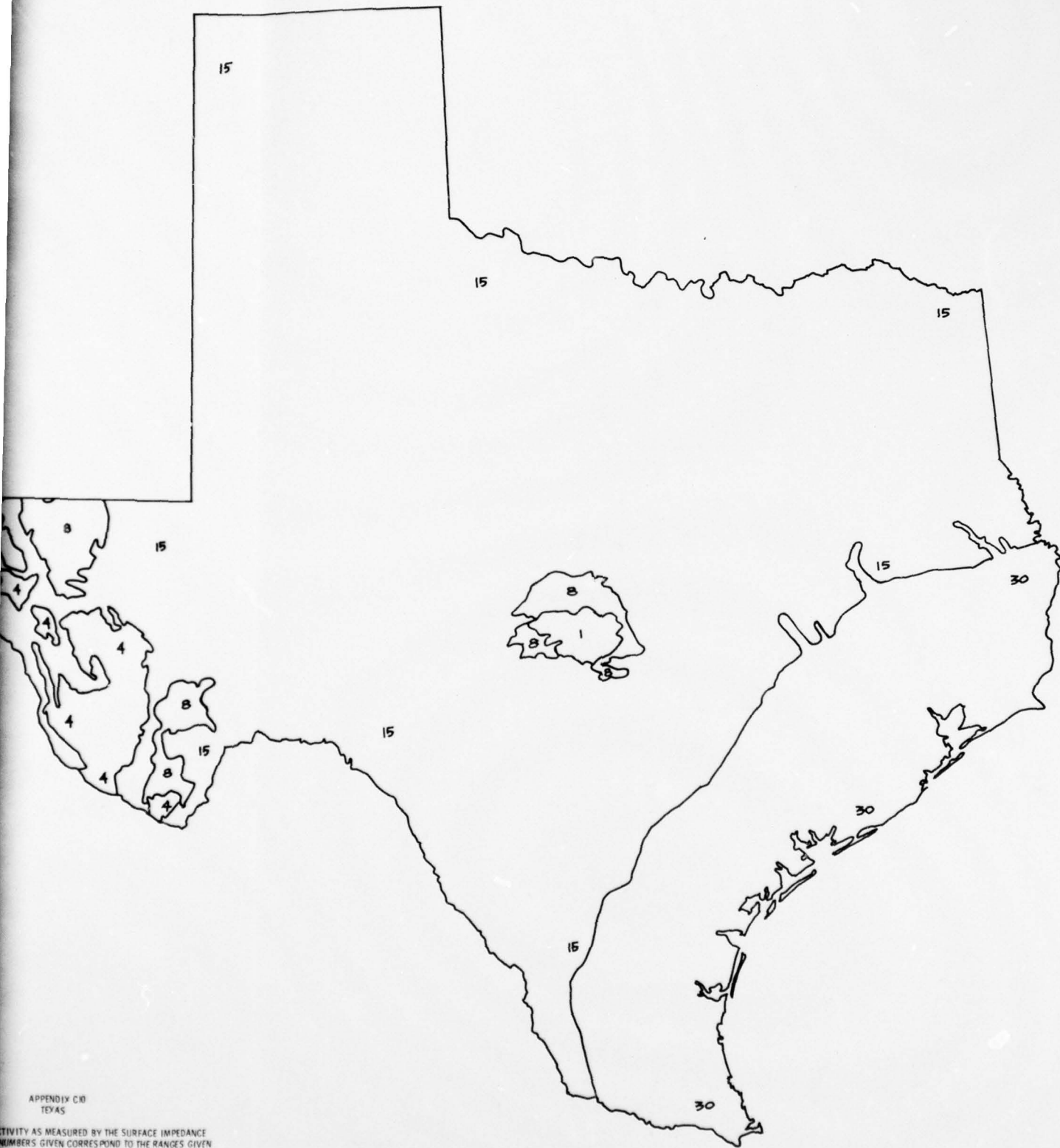
2.



APPENDIX C10  
TEXAS

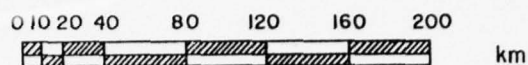
ESTIMATED RANGES OF GROUND CONDUCTIVITY AS MEASURED BY THE SURFACE IMPEDANCE METHOD BETWEEN 200 AND 45 KHZ. THE NUMBERS GIVEN CORRESPOND TO THE RANGES GIVEN IN TABLE I AND ARE APPROXIMATELY THE MID-VALUE OF THOSE RANGES IN MILLIMHOS/M.

0 10 20 40 80 120 160 200 km



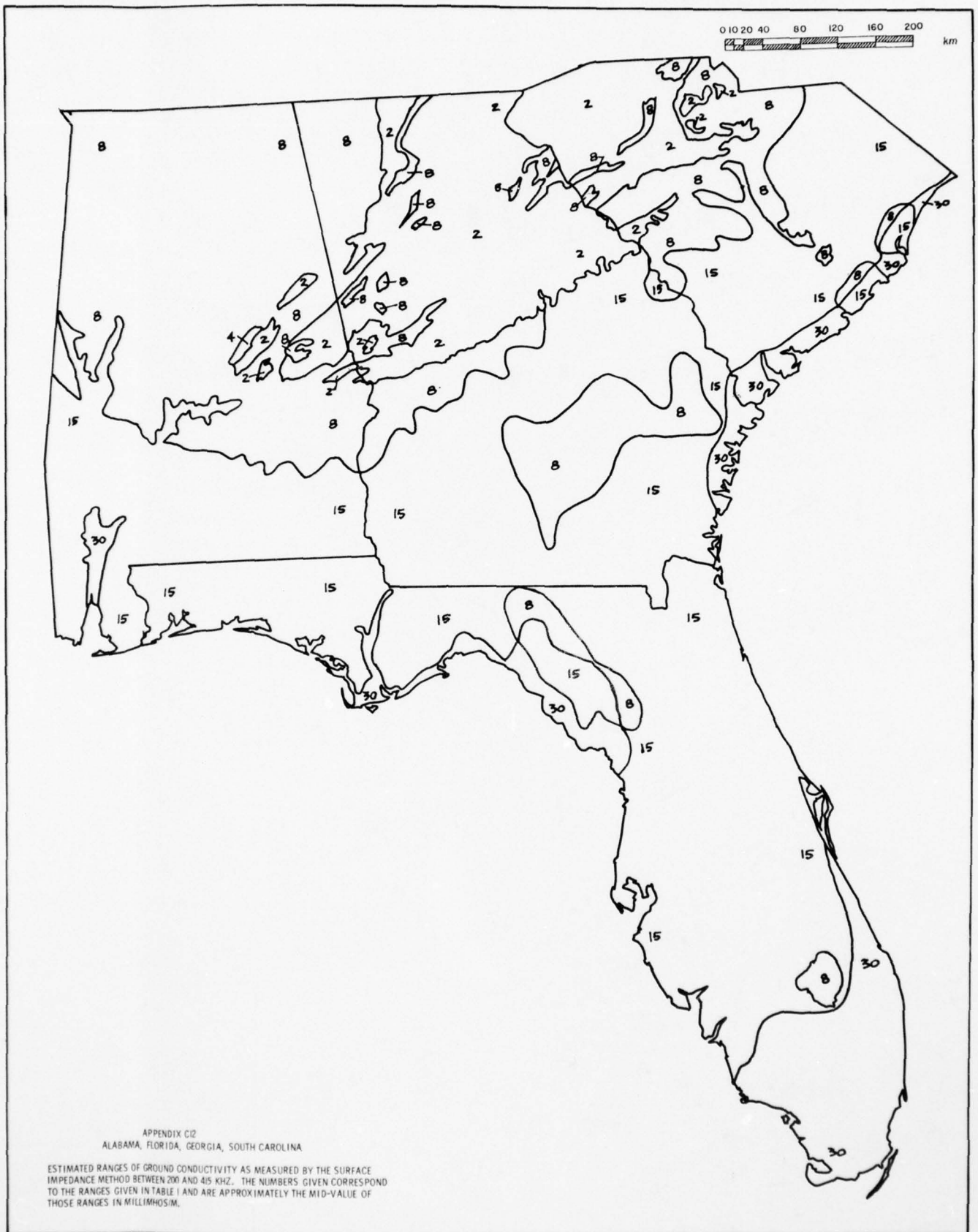
APPENDIX C/D  
TEXAS

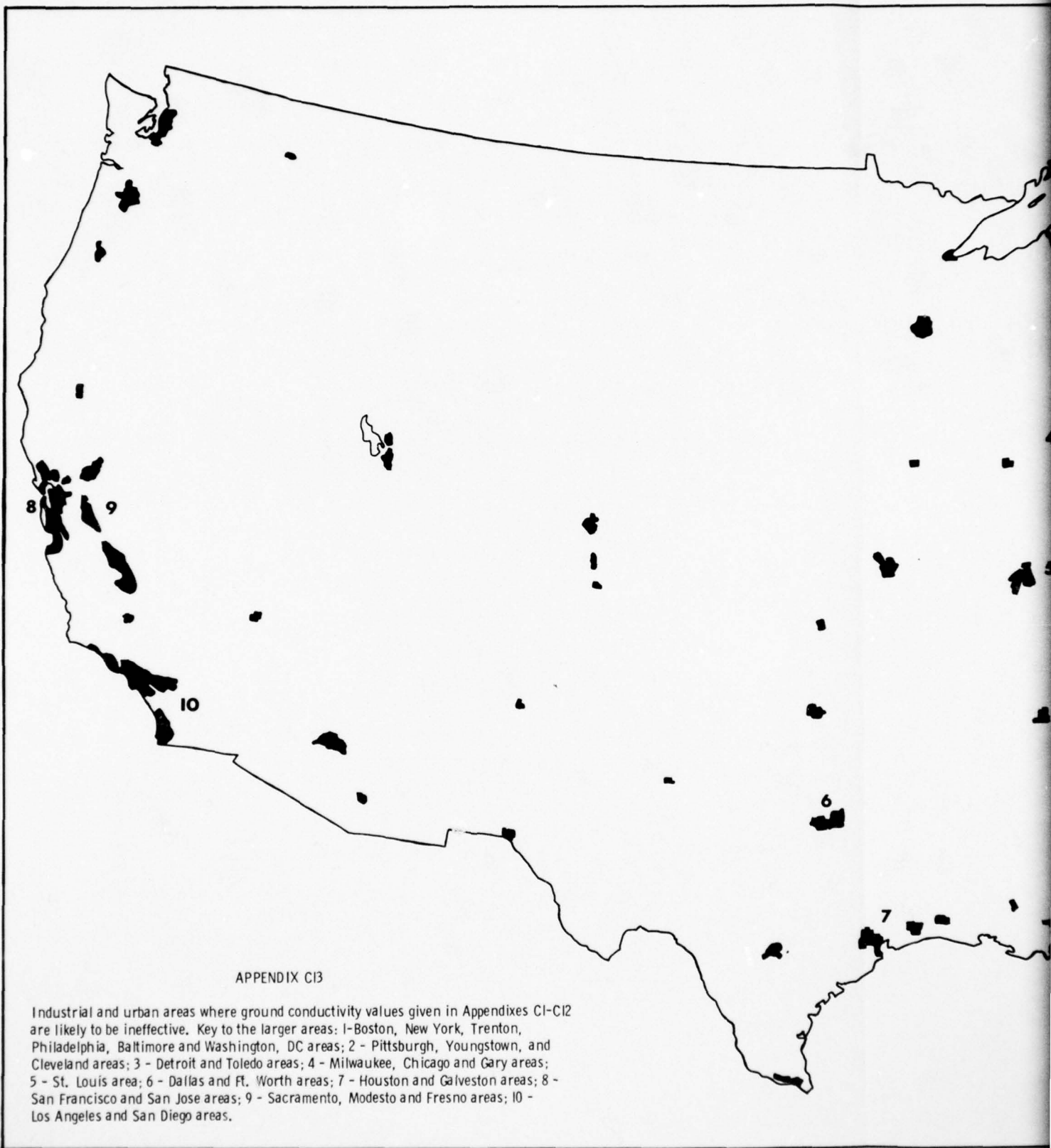
ACTIVITY AS MEASURED BY THE SURFACE IMPEDANCE  
NUMBERS GIVEN CORRESPOND TO THE RANGES GIVEN  
THE MID-VALUE OF THOSE RANGES IN MILLIMHOS/M.



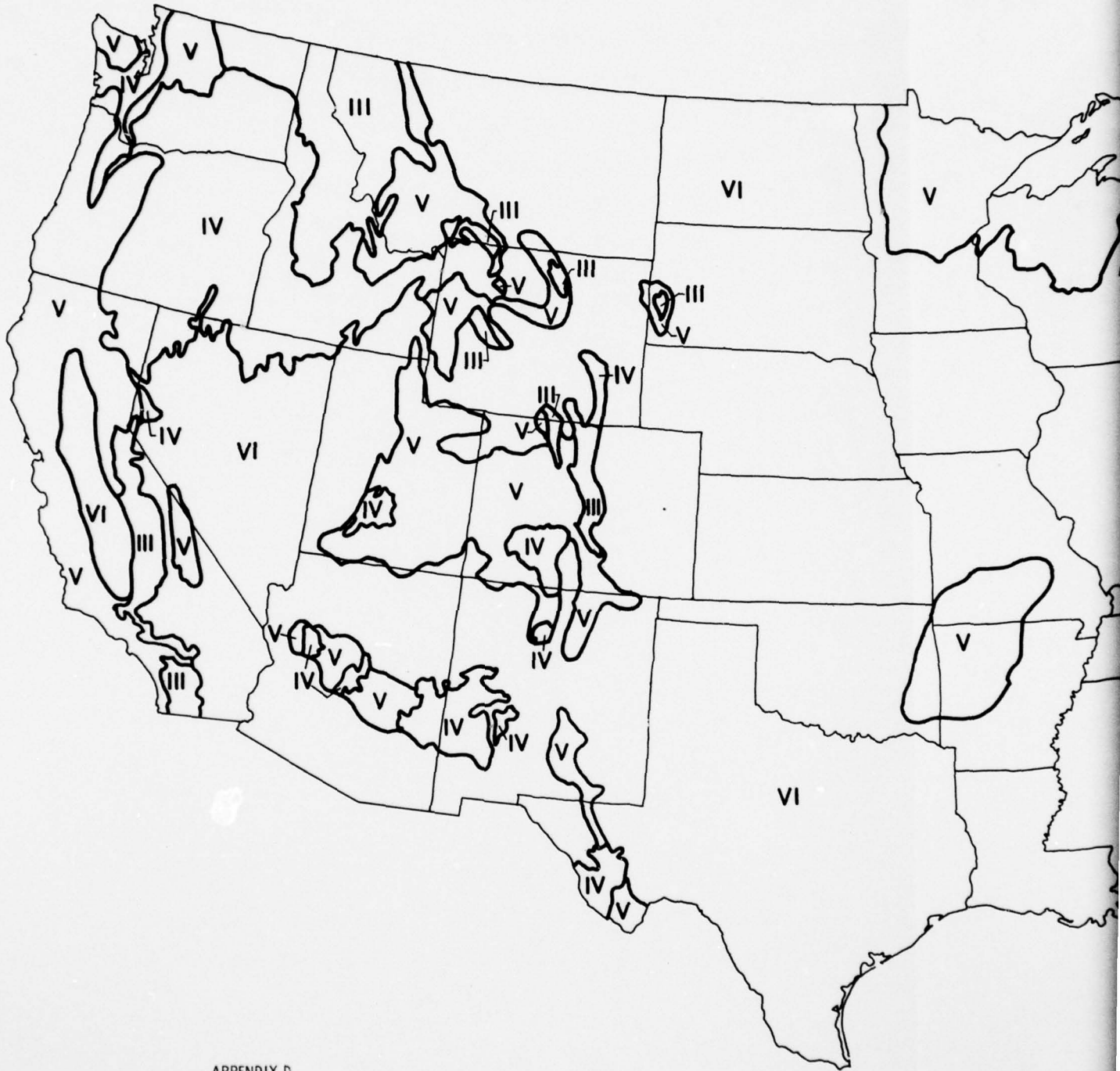
APPENDIX CII  
LOUISIANA, MISSISSIPPI

ESTIMATED RANGES OF GROUND CONDUCTIVITY AS MEASURED BY THE IMPEDANCE METHOD BETWEEN 200 AND 415 KHZ. THE NUMBERS GIVEN CORRESPOND TO THE RANGES GIVEN IN TABLE I AND ARE APPROXIMATELY THE MID-VALUE OF THOSE RANGES IN MILLIMHOS/M.







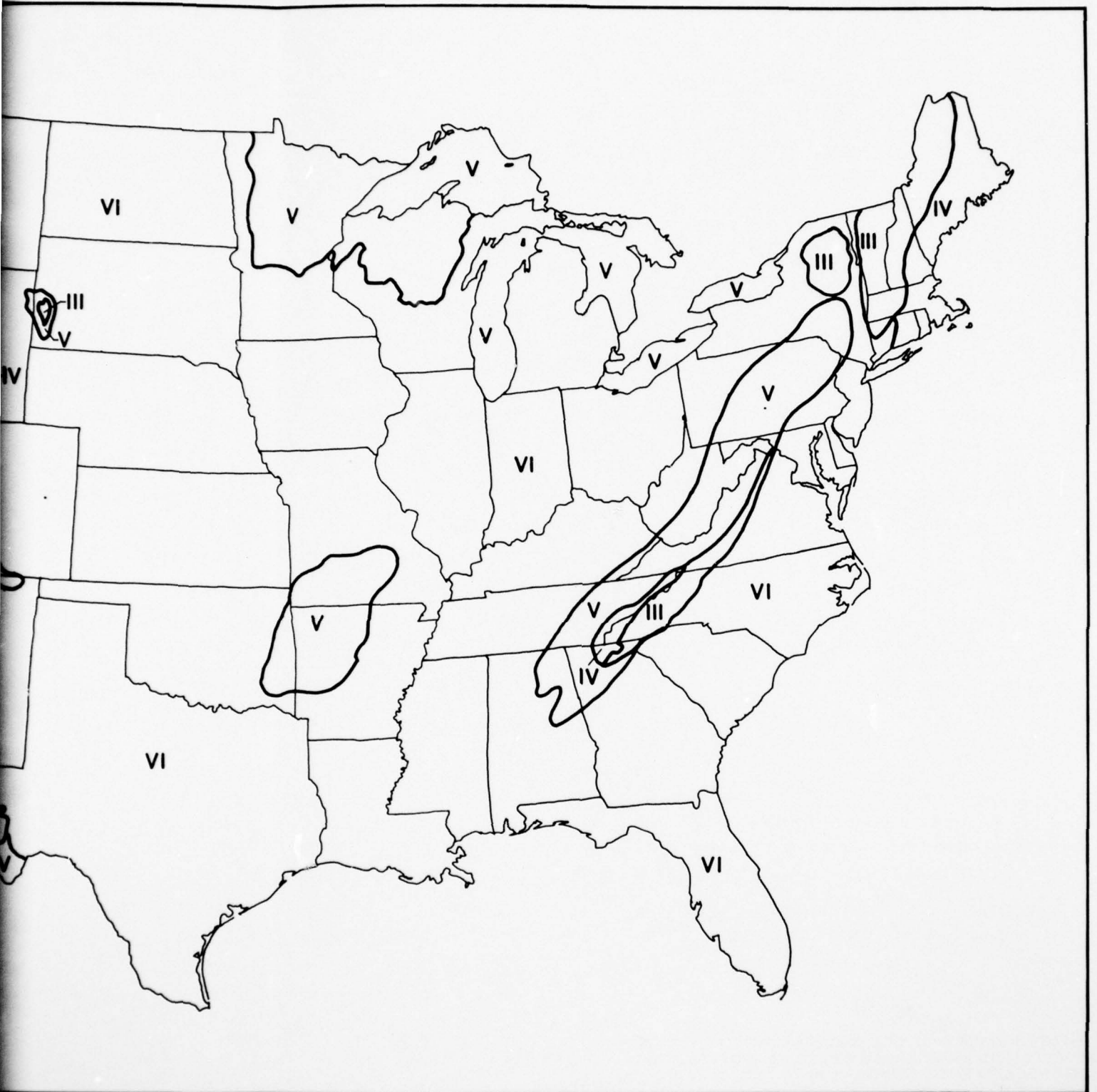


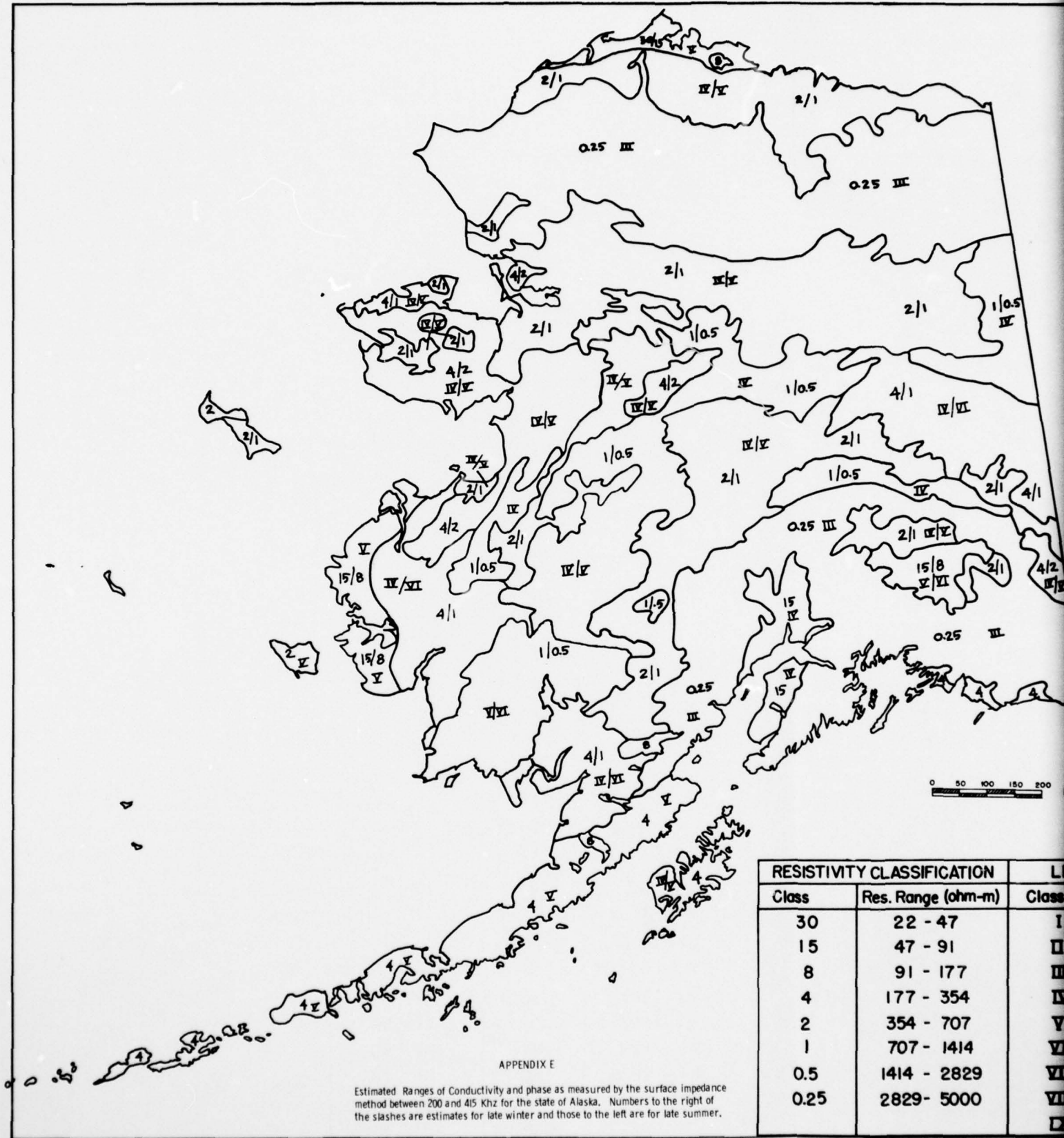
APPENDIX D

ESTIMATED RANGES OF PHASE FOR THE CONTIGUOUS UNITED STATES AS MEASURED BY THE SURFACE IMPEDANCE METHOD BETWEEN 200 AND 415 KHZ. THE NUMBERS CORRESPOND TO THE RANGES GIVEN IN TABLE VI.

1.

2.





APPENDIX E

Estimated Ranges of Conductivity and phase as measured by the surface impedance method between 200 and 415 KHz for the state of Alaska. Numbers to the right of the slashes are estimates for late winter and those to the left are for late summer.

RESISTIVITY CLASSIFICATION		LF
Class	Res. Range (ohm-m)	Class
30	22 - 47	I
15	47 - 91	II
8	91 - 177	III
4	177 - 354	IV
2	354 - 707	V
1	707 - 1414	VI
0.5	1414 - 2829	VII
0.25	2829 - 5000	VIII

